

## **Distribution Agreement**

In presenting this thesis or dissertation as a partial fulfillment of the requirements for an advanced degree from Emory University, I hereby grant to Emory University and its agents the non-exclusive license to archive, make accessible, and display my thesis or dissertation in whole or in part in all forms of media, now or hereafter known, including display on the world wide web. I understand that I may select some access restrictions as part of the online submission of this thesis or dissertation. I retain all ownership rights to the copyright of the thesis or dissertation. I also retain the right to use in future works (such as articles or books) all or part of this thesis or dissertation.

---

Rebecca M. Lynch

---

Date

Mechanisms of Viral Escape from Neutralizing Antibodies during Subtype C HIV-1 Infection

By

Rebecca M. Lynch  
Doctor of Philosophy

Graduate Division of Biological and Biomedical Science  
Immunology and Molecular Pathogenesis

---

Cynthia A. Derdeyn, Ph.D.  
Advisor

---

Eric Hunter, Ph.D.  
Committee Member

---

Hinh Ly, Ph.D.  
Committee Member

---

David Steinhauer, Ph.D.  
Committee Member

Accepted:

---

Lisa A. Tedesco, PhD  
Dean of the James T. Laney School of Graduate Studies

---

Date

Mechanisms of Viral Escape from Neutralizing Antibodies during Subtype C HIV-1 Infection

By

Rebecca M. Lynch  
B.S., Yale University, 2003

Advisor: Cynthia A. Derdeyn, PhD.

An abstract of  
A dissertation submitted to the Faculty of the  
James T. Laney School of Graduate Studies of Emory University  
In partial fulfillment of the requirements for the degree of  
Doctor of Philosophy  
in Graduate Division of Biological and Biomedical Science  
Immunology and Molecular Pathogenesis  
2010

## Abstract

### Mechanisms of Viral Escape from Neutralizing Antibodies during Subtype C HIV-1 Infection

By Rebecca M. Lynch

Human immunodeficiency virus type 1 (HIV-1) group M is responsible for the current AIDS pandemic and exhibits exceedingly high levels of viral genetic diversity around the world. This diversity reflects the remarkable ability of the virus to adapt to selective pressures, the bulk of which is applied by the host immune response, and represents an obstacle for developing a vaccine capable of broad coverage. Studying how the virus escapes this immune pressure at both a population as well as an individual level will ultimately aid in vaccine design. The V3 region of the HIV-1 envelope (Env) glycoprotein gp120 is a key functional domain yet it exhibits distinct mutational patterns across subtypes. Here an invariant residue in V3 (Ile 309) is replaced with Leu in subtype C patient-derived Envs. The results demonstrate that conservation of Ile 309 preserves a V3-mediated masking function that occludes the CD4 binding site, revealing a novel immune evasion strategy that subtype C HIV-1 uses to protect this immune target. Within individual subjects, however, the virus can elicit diverse neutralizing antibody (Nab) responses, leading to different escape pathways. In order to elucidate this process in more detail, the early Nab response in a Zambian seroconverter is characterized for the first time at the autologous monoclonal antibody (Mab) level. Here five Mabs are described, and autologous neutralization by Mabs representative of three distinct B-cell clones are mapped to two residues (134 in V1 and 189 in V2). Mutational analysis reveals cooperative effects between glycans and residues at these two positions, arguing that they contribute to a single novel epitope. Further data demonstrates that although independent B cells in this subject repeatedly target a single structure in V1V2, this pressure is escaped by a single residue change with no demonstrable effect on replication. Together this thesis suggests that subtype C HIV-1 can evade the potent but limited humoral immune response using both sequence variation and conservation, and thus I would propose that a successful vaccine might need to expand the narrow response of natural infection by targeting multiple domains of gp120 in order to achieve ultimate effectiveness.

Mechanisms of Viral Escape from Neutralizing Antibodies during Subtype C HIV-1 Infection

By

Rebecca M. Lynch  
B.S., Yale University, 2003

Advisor: Cynthia A. Derdeyn, Ph.D.

A dissertation submitted to the Faculty of the  
James T. Laney School of Graduate Studies of Emory University  
in partial fulfillment of the requirements for the degree of  
Doctor of Philosophy  
in Graduate Division of Biological and Biomedical Science  
Immunology and Molecular Pathogenesis  
2010

## Acknowledgments

I would like to thank the interns, staff, participants, and Project Management Group at ZEHRP, without whom this work would not have been possible. I would like to thank Dr. Cynthia Derdeyn for invaluable mentorship. I would like to thank my friends and family for their support during my graduate work.

# Table of Contents

|  |           |
|--|-----------|
| <b>Chapter One: Thesis Introduction</b>  | <b>1</b>  |
| Origins of HIV   | 1         |
| HIV Diversity  | 2         |
| Function and structure of HIV Envelope   | 3         |
| Subtype-specific Nab responses during HIV-1 infection  | 6         |
| Targets of Nabs and subsequent viral escape  | 8         |
| Consequences of viral escape   | 11        |
| Summary  | 13        |
| <b>Chapter Two: Subtype-specific Conservation of Isoleucine 309 in the Envelope V3 Domain is Linked to Immune Evasion in Subtype C HIV-1 Infection</b> | <b>15</b> |
| <b>I. Abstract</b>   | <b>15</b> |
| <b>II. Introduction</b>  | <b>16</b> |
| <b>III. Materials and Methods</b>  | <b>18</b> |
| Env clones   | 18        |
| PCR-based site mutagenesis   | 18        |
| Virus neutralization and inhibition assays   | 20        |
| Replication in CD4 and monocyte-derived macrophages (MDM) using an NL4.3 proviral cassette   | 20        |
| Receptor-dependent pseudovirus entry assay   | 22        |
| Statistical analysis   | 22        |
| <b>IV. Results</b>   | <b>23</b> |
| I309L was created in a representative panel of diverse subtype C Envs  | 23        |
| The I309L mutation does not decrease replication in primary CD4 T cells  | 26        |

|  |           |
|--|-----------|
| The I309L mutation leads to a moderate enhancement of replication in<br>monocyte-derived macrophages_____  | 29        |
| The I309L mutation confers increased entry into a cell line expressing low<br>CD4_____   | 32        |
| The I309L mutation confers increased sensitivity to sCD4_____  | 35        |
| The I309L mutation moderately increased sensitivity to monoclonal antibodies<br>directed against V3 and a CD4-induced epitope_____                         | 38        |
| <b>V. Discussion_____</b>  | <b>43</b> |
| Replication is not dependent on conservation of I309_____  | 43        |
| Conservation of I309 prevents exposure of neutralization targets_____  | 44        |
| V3-mediated masking of the CD4 binding site_____   | 45        |
| <b>VI. Acknowledgements_____</b>   | <b>50</b> |
| <b>VII. Contributors_____</b>  | <b>51</b> |
| <b>Chapter Three: The B cell response is redundant and highly focused<br/>on V1V2 during early subtype C infection in a Zambian<br/>seroconverter_____</b> |           |
| <b>I. Abstract_____</b>  | <b>52</b> |
| <b>II. Introduction_____</b>   | <b>53</b> |
| <b>III. Materials and Methods_____</b>   | <b>56</b> |
| Env clones_____  | 56        |
| PCR-based site mutagenesis and virus preparation_____  | 56        |
| Generation of human monoclonal antibodies_____   | 58        |
| Screening ELISA for Mabs _____   | 58        |
| Neutralization Screening Assay for Mabs_____   | 59        |
| Pseudovirus inhibition assays_____   | 59        |
| Homology modeling of residues 134 and 189 in the V1V2 domain_____  | 60        |



|   |           |
|---|-----------|
| Replication in CD4+ cells using an NL4.3 proviral cassette_____   | 60        |
| <b>IV. Results_____</b>   | <b>62</b> |
| Characterization of monoclonal antibodies isolated from a subtype C infected patient<br>and selected for neutralization activity against the founder Env_____ | 62        |
| The monoclonal antibodies likely arose before eight months<br>post-seroconversion_____  | 66        |
| Glycosylation in V1 can confer sensitivity to monoclonal antibodies_____  | 68        |
| Amino acid sequence rather than glycosylation status in V2 defines neutralization<br>sensitivity to Mabs_____   | 71        |
| Residues 134 and 189 may contribute to a single epitope near the V1V2 stem____  | 74        |
| Amino acid changes at residues 134 and 189 do not overtly affect replication fitness in<br>vitro_____   | 76        |
| <b>V. Discussion_____</b>   | <b>79</b> |
| By 8-months post-seroconversion, multiple B-cell clones produced somatic variations<br>of antibodies that neutralize the virus_____                           | 79        |
| Mutational analysis reveals that residues 134 and 189 contribute to a novel epitope<br>near the V1V2 stem_____  | 80        |
| Glycosylation plays varying roles in neutralization during early infection_____   | 81        |
| Replication kinetics of neutralization resistant Envs is similar to neutralization<br>sensitive Envs_____   | 82        |
| <b>VI. Acknowledgements_____</b>  | <b>86</b> |
| <b>VII. Contributors_____</b>   | <b>87</b> |
| <b>Chapter Four: Thesis Discussion_____</b>   | <b>88</b> |
| Conclusion_____   | 96        |
| <b>Bibliography_____</b>  | <b>98</b> |

# List of Tables and Figures

## Chapter One: Thesis Introduction

**Figure 1.** Atomic fluctuations in gp120 \_\_\_\_\_5

## Chapter Two: Subtype-specific Conservation of Isoleucine 309 in the Envelope V3 Domain is Linked to Immune Evasion in Subtype C HIV-1 Infection

**Table 1.** \_\_\_\_\_24

**Figure 1.** Alignment of V3 sequences from subject Envs\_\_\_\_\_25

**Figure 2.** Replication of virus containing a wildtype and I309L mutated Envs in PBMC\_\_\_\_\_27

**Figure 3.** Replication of I309 and I309L Env viruses in MDM\_\_\_\_\_30

**Figure 4.** Lower dependence on CD4 but not CCR5 levels for entry by I309L Envs\_\_\_\_\_34

**Figure 5.** I309L mutation increases sCD4 sensitivity in multiple subtype C Envs\_36

**Figure 6.** I309L increases neutralization by anti-V3 antibodies\_\_\_\_\_39

**Figure 7.** I309L slightly increases neutralization of pre-triggered Envs by an anti-coreceptor binding site antibody 17b \_\_\_\_\_41

**Supplemental Figure 1.** Phylogenetic tree of representative subtype C Envs\_\_\_47

**Supplemental Figure 2.** Replication of virus containing a wildtype and I309L mutated Envs in PBMC\_\_\_\_\_48

**Supplemental Figure 3.** Replication of I309 and I309L Env viruses in MDM\_\_49

**Chapter Three: The B cell response is redundant and highly focused on V1V2 during early subtype C infection in a Zambian seroconverter**

|   |    |
|---|----|
| <b>Figure 1.</b> Timeline of seroconverter 205F from a Zambian cohort _____                       | 64 |
| <b>Figure 2.</b> Sequence analysis of Mabs isolated from seroconverter 205F _____                 | 65 |
| <b>Table 1.</b> _____   | 67 |
| <b>Figure 3.</b> Mab neutralization of Env 6.3 and V1 mutants _____                               | 70 |
| <b>Figure 4.</b> Mab neutralization of Env 6.3 and V2 mutants _____                               | 73 |
| <b>Figure 5.</b> Model of residues 134 and 189 in the V1V2 domain of 0-month FPL<br>Env 6.3 _____ | 75 |
| <b>Figure 6.</b> Replication kinetics of parent and mutant Envs in PMBC _____                     | 78 |
| <b>Supplemental Table 1.</b> _____  | 85 |

**Chapter Four: Thesis Discussion**

|   |    |
|---|----|
| <b>Figure 1.</b> Regions in core gp120 that could potentially interact with Ile 309 _____ | 92 |
|---|----|

## **Chapter One:**

### **Thesis Introduction**

#### **Origins of HIV**

For 2008, the UNAIDS organization estimated that over 30 million people were living with HIV worldwide, underscoring the profound nature of the global HIV pandemic (171). Human Immunodeficiency Virus or HIV is a lentivirus in the family retroviridae consisting of nine genes that, with the help of viral reverse transcriptase, are transcribed from RNA into DNA and integrated into the host cell genome. Integration leads to production of both viral proteins and copies of the genome, all of which are packaged together at the plasma membrane of an infected cell to bud off as virions. The *env*, *pol* and *gag* genes encode essential proteins that provide receptor binding and fusion domains, viral polymerase, and virion structure. The genes *tat*, *rev*, *nef*, *vif*, *vpr*, and *vpu* are known as accessory genes and encode proteins that promote viral escape from immune pressure and that enhance viral infectivity. The virus uses CD4 as its receptor (103, 107) and mainly CCR5 or CXCR4 as its co-receptor (40, 44, 48, 168) leading to productive infection and eventual loss of CD4 T cells in its host (71).

The transmission of this retrovirus into humans is thought to have occurred from at least three independent cross-species transmission events of simian immunodeficiency virus (SIV) from its natural chimpanzee host, giving rise to the three circulating groups of HIV-1 (M, N, and O) (51, 68) in addition to the introduction of SIV from sooty mangabeys into humans, which gave rise to HIV-2

(52, 70, 150). HIV-1 groups N and O, and HIV-2 have been geographically limited to individuals in west Africa while viruses of the HIV-1 group M lineage are responsible for the current global pandemic (106, 126). The last common ancestor for group M HIV-1 was dated to the early 20<sup>th</sup> century (85, 180), and, based on phylogenetic characterization of HIV-1 sequences recovered from frozen specimens, divergent HIV-1 subtypes were already circulating in west-central Africa by the 1960s (180, 188). As of 2008, the average infection prevalence of adults was 5% in sub-Saharan Africa (171), highlighting the urgent need for a vaccine.

### **HIV Diversity**

An unexpected challenge for vaccine design has been the incredible amount of viral genetic diversity generated by features of HIV such as an error prone viral encoded polymerase (31, 125), high levels of persistent virus replication (71, 177), and frequent genomic recombination events (138, 185), characteristics which allow the virus to rapidly adapt to changing selective pressures. This cumulative genetic variability of HIV-1 is managed on paper by classifying viral sequences into one of 13 currently recognized subtypes or sub-subtypes (A1-A4, B, C, D, F1-F2, G, H, J, K) or 43 circulating recombinant forms (161). As of 2004, HIV-1 subtype A, C, and D accounted for 65% of worldwide HIV-1 infections, with subtype C alone being responsible for half of all global infections (69).

Most of these genetic differences reflect variability in the *env* gene, which can encode glycoproteins exhibiting 35% amino acid diversity between subtypes and

20% within a subtype (84). This sequence evolution is thought to be in response to immune pressure because Env is a target for both cell-mediated and humoral immune responses during HIV-1 infection (15, 19, 50, 115, 118, 144-146, 159, 176). Interestingly, patterns of adaptive evolution in the *env* gene of HIV-1 group M have been found to be similar but distinct between subtypes (27, 167). This genetic divergence between subtypes may lead to structural and/or antigenic variation that must be considered during HIV vaccine design.

### **Function and structure of HIV Envelope**

The HIV *env* gene encodes the envelope (Env) precursor 160kDa glycoprotein (gp160), which is proteolytically cleaved into the surface unit gp120 and transmembrane unit gp41 (75). Together, these Env proteins form a complex that protrudes from the virion surface as a trimer. The transmembrane unit gp41 contains heptad repeat regions 1 and 2 (HR1 and HR2), which reside in the ectodomain portion of gp41 (external to the viral membrane). These regions come together to form a six helix bundle that facilitates entry of the virus into the target cell after gp120 binding to receptor molecules and insertion of the fusion peptide into the target cell membrane (75). The surface protein, gp120, contains the CD4 binding site (CD4bs) and the co-receptor binding site, but to avoid recognition by the humoral immune response, conformational masking hides these two important sites. The first, the CD4bs is hidden within a hydrophobic pocket of gp120 (88). The second, the co-receptor binding site, is not available on the un-liganded gp120 trimer as it is formed by conformational changes that occur after CD4 binding, allowing four  $\beta$ -sheets to come together to form a bridging sheet that binds to CCR5 or CXCR4 (141, 142).

Much of what is currently known about the conformation of gp120 is based on crystal structures of the truncated, de-glycosylated, CD4-liganded subtype B and C protein core or the truncated, glycosylated, unliganded core of simian immunodeficiency virus (SIV) (24, 42, 89, 90). The structure and position of the 'hyper-variable' domains contained within gp120 have been difficult to determine because of their conformational flexibility. It is, therefore, not fully understood how these variable domains might influence the overall conformation of a functional trimer. Structures of CD4-liganded, truncated gp120 with an intact, antibody bound V3 domain (73) and a truncated gp120 bound to monoclonal antibody b12 (an anti-CD4bs antibody) (187), as well as a subtype C core bound to CD4 and 21c (an anti-coreceptor binding site antibody) (42) have also been recently deduced. In all of these structures, the outer-domain of gp120 appears to be similar; however, the inner domain is predicted to undergo significant conformational change upon binding to CD4, as reflected by its relative flexibility as compared to the outer domain ((101) and Fig. 1). Furthermore, comparisons between subtype B and C gp120s have shown that sequence differences in the CD4bs do indeed lead to differential binding and neutralization patterns by monoclonals (42, 182). Thus, it is imperative that HIV vaccine designs based on structure, such as immunogens aimed at inducing an antibody response, take into account these differences.

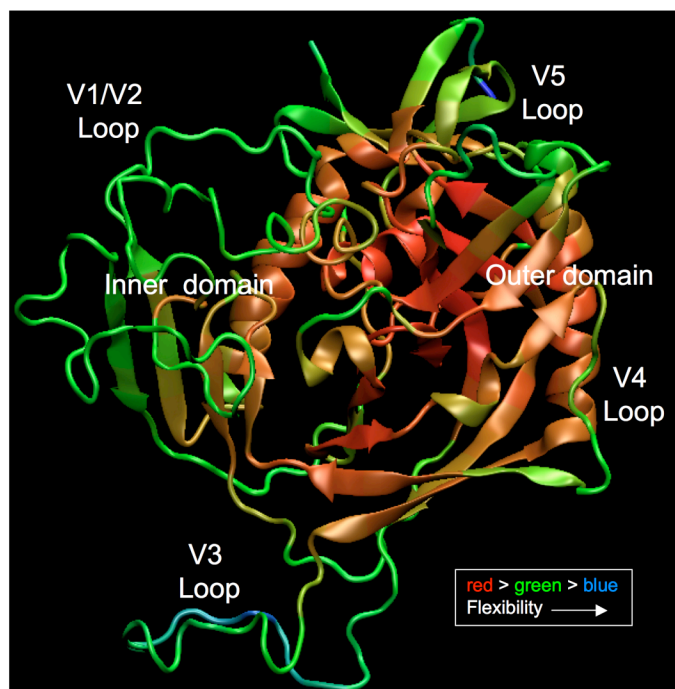


**Figure 1. Atomic fluctuations in gp120.** Backbone flexibility of the YU2 gp120 molecule was calculated from long time scale equilibrium molecular dynamics simulations. These all atom simulations were carried out with gp120 solvated in explicit solvent molecules. The calculated B-factors correspond to backbone atomic fluctuations and are graphically mapped on an arbitrary structure of a liganded gp120 with modeled loops using a color gradient. The red to blue indicates small to large atomistic fluctuations (rigid to flexible) in the backbone of the structure. The outer domain is relatively more rigid than the inner domain, while the loop regions are also more flexible than the core. Even though the starting conformation of gp120 corresponds to that of the CD4-liganded structure, the CD4 molecule was not included in the calculations. Despite the incomplete sampling of the gp120 conformational space, significant



flexibility is observed in the inner domain, some of which is associated with the relief of the conformational constraints induced by binding to CD4.

### **Subtype-specific Nab responses during HIV-1 infection**

Studying the evolution of the humoral immune response during natural HIV infection may also give clues as to how to induce a more effective antibody response in a vaccine setting. The majority of antibodies that arise are directed against Env (154, 165, 172). Given the subtype differences in Env proteins outlined above, it would not be surprising to find variation in the serology of infection with diverse subtypes. During infection, subtype B HIV-1 elicits neutralizing antibody activity against the autologous virus that is usually detectable in patient plasma within the first few months of infection (1, 4, 19, 92, 112, 140, 165, 176). Subtype C HIV-1 elicits a Nab response with similar kinetics (20, 63, 92). However, when the autologous Nab response in 6 subtype B infected seroconverters was compared directly against 11 subtype C infected seroconverters from Zambia, a 3.5-fold higher 50% inhibitory titer of Nab was found in the C subjects (92). This study suggests that early subtype C antibodies may be more potent than subtype B.

In addition to the issue of potency, the inability to induce antibodies during natural infection that can broadly neutralize across subtypes, much less via immunization, has hampered attempts to generate an effective vaccine. Recent studies of the cross-neutralization properties of individual and pooled subtype-specific plasma using both pseudo-virus and PBMC-based assays have determined that in general, subtype specific relationships do exist between

neutralizing antibody and virus sensitivity (11, 12, 18, 20, 137). Surprisingly, one study found, that subtype C patient plasma was not more likely to cross-neutralize a heterologous virus genetically similar to the autologous virus as opposed to a heterologous virus that was more distantly related (137). Thus, it is important to note that there could be poor concordance between neutralization epitopes (which are often conformational), and linear Env sequences (which are often gap-stripped) that are analyzed with phylogenetic methods. In fact it has been recently demonstrated that the presence of a defined Mab epitope in an Env is not always sufficient for neutralization (12, 182), providing further evidence that exposure of neutralization determinants on the native trimer is also important. Thus there are both sequence and structural differences amongst subtypes that can hinder vaccine efforts to elicit antibodies capable of broad neutralization.

A separate report, which found higher in vitro autologous Nab titers in early subtype C vs. B infection (as discussed above), also observed that plasma from these subtype C subjects had less cross-reactive activity against heterologous Envs of the same subtype, compared to plasma from the subtype B patients (92). This study suggests that the initial Nab response in subtype C infection, although potent, is directed against strain-specific epitopes. This lack of cross-reactivity in early subtype C infection was corroborated in an independent study of 14 South African patients (63). Intriguingly, in one study, subtype C pooled plasma was highly cross-neutralizing against viral Envs of almost all subtypes measured (A, B, C, D, AE and AG) using a sensitive pseudovirus assay (18). One explanation for

this apparent contradiction would be that when these plasma samples are pooled, the breadth of targets recognized is increased substantially. In contrast, if autologous Nab across subtype B infected patients recognized similar targets, as suggested in (19), pooling the plasma would not be expected to dramatically increase the breadth (18).

With respect to monoclonal antibodies (Mabs), a few 'broadly reactive' Mabs have been derived from subtype B infected patients, but most lack neutralizing activity against non-B viruses (11-13, 20, 64). For example, antibodies 2F5 and 2G12 have limited activity against subtypes A, C, and D viruses (12), and for 2G12, simply reconstituting the epitope in subtype C Env does not necessarily result in neutralization, suggesting that conformational constraints prevent formation or exposure of this epitope (64). Recently, monoclonals from a subtype A infected patient (PG9 and PG16) and a subtype B patient (VRC01) have shown promise by demonstrating both potency and wide breadth. Together these findings indicate that Envs of different subtypes have distinct antigenic properties, leading to differences in potency and breadth of the resulting antibody response. When these differences are taken into account, however, it does appear possible to isolate Mabs with the ability to neutralize across subtypes.

### **Targets of Nabs and subsequent viral escape**

An ideal vaccine candidate would induce Nabs against a well-conserved, immunogenic target. Thus studying the targets of Nab during natural infection

may provide insight into achieving this goal. Presumably breadth arises from either an antibody-specificity against a conserved epitope, diverse antibody specificities that target 'enough' epitopes, or some combination of the two. There is no consensus as of yet as to what comprises 'breadth' although the specificities of these antibodies have been studied by numerous groups. Most of the patients with plasma that possess this desirable quality have been found to have antibodies directed against gp120 and more specifically, the CD4bs (10, 95, 96, 151, 154, 173). Mabs isolated from two of these subjects suggest that breadth may be attributed to particular specificities such as the CD4bs (Mab VRC01) or quaternary epitopes involving V2 and V3 (Mabs PG9 and PG12). However, it has also been reported that neutralization breadth correlates with anti-MPER (in gp41) specificities (62, 65, 151, 157). One explanation for these different observations could be the different cohorts studied, or it could be that the anti-MPER specificities do confer breadth, but in a smaller number individuals, as found by Walker, et al. and Sather, et al. (151, 172). Interestingly, in one study, the breadth demonstrated by polyclonal plasma could not be recreated by combining autologous monoclonals at a one to one ratio (154). Thus, although cross-subtype neutralization is a major goal for vaccine design, the path that leads to antibody breadth is still not fully understood.

Furthermore, why is breadth so uncommon? As described in a previous section, antibody responses have been found to be potent, but often strain-specific (92, 112). In a SHIV model of infection, it was found that the V1V2 domain is responsible for this specificity. This finding corresponds with evidence from

multiple labs reporting that antibodies often target V1V2 during HIV-1 infection as well (59, 60, 72, 81, 172). In fact studies of the early antibody response in subtype C patients have shown that antibodies have limited specificities (targeting only V1V2, C3 and V5) and thus are easily escaped (116, 146). Together, these data potentially explain the lack of viral control by the humoral arm of the immune response, in that early antibodies appear to target one highly variable region at a time, which means the response is both lacking in breadth and fairly simple to evade.

In these latter studies by Moore et al. and Rong et al., subsequent viral escape was suggested to be through sequence changes in the V1V2 domain as well as through potential glycan shifts and indels. Others have demonstrated both the importance of both glycan shifting in Nab escape (176) as well as changing loop length (41, 144, 147), methods of escape used by HIV-1 regardless of subtype. The virus may further evade the immune system by structurally concealing targets of Nabs. The CD4bs is hidden in a hydrophobic pocket that may sterically prevent antibody binding and may necessitate the virus to bind multiple CD4 molecules to gain sufficient avidity for entry (88). The coreceptor binding site is “hidden” as well in that it is only formed after conformational changes that occur following receptor binding. Structural concealment of both these sites has been demonstrated to prevent antibody neutralization of the virus (38, 88). Less defined is the role of structural masking of the V3 domain, another possible target of neutralizing antibodies.

The V3 domain is the most conserved of the “hyper-variable” domains (73), and it is the only one of these domains to have a defined role in viral entry (21, 34, 168). However, lineage specific sequence and mutational patterns have been identified in V3 across all HIV-1 subtypes (86, 124). For instance, the subtype C V3 domain lacks sites of strong positive selection analogous to those found in the subtype B V3 (54, 145). One possible explanation is that the former may not be driven to vary its sequence in reaction to immune pressure, but at odds with this theory is the fact that anti-V3 antibodies are in fact detectable in subtype C plasma (10, 20, 37, 115). A second possibility is that since sequence variation in V3 appears to facilitate the switch to CXCR4 usage in subtype B viruses, V3 conservation may just be a general feature of CCR5-using viruses, but analysis using the HIV Sequence Database (data not shown) does not support this theory. Thus, despite their presence in both subtype C and B plasma, anti-V3 antibodies in these respective subtypes have been shown to both target diverse epitopes on V3 and have varying neutralizing abilities against primary viruses, suggesting antigenic differences between the V3 in these two subtypes (10, 110, 112, 124, 189). Whether these different mutational patterns are a result of conformational differences or are the cause is uncertain.

On the contrary, cross-subtype reactive anti-V3 antibodies can be elicited in patients, indicating that there are also conserved features of V3. Recently, crystal structures of cross-neutralizing anti-V3 antibodies bound to diverse V3 peptides were characterized (78). This study reveals that despite the sequence variation that occurs in V3, there are four conserved structural elements termed arch,

circlet, band and backbone, and when antibodies target these latter regions, they possess cross-neutralizing ability. Subtype A infections in particular appear to elicit antibodies that recognize features of V3 that are conserved across subtypes. For example, plasma from Cameroonian patients infected with subtype A or CRF02\_AG more frequently harbored anti-V3 antibodies that were cross-reactive than did North American patients infected with subtype B (87), and two of the three cross-reactive antibodies crystallized in the former study were from Cameroonian patients (78). Nevertheless, anti-V3 specificities rarely contribute to broad neutralization despite their omnipresence. Intriguingly, in studies of subtype C South African patients, antibodies directed against the V3 domain were present in the plasma of all subjects during early infection, and were capable of binding to autologous and heterologous V3 peptides, yet these antibodies did not contribute to neutralization of autologous virus in most of the patients (20, 115). This phenomenon has been observed in subtype B infection as well (112). The ubiquitous presence of anti-V3 antibodies could suggest recognition of 'decoy' V3 epitopes exposed on defective Env forms (i.e. monomeric Env), but it is also possible that sequestration of V3 on the native, trimeric Env, prevents neutralizing activity as well (114) and structural concealment of V3 epitopes has been reported (10, 37, 115). Thus the role of the V3 domain in antibody escape remains incompletely described.

### **Consequences of viral escape**

An important question that arises from these studies of viral escape is whether there is a fitness cost to the virus by immune system evasion. One measure of

'fitness' is the ability to replicate, and viral replication can be examined in vitro in cell culture or in vivo by viral load. Drug resistance mutations in the reverse transcriptase enzyme (RT) have been shown to negatively impact viral replication in vitro (5, 133, 174), and some mutations associated with escape from the cytotoxic lymphocyte (CTL) immune response have been observed to dampen viral replication as well (17, 35, 134, 155, 170). Intriguingly, some of these escape mutations have been associated with lower viral loads in vivo (58, 123). This observation suggests that although the virus can escape and possibly gain compensatory mutations, the selective pressure of drugs or the cellular immune response can play a role in viral control, however slight. Because Env exhibits high levels of diversity, it might be hypothesized that immune escape in Env in particular would not carry a viral replication cost. It has been reported that CTL escape mutations in this region have varying effects on viral replication in vitro (170). As for the humoral arm of the immune response, its role in viral control is ambiguous as well. One study found a negative correlation between autologous titer and viral load in chronic infection, implying a role for Nabs in lowering viremia (39). Furthermore, in a South African subject, the appearance of certain autologous Nab specificities was shown to parallel a slight dip in viral load (116). In long-term non-progressors; however, no correlation between autologous Nab and viral load was found suggesting that the exquisite control exhibited by these particular subjects is not attributable to Nabs (104). To date, in vitro studies have reported different conclusions as well. There is no correlation between resistance to antibodies b12, 2G12, 2F5 and 4E10 and replication ability (136), but another group found that alanine mutations in an epitope targeted by anti-gp120 core



antibodies resulted in loss of infectivity (130). Thus, specific mutations that arise naturally during infection and confer resistance to autologous Nabs have not been examined for their effect on replication kinetics in vitro, and so the question of fitness cost remains unanswered.

Thus through a combination of steric hindrance, glycan shifts and sequence change, the virus is able to escape from potent Nabs, which may target different regions of gp120 such as V1V2 or V3, yet rarely achieve 'enough' breadth in an individual to effectively control virus during natural HIV-1 infection. The manner in which the virus escapes without crippling consequences, and how we might exploit any vulnerability in this process for vaccine design, demands close examination.

### **Summary**

In summary, because of high levels of replication, recombination and an error-prone polymerase, HIV-1 is able to generate a tremendous level of diversity. This genetic variation leads to antigenic differences amongst subtypes, a fact that has greatly hindered vaccine design. Subtype C, however, accounts for the majority of infections worldwide, and therefore, it is especially important to study.

Additionally, studying subtype C HIV-1 in the setting of natural infection and the subsequent development of the immune response may provide important insight for vaccine development.

The struggle between host and virus is actively being characterized. Within the first months of infection, people (especially with subtype C) mount a potent but

strain-specific antibody response against limited targets. It has also been shown that the virus rapidly escapes this constant immune pressure and these mechanisms of evasion are important to deduce to avoid this pitfall with a vaccine. HIV-1 has multiple pathways to escape. The glycoprotein spikes on the virion are covered by oligosaccharides forming what is commonly referred to as a 'glycan shield'. Env proteins can tolerate high levels of sequence change and they also contain five 'hypervariable' loops that can vary in length and mask epitopes. Here in chapter two, I demonstrate that conservation as opposed to sequence change of a residue in the V3 domain of subtype C Envs contributes to Nab evasion by structural masking of neutralization epitopes. This phenomenon occurs in multiple, genetically diverse subtype C Envs, suggesting that conservation of hydrophobic residues in V3 may be a feature of subtype C gp120 in general. In chapter three I closely examine the types of antibodies that comprise the early Nab response. I establish that this early Nab response in a Zambian seroconverter is composed of multiple B cell clones producing antibodies against a single conformationally complex target in V1V2. Because the Mabs are narrowly targeted, escape from these multiple antibodies is achieved by a single residue change. Although the mechanism behind this escape appears to require insertion of a potential glycan motif, I verify that it is the sequence change itself as opposed to the glycan that actually confers escape from these Mabs. Thus, in this thesis, multiple mechanisms of HIV-1 escape from Nab pressure are explored, and hopefully the conclusions can inform vaccine design.

## **Chapter Two:**

### **Subtype-specific Conservation of Isoleucine 309 in the Envelope V3 Domain is Linked to Immune Evasion in Subtype C HIV-1 Infection**

#### **I. Abstract**

The V3 region of the HIV-1 envelope (Env) glycoprotein gp120 is a key functional domain yet it exhibits distinct mutational patterns across subtypes. Here an invariant residue (Ile 309) was replaced with Leu in 7 subtype C patient-derived Envs from recent infection and 4 related neutralizing antibody escape variants that emerged later. For these 11 Envs, I309L did not alter replication in primary CD4 T cells; however, replication in monocyte-derived macrophages was enhanced. Infection of cell lines with low CD4 or CCR5 revealed that I309L enhanced utilization of CD4 but did not affect the ability to use CCR5. This CD4-enhanced phenotype tracked with sensitivity to sCD4, indicating increased exposure of the CD4 binding site. The results suggest that Ile 309 preserves a V3-mediated masking function that occludes the CD4 binding site. The findings point to an immune evasion strategy in subtype C Env to protect this vulnerable immune target.

## II. Introduction

HIV-1 group M is a collection of genetically diverse viruses that have been classified into 9 major subtypes as well as multiple circulating and unique recombinant forms (for a complete listing see <http://www.hiv.lanl.gov>). The envelope (*env*) gene is a major source of this genetic diversity, varying by approximately 10% within an individual, 20% within a subtype, and 35% between subtypes (84). The product of the *env* gene is a 160kDa polyprotein precursor that is proteolytically processed into individual subunits, gp41 and gp120, which associate non-covalently to form trimeric 'spikes' on the surface of the virion. The gp120 subunit protrudes from the virion surface, and contains the binding sites for the CD4 receptor and the coreceptors CCR5 or CXCR4. The gp120 is also the major target for neutralizing antibodies (Nab) but its genetic variability poses a significant obstacle for vaccine-induced protection (10, 61, 65, 154). Much of what is currently known about the organization of gp120 is based on crystal structures of a truncated, de-glycosylated, CD4-bound subtype B core or a truncated, glycosylated, unliganded SIV core (24, 89, 90). The structure and position of the five 'hyper-variable' domains (V1-V5) on gp120 have been difficult to determine because of their conformational flexibility; it is, therefore, not fully understood how these domains could influence the overall conformation and immunogenicity of the native protein. Consequently, the positions, inter-molecular interactions, and genetic diversity of the hyper-variable domains could lead to subtle but important structural differences, particularly between viral subtypes (56, 64, 101, 124, 145).

Of the five hyper-variable domains, V3 is relatively conserved (73) and does not exhibit the dramatic insertions, deletions, and shifts in potential N-linked glycosylation sites that are characteristic of the V1V2 and V4 domains. Perhaps this reflects that the V3 domain participates directly in coreceptor binding, which is a critical step in viral entry (21, 34, 168). Nevertheless, the amino acid sequence of V3 and its mutational pattern exhibit differences across subtypes (47, 54, 86, 124). One striking example is that subtype A and C V3 domains contain a highly conserved GPGQ amino acid motif at the crown, while GPGR is predominant in subtype B Envs (86, 158). Subtype D Envs, on the other hand, carry a mixture of residues at the R/Q position ([www.hiv.lanl.gov](http://www.hiv.lanl.gov)). The subtype B V3 domain facilitates a switch in tropism, from CCR5 to CXCR4 usage in about 50% of patients (33, 139, 156, 162), whereas CXCR4 usage among subtype C viruses is infrequent, even in advanced stage patients (26, 28, 30, 77, 117, 160). Consistent with possible functional constraints, the subtype C V3 domain exhibits less sequence variation compared to subtype B (54, 55, 86, 124, 145, 158). Even during escape from autologous Nab in subtype C HIV-1 infection, the V3 domain remains remarkably conserved amid ongoing sequence evolution in other Env regions (116, 146). It has recently been shown that distinct mutational patterns in subtype B and C lead to conformational differences as well (124). Interestingly, position 309 in V3 exhibits extreme conservation as Ile in subtype C but in subtype B, Leu, Met, and Val also occur with relative frequency (124). Thus, while lineage-specific genetic differences in the V3 domain have been firmly established, their underlying biology is not clearly understood.

Here we have begun to explore the biological basis for conservation of V3 sequence by creating an I309L substitution in a panel of eleven diverse, patient-derived subtype C Envs that includes recently transmitted viruses and defined autologous Nab escape variants. We evaluated changes in both function and antigenicity of the wildtype and mutated Envs and uncovered evidence suggesting that in subtype C, I309 participates in immune evasion by masking the CD4bs and possibly other vulnerable sites, even though this residue is not critical for interactions with CCR5.

### III. Materials and Methods

**Env clones.** Details of the ZEHRP cohort, sample collection, and processing have been described previously (41, 108, 166). The Envs studied here were derived from seven newly infected subjects from this cohort (185F, 153M, 205F, 221M, 109F, 106F, and 55F). The Emory University Institutional Review Board, and the University of Zambia School of Medicine Research Ethics Committee approved informed consent and human subjects protocols. None of the subjects received antiretroviral therapy during the evaluation period. PCR amplification and cloning of the Envs has been described (41, 67, 146). The env genes were cloned into one of the CMV-driven expression plasmids pCR3.1 or pcDNA 3.1/V5-His TOPO (Invitrogen), which were then used to generate viral pseudotypes. All Envs were derived from plasma or PBMC DNA according to protocols previously described (92) and are subtype C. Nucleotide sequences (either V1-V4 or full-length) have been deposited into Genbank under the following accession numbers: 55 FPB4a AY423973, 106 FPB9 AY424163, 109 FPB32 AY424141, 205FPB 12MAY05ENV5.1 GQ485442, 205FPL27MAR03ENV5.2 GQ485418, 185FPL 10JUL04ENV1.1 GQ485388, 185FPB 24AUG02 ENV3.1 GQ 485314, 153MPL 13MAR02 ENV5.1 HM068596, 153MPL 13MAR04 ENV4.1 HM068597, 221MPL 7MAR03 ENV2.1 HM068598, 221MPL 26FEB05 ENV3.1 HM068599. All amino acid positions are based on HXB2 gp160 numbering.

**PCR-based site mutagenesis.** To generate I309L mutations, PCR-directed site mutagenesis was performed using two overlapping primers that contained

the mutated sequence for each Env using a strategy similar to that described in (144). Briefly, each *env* gene (plus Rev and partial Nef coding sequences) was amplified using primer sequences similar to the following, which were used with 185F o-Month EnvPB3.1 (substituted nucleotide is underlined and HXB2 locations are provided): 7124-7162 (5'-CAA TAA TAC AAG GAA AAG TGT GAG ACT AGG ACC-3') and 7134-7167 (5'-GTC CTG GTC CTA GTC TCA CAC TTT TCC-3'). The amplification conditions were: 1 cycle of 95°C for 30 sec.; 18 cycles of 95°C for 30 sec.; 45°C for 1 min. (optimal annealing temperature was determined for each primer set), and 68°C for 9 min.; storage at 4°C. The 50 µl PCR reactions contained 100ng of each primer, 10 ng of the plasmid template, 0.2 mM dNTP, and 1X reaction buffer. PfuUltra II Fusion Hotstart DNA polymerase (Stratagene) was used to generate the PCR amplicons, which were digested with DpnI to remove contaminating template DNA, and then transformed into maximum efficiency XL2-Blue ultracompetent cells (>5 x 10<sup>9</sup> cfu/µg DNA; Stratagene) so that the DNA volume did not exceed 5% of the cell volume. The entire transformation was plated onto LB-Ampicillin agar plates, generally resulting in 10 to 50 colonies.

Colonies were inoculated into LB-Ampicillin broth for overnight cultures and the plasmid was prepared using the QIAprep Spin Miniprep Kit. Each plasmid was screened for biological function as previously described (41, 92). Briefly, 600 ng of Env DNA was co-transfected into 293T cells along with 1200 ng of an Env-deficient subtype B proviral plasmid, pSG3ΔEnv, using Fugene-6 according to the manufacturer's instructions (Hoffman-La Roche). Seventy-two hours later, the



transfection supernatant was transferred to JC53-BL (TZM-bl) indicator cells. At 48 hours post-infection, each well was scored positive or negative for blue foci using b-gal staining. For clones that produced functional Env pseudotypes, the plasmids were re-transfected into 293T cells on a larger scale to produce a working pseudotype virus stock. Transfection supernatants were collected at 48 hours post-transfection, clarified by low speed centrifugation for 20 minutes, aliquoted into 0.5 ml or less portions, and stored at  $-80^{\circ}\text{C}$ . The titer of each pseudotyped virus stock was determined by infecting JC53-BL cells with 5-fold serial dilutions of virus as described previously (41, 92). All *env* sequences were confirmed by nucleotide sequencing.

**Virus neutralization and inhibition assays.** Neutralization assays using sCD4, monoclonal 17b, and a pool of anti-V3 monoclonal antibodies derived from subtype C infected Indian patients were performed using viral pseudotypes to infect JC53-BL (Tzm-bl) indicator cells using a luciferase readout as described previously (41, 92, 144-146). A human IgG isotype control was used in all monoclonal antibody experiments. Briefly, 2000 IU of pseudovirus was incubated for 1 hour in DMEM + 10% FBS (Hyclone) + 40 $\mu\text{g}/\text{ml}$  DEAE-Dextran with serial dilutions of sCD4 or monoclonal antibody and 100 $\mu\text{l}$  was then added to the indicator cells for a 48 hour infection before being lysed and evaluated for luciferase activity. To pre-trigger Envs, the pseudovirus was incubated for one hour with either its  $\text{IC}_{50}$  of sCD4 or 100nM sCD4 if 50% inhibition was not achieved. After incubation for another hour with serial dilutions of 17b, 100 $\mu\text{l}$  of sCD4-17b-virus was added to JC-53BL cells for a 48 hour infection. The 17b

monoclonal antibody (contributed by Dr. James Robinson) (163) and sCD4-183 (2-domain) (contributed by Progenics Pharmaceuticals) (53) were obtained from the NIH AIDS Research and Reference and Reagent Program, Division of AIDS, NIAID, NIH. The anti-CD4 antibody B13.8.2 was kindly provided by Dr. Quentin Sattentau (University of Oxford) (152). A pool of three monoclonal antibodies against the V3 domain isolated from Indian patients infected with subtype C viruses was contributed by Dr. Susan Zolla-Pazner.

**Replication in CD4 and monocyte-derived macrophages (MDM) using an NL4.3 proviral cassette.** A panel of Envs was subcloned into a replication competent NL4.3 backbone that has been described previously (98, 121). This system is amenable to accepting diverse *env* genes, and facilitates substitution of virtually the entire coding region (only 36 and 6 amino acids at the N and C terminus respectively are derived from NL4.3). We have previously shown that patient-derived Envs retain their entry phenotype in comparison with the primary isolate, indicating that the NL4.3 backbone is neutral to Env entry properties (121). Peripheral blood mononuclear cells (PBMC) were isolated from the whole blood of a normal, seronegative donor by ficoll-hypaque centrifugation. CD8-depleted PBMC cultures were prepared by negative selection using Dynabeads (Invitrogen). The CD4-enriched PBMC were cultured in complete RPMI for 3 days in the presence of 3mg/ml phytohemagglutinin (PHA) for activation prior to infection. Infected cultures were maintained in complete RPMI supplemented with 30 U/ml recombinant human IL-2 (Roche) for up to 10 days. Every two days, 200 $\mu$ l of supernatant was collected for p24 analysis

(Perkin-Elmer), and this volume was replaced with fresh complete media with IL-2. MDM were prepared from whole blood as described in (148). Briefly,  $3 \times 10^6$  PBMC per well were subject to adherence for 2 hours in a 24-well plate, and non-adherent cells were aspirated off. The remaining cells were incubated in DMEM with 10% Giant Tumor Cell-Conditioned Media (GCT) (Irvine Scientific), 10% Human AB Serum (Sigma) and 50ng/ml recombinant human Macrophage Colony-Stimulating Factor (rhMCSF) (R&D Systems). After 3 days, the cells were washed 3 times with PBS and media was replaced with 800 $\mu$ l of Macrophage media (DMEM + 10% FBS (Hyclone) + 10% GCT + 50ng/ml rhMCSF). On day 6, 100,000 IU of virus was added in 300 $\mu$ l serum-free DMEM for 2 hours, and 500 $\mu$ l of Macrophage media was added for overnight infection. Every 3 days for 13 days after infection, 250 $\mu$ l of supernatant was collected for p24 analysis, and 1.5 ml of media was removed and then replaced with fresh media. Subtype B Envs NL4.3 and YU-2 and subtype C Env MJ-4 were cloned into the NL4.3 backbone and used as controls for these experiments. The infectious subtype C proviral clone MJ4 (contributed by Drs. Thumbi Ndung'u, Boris Renjifo, and Max Essex) (119) was obtained from the NIH AIDS Research and Reference and Reagent Program, Division of AIDS, NIAID, NIH.

**Receptor-dependent pseudovirus entry assay.** Pseudovirus entry assays were performed as described above except that a panel of HeLa cells (provided by Drs. Emily Platt and David Kabat, Oregon Health and Science University) stably transduced to express varying levels CD4 and CCR5 were used instead of JC53-BL cells and the Env-deficient subtype B proviral plasmid pNL4.3 $\Delta$ Env, kindly

provided by Dr. Ron Collman, expressing a luciferase reporter gene was used instead of pSG3DEnv (which does not express a reporter gene) (79, 132). Briefly, transfection supernatants were normalized to p24 and equivalent amounts were added per well in each experiment to infect each cell line. The cell lines used were JC.53 ( $1.5 \times 10^5$  CD4 and  $1.3 \times 10^5$  CCR5 molecules/cell), JC.10 ( $1.5 \times 10^5$  CD4 and  $2.0 \times 10^3$  CCR5 molecules/cell) and RC.49 ( $1.0 \times 10^4$  CD4 and  $8.5 \times 10^4$  CCR5 molecules/cell).

**Statistical analysis.** To compare groups, a non-parametric Wilcoxon signed rank test was used for paired comparisons. All analyses were performed using a two-tailed p-value in Graphpad Prism 4.0c, and p-values  $\leq 0.05$  were considered statistically significant.

## IV. Results

### **I309L was created in a representative panel of diverse subtype C**

**Envs.** The major goal of this study was to investigate the biological effects of mutating Ile 309 in Envs of HIV-1 subtype C, in which this residue is 99% conserved. We chose Leu because this amino acid occurs naturally, albeit in less than 1% of subtype C Envs, and has been associated with structural changes in V3 (158). We therefore selected a panel of seven Envs that were each cloned during acute/early infection from a different subject enrolled in the Zambia-Emory HIV Research Project (Table 1). The newly transmitted Envs were cloned within 129 days of the last seronegative test, with Envs from 185F, 221M, and 205F being within an estimated 48 days of infection. To broaden the relevance of this study, we also included four Envs cloned at a time point between 23 and 25 months after infection that had developed resistance against the contemporaneous autologous neutralizing antibody (Nab) pool ((146) and data not shown) (Table 1). These later Envs allowed us to evaluate the effects of the I309L mutation specifically within Envs known to have adapted to Nab immune pressure during natural infection. Supplemental Fig. 1 demonstrates that all of the Envs cluster phylogenetically as subtype C, and that their genetic diversity is representative of subtype C variants circulating across multiple geographic regions. This figure also shows that the newly transmitted Envs from subjects 205F, 153M, 185F, and 221M each cluster with the Nab escape variant from the same patient. The I309L mutation was created in the V3 domain of each of the 11 Envs (Fig. 1) and used in the biological studies described in the following sections.

Table 1.

| Subject ID | Sample date | SGA <sup>a</sup> | Days since seronegative | Estimated days since infection | Nab escape variants |
|------------|-------------|------------------|-------------------------|--------------------------------|---------------------|
| 106F       | 8-Jun-98    | no               | 129                     | ND <sup>b</sup>                | NT <sup>c</sup>     |
| 55F        | 13-Aug-98   | no               | 90                      | ND                             | NT                  |
| 109F       | 16-Mar-00   | no               | 96                      | ND                             | NT                  |
| 153M       | 13-Mar-02   | yes              | 88                      | ND                             | 24-months           |
| 185F       | 17-Aug-02   | yes              | 11                      | 33                             | 23-months           |
| 221M       | 7-Mar-03    | yes              | 100                     | 31                             | 23-months           |
| 205F       | 27-Mar-03   | yes              | 26                      | 48                             | 25-months           |

<sup>a</sup>Single Genome Amplification

<sup>b</sup>Not determined

<sup>c</sup>Not tested

| CONSENSUS | SUBTYPE C         | CTRPNNNTRK | SIRIGPGQTF | YATGDIIGDI | RQAHC |
|-----------|-------------------|------------|------------|------------|-------|
| 109F      | 0-Month EnvPB32   | -I--G----- | ---        | -----V---- | -K-Y- |
| 106F      | 0-Month EnvPB9    | -----      | ---        | -----E---- | -K-Y- |
| 55F       | 0-Month EnvPB4a   | -----      | -M-----    | -----      | ----- |
| 185F      | 0-Month EnvPB3.1  | -V-----    | -V-----    | -----E---- | ---Y- |
| 185F      | 23-Month EnvPL1.1 | -V-----    | -V-----    | -----G---- | ---Y- |
| 153M      | 0-Month EnvPL5.1  | -V-----    | -V-----    | -----A---- | -K--- |
| 153M      | 24-Month EnvPL4.1 | -V-----    | -V-----    | -----      | -K--- |
| 205F      | 0-Month EnvPL5.2  | -----SR    | G-----     | F---R---N- | ---Y- |
| 205F      | 25-Month EnvPB5.1 | -----SR    | G-----     | F---R----- | ---Y- |
| 221M      | 0-Month EnvPL2.1  | -----      | ---        | ---DG---N- | ----- |
| 221M      | 23-Month EnvPL3.1 | -----      | ---        | ---DG---N- | ----- |

**Figure 1. Alignment of V3 sequences from subject Envs.**

Amino acid sequences of the V3 domain from the 11 patient-derived Envs used in the mutagenesis experiments were aligned using SeqPublish (Los Alamos Database) and are shown in comparison to the consensus sequence for subtype C. The 7 Envs from an acute/early time point of infection are shown in red and the four Nab escape variants from a longitudinal time point two years post-infection are shown in blue. The consensus subtype C sequence is shown in black. Dashes indicate residues that are the same as the subtype C consensus sequence. A green box designates the I309 residue that was mutated to an L309 in each Env using site-directed mutagenesis.

**The I309L mutation does not decrease replication in primary CD4 T cells.** Purifying selection imposed upon I309 could indicate that changes at this position are not tolerated because they decrease replication capacity. We therefore evaluated whether the I309L change would be detrimental to replication in activated CD4 T cells. Ten of the eleven Envs, with and without I309L, were transferred into a replication competent NL4.3 proviral backbone and used to infect PBMC enriched for CD4 T cells by CD8 depletion. A replication competent virus containing 185F 23-month EnvPL1.1 could not be generated using this system due to internal restriction sites. Supernatant was collected every two days and viral p24 was quantified for a measure of viral replication (Fig. 2A and Suppl. Fig. 2). The subtype C provirus MJ4 was used as a positive control for replication in CD4 T cells (119).

The acute/early subtype C Envs mediated replication with variable magnitude and kinetics, but day 10 represented the peak p24 level for the majority of the subtype C Envs (Fig 2A and Suppl. Fig. 2). Therefore, this time point was used to compare the overall replication between paired sets of wildtype and I309L mutant Envs. Each wildtype Env and its I309L mutant displayed comparable replication kinetics and p24 levels (Fig 2A and Suppl. Fig. 2), and there was no statistical difference in day 10 p24 levels between of the two groups (Fig. 2B). To ensure that the I309L mutation had not reverted, the V3 domain of each mutant virus was sequenced using virion-associated RNA in supernatant collected at day 10 during one experiment (data not shown). This result demonstrates that I309L-containing Envs are replication competent in activated CD4 T cells, and suggests



that the strong conservation of I309 is not due to a detrimental effect on viral replication, at least as measured by this *in vitro* assay.

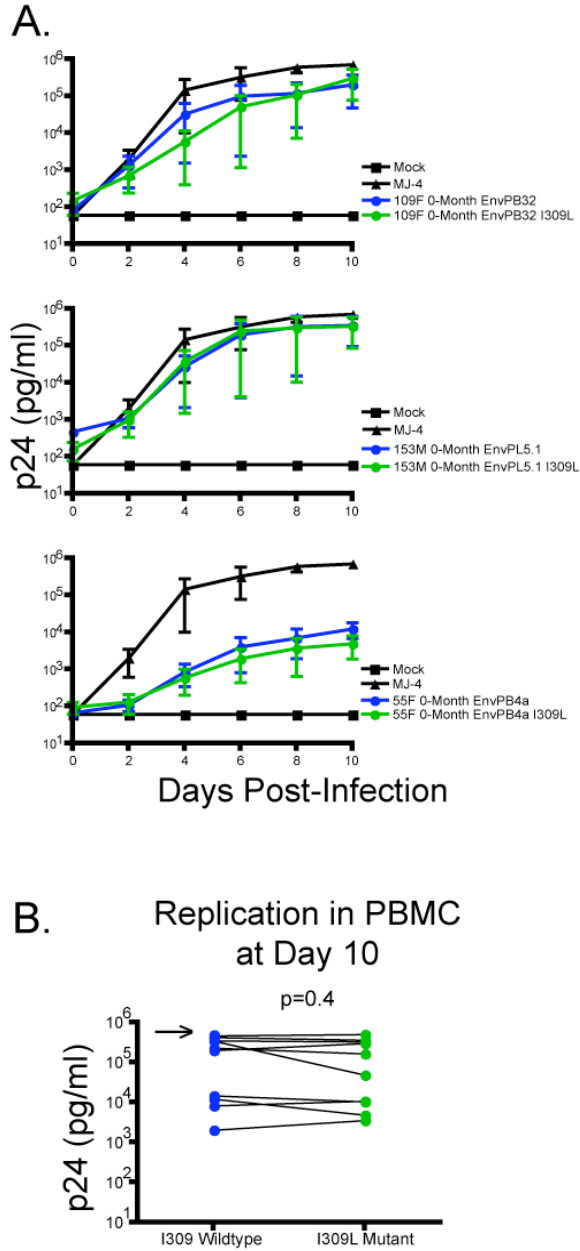


**Figure 2. Replication of virus containing a wildtype and I309L mutated Envs in PBMC.**

10 wildtype and 10 I309L mutated Envs were placed into a replication competent NL4.3 backbone and used to infect CD8-depleted human PBMC; representative graphs of 3 of these pairs are shown in panel (A). Viral p24 antigen production in the supernatant was measured by ELISA and is plotted (pg/ml) on the vertical

axis on a log<sub>10</sub> scale while days post infection are on the horizontal axis. Mock-infected (squares) and positive control virus NL4.3 (triangles) are shown in black. Wildtype Envs are blue and I309L mutant Envs are green. The error bars represent two independent experiments using two different donors. Total p24 at day 10 of infection is shown as a dot plot (B). The residue at position 309 is indicated on the horizontal axis, and a comparison of p24 antigen levels between I309 Envs (blue) and L309 (green) Envs was performed using Graphpad Prism. Each dot represents the mean p24 for one Env. The p-value was determined using a paired Wilcoxon test. The p24 level for the positive control virus NL4.3 is represented by a black arrow.

**The I309L mutation leads to a moderate enhancement of replication in monocyte-derived macrophages.** In addition to CD4 T cells, human monocyte-derived macrophages (MDM) can also serve as a target cell for HIV-1 *in vivo*. We therefore evaluated whether I309L altered *in vitro* replication in MDM cultures. For these experiments, the subtype B Env YU-2 was used as a positive control for replication in MDM, and NL4.3 was used as a negative control (Fig 3A and Suppl. Fig. 3) (94). None of the subtype C Envs replicated as efficiently as the 'control' strain YU-2, which is consistent with our previous finding that subtype C Envs, while CCR5-tropic, do not infect MDM with high efficiency (77). Nevertheless, using p24 level at day 13 post-infection for comparison, the I309L Envs overall replicated to moderately higher levels than their wildtype counterparts (Fig. 3B;  $p=0.02$ ). This enhanced ability to replicate in MDM cultures could be linked to augmented usage of low amounts of CD4 found on these cells, as compared to levels found on T-cells (7, 32, 45, 164).

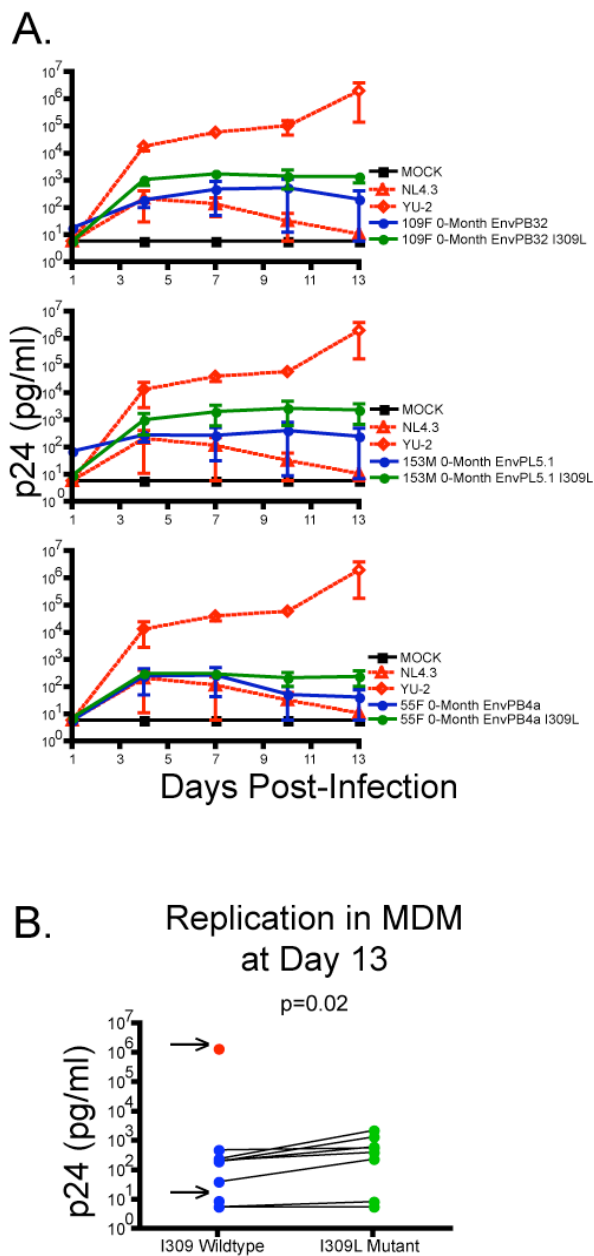


**Figure 3. Replication of I309 and I309L Env viruses in MDM.**

10 wildtype and 10 I309L mutated Envs were placed into a replication competent NL4.3 backbone and used to infect MDM; representative graphs of 3 of these pairs are shown in panel (A). Viral p24 antigen production in the supernatant was measured by ELISA and is plotted (pg/ml) on the vertical axis on a log<sub>10</sub> scale while days post infection are on the horizontal axis. Mock-infected is shown

in black squares, negative control virus NL4.3 (triangles) and positive control virus YU-2 (diamonds) are shown in red, wildtype I309 Envs are blue and I309L mutant Envs are green. The error bars represent two independent experiments from two different donors. Total p24 at day 13 of infection is shown as a dot plot (B). The residue at position 309 is indicated on the horizontal axis, and a comparison of p24 antigen levels between I309 Envs (blue) and L309 (green) Envs was performed using Graphpad Prism. Each dot represents the mean p24 for one Env. The p-value was determined using a paired Wilcoxon test. The p24 level for the positive control viruses YU-2 (shown as a red dot) and the negative control virus NL4.3 are represented by black arrows.

### **The I309L mutation confers increased entry into a cell line**

**expressing low CD4.** We next investigated whether differences in infection efficiency would be observed in HeLa-based cell lines that express known quantities of CD4 and CCR5. JC.53 cells, which express high levels of CCR5 and CD4, were used to determine relative infectivity in two different cell lines: JC.10, which express low CCR5/high CD4, and RC.49, which express high CCR5/low CD4 (see methods) (132). These cell lines were infected with pseudoviruses created by expressing the wildtype or I309L mutant Envs with an HIV-1 *env*-deficient backbone that encodes luciferase. Under the condition of high CD4 and limited CCR5, there was no statistically significant difference between the wildtype and I309L Envs in ability to enter the JC.10 cells (Fig 4A). There was one pair of Envs from subject 221 for which the I309L did appear to decrease infectivity, although this effect may be due to an inherent property of the V3 loop (perhaps the D321, see Fig. 1) in these two Envs. Overall, however, infectivity of JC.10 cells was decreased by approximately 10-fold for all Envs, compared to the JC.53 cells (high CCR5, high CD4), suggesting that the wildtype and I309L Envs were equally dependent on CCR5 for entry into JC.10 cells. Dependence on CCR5 was confirmed using the HI-J cell line, which expresses CD4 and endogenous CXCR4 but no CCR5 (data not shown). When CD4 levels were reduced, however, the I309L containing Envs consistently had higher relative infectivity in the RC.49 cells, ranging from a 1.1- to an 18.6-fold increase over the matched wildtype Env (Fig. 4B;  $p=0.003$ ). It should be noted that the infectivity of all Envs for RC.49 cells was generally about 1% of that achieved on the JC.53 cells. Thus, all of the Envs were highly dependent on CD4 levels, consistent with other

studies by our group using patient-derived subtype C Envs from acute/early and chronic infection (3). The I309L mutation did not, therefore, “pre-trigger” the coreceptor binding domain, leading to CD4 independence, as has been described for subtype B Envs carrying non-consensus residues at position 309 (38, 186). Thus, although both I309L and wildtype Envs were inefficient at infecting cells with limiting levels of CD4, the I309L Envs consistently had higher relative infectivity, suggesting more efficient binding to CD4 and/or increased exposure of the CD4bs.



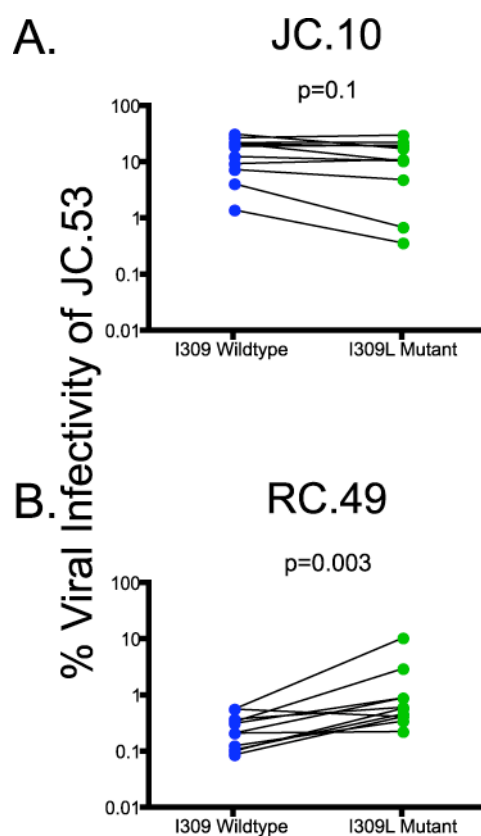


**Figure 4. Lower dependence on CD4 but not CCR5 levels for entry by I309L Envs.**

The infectivity of the 11 wildtype and 11 I309L mutated pseudotyped Envs were measured in HeLa cell-lines JC.10 with high CD4 and low CCR5 (A) and RC.49 expressing low CD4 and high CCR5 (B). The relative infectivity compared to JC.53 cells, which express high CD4 and high CCR5, was determined by provirally-encoded luciferase and is shown on the vertical axis. The I309 wildtype Envs are blue while the I309L mutated Envs are green. Each point represents the mean relative infectivity of an individual Env pseudovirus from 2 independent experiments. A paired Wilcoxon test was used to determine the p-value.

**The I309L mutation confers increased sensitivity to sCD4.** Patient-derived virus Envs are typically resistant to inhibition by the soluble form of the CD4 receptor, sCD4, reflecting the cryptic nature of the CD4 binding site (CD4bs) (6, 20, 36, 111, 113, 135, 178, 182). However, the ability to infect MDM and RC.49 cells has been associated with increased sensitivity to sCD4 inhibition (45, 127, 128). Fig. 5 demonstrates that all of the wildtype Envs were relatively resistant to sCD4 out to 100 nM in a single round pseudovirus assay. The I309L substitution, however, led to an almost universal increase in sCD4 sensitivity, although the magnitude varied between Envs (Fig 5A). For 9 of the 11 Envs, I309L resulted in an increase in sensitivity compared against wildtype at the highest concentration of sCD4 (100nM). Overall, viral infectivity was significantly lower with the I309L mutation at both 100nM and 20nM concentrations of sCD4 (Fig. 5B;  $p=0.001$  and  $p=0.005$ , respectively), suggesting a consistent increase in exposure of the CD4bs in the mutant Envs as compared to the wildtype Envs. Binding to CD4 was further assessed by incubating the pseudotyped Envs with an anti-CD4 monoclonal antibody B13.8.2, and subsequently calculating the concentration of antibody necessary to reduce viral infectivity by 50% (IC<sub>50</sub>). The I309L Envs required higher concentrations of anti-CD4 to inhibit infection (with a higher IC<sub>50</sub>) than wildtype, confirming their more efficient utilization of the CD4 receptor (Fig. 5C;  $p=0.01$ ).

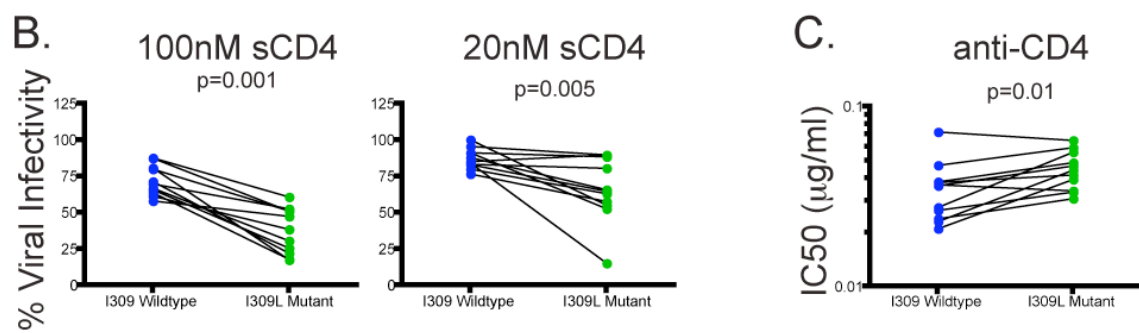
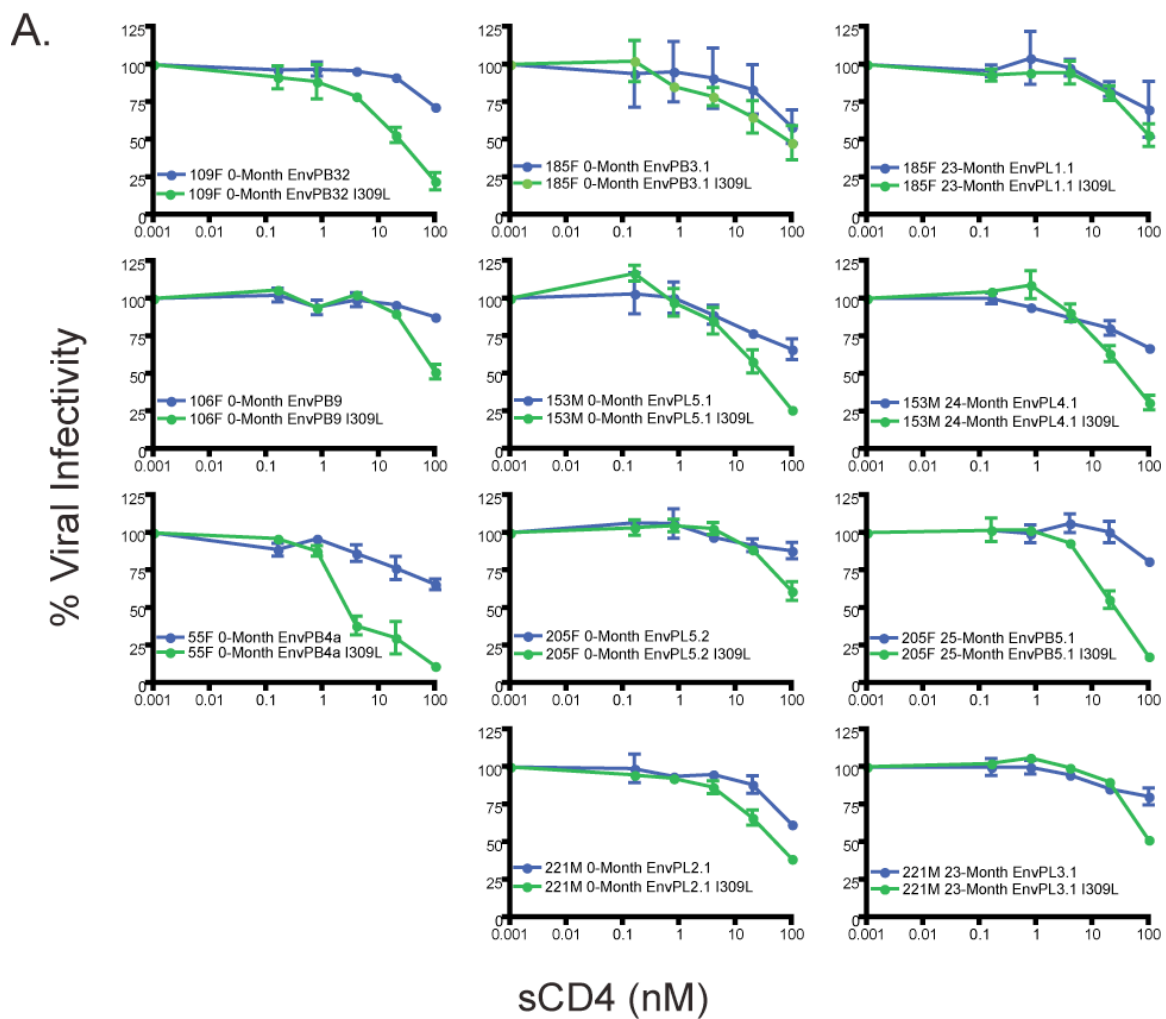


**Figure 5. I309L mutation increases sCD4 sensitivity in multiple subtype C Envs.**

The parent and wildtype Envs were assessed for sensitivity to sCD4 using pseudoviruses (A). Mutant I309L Envs are shown by green lines and wildtype Envs are shown by blue lines. Each line on the graph represents an individual Env pseudovirus. Percent viral infectivity compared to no sCD4 is shown on the vertical axis and was calculated from luciferase units by dividing virus-infected wells in the presence of inhibitor by the virus-infected well in the absence of inhibitor. The concentration of sCD4 (in nanomolar) is plotted on the horizontal axis on a log<sub>10</sub> scale. Error bars represent the standard error of the mean of at least 2 independent experiments. Vertical point plots of the mean percent viral infectivity for each Env pseudovirus at 100nM and 20 nM sCD4 respectively were generated using Graphpad Prism (B) while the IC<sub>50</sub> (μg/ml) of pseudovirus in the presence of anti-CD4 binding antibody B13.8.2 is shown in (C). I309 Envs in blue were compared to L309 Envs in green. A paired Wilcoxon test was performed to determine the p-value.

**The I309L mutation moderately increased sensitivity to monoclonal antibodies directed against V3 and a CD4-induced epitope.** If I309L induces conformationally based changes in gp120 that increase exposure of the CD4bs, we hypothesized that other Env domains could also be affected. Patient derived Envs, and in particular those of subtype C, are typically refractory to neutralization by anti-V3 antibodies (11, 37, 82, 115, 148, 181). Therefore, a pool of three anti-V3 directed monoclonal antibodies from Indian patients infected with subtype C viruses were used to assess changes in susceptibility to V3-targeted neutralization. In 6 of the 11 Envs, there was an increase in sensitivity to anti-V3 mediated neutralization with the I309L mutation (Fig. 6A), suggesting a local unmasking of the V3 domain. Taken as a whole, when infectivity at the highest concentration of antibody (10 $\mu$ g/ml) was compared in a pairwise manner, there was a statistically significant difference between wildtype and mutant Envs (Fig. 6B;  $p=0.04$ ).

We next investigated whether the I309L Envs were also more susceptible to sCD4-triggering of the coreceptor binding site, which contains an epitope recognized by the monoclonal antibody 17b (163). The Envs were pre-incubated with their IC<sub>50</sub> of sCD4, or 100nM if an IC<sub>50</sub> was not determined, and then neutralization by 17b was evaluated. Four of the 11 Envs showed a moderate increase in neutralization sensitivity to 17b after incubation with sCD4 (Fig. 7A). Overall the difference between the wildtype and I309L Envs reached the borderline of statistical significance in a paired analysis (Fig. 7B;  $p=0.05$ ),

suggesting that this mutation did also affect efficiency with which the coreceptor binding site was formed, albeit in a context dependent manner.

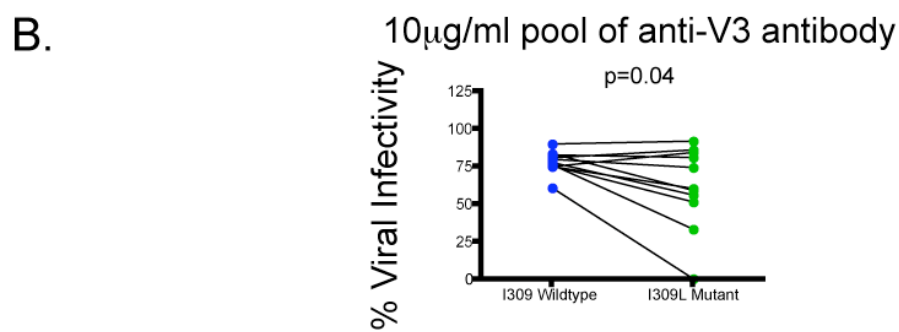
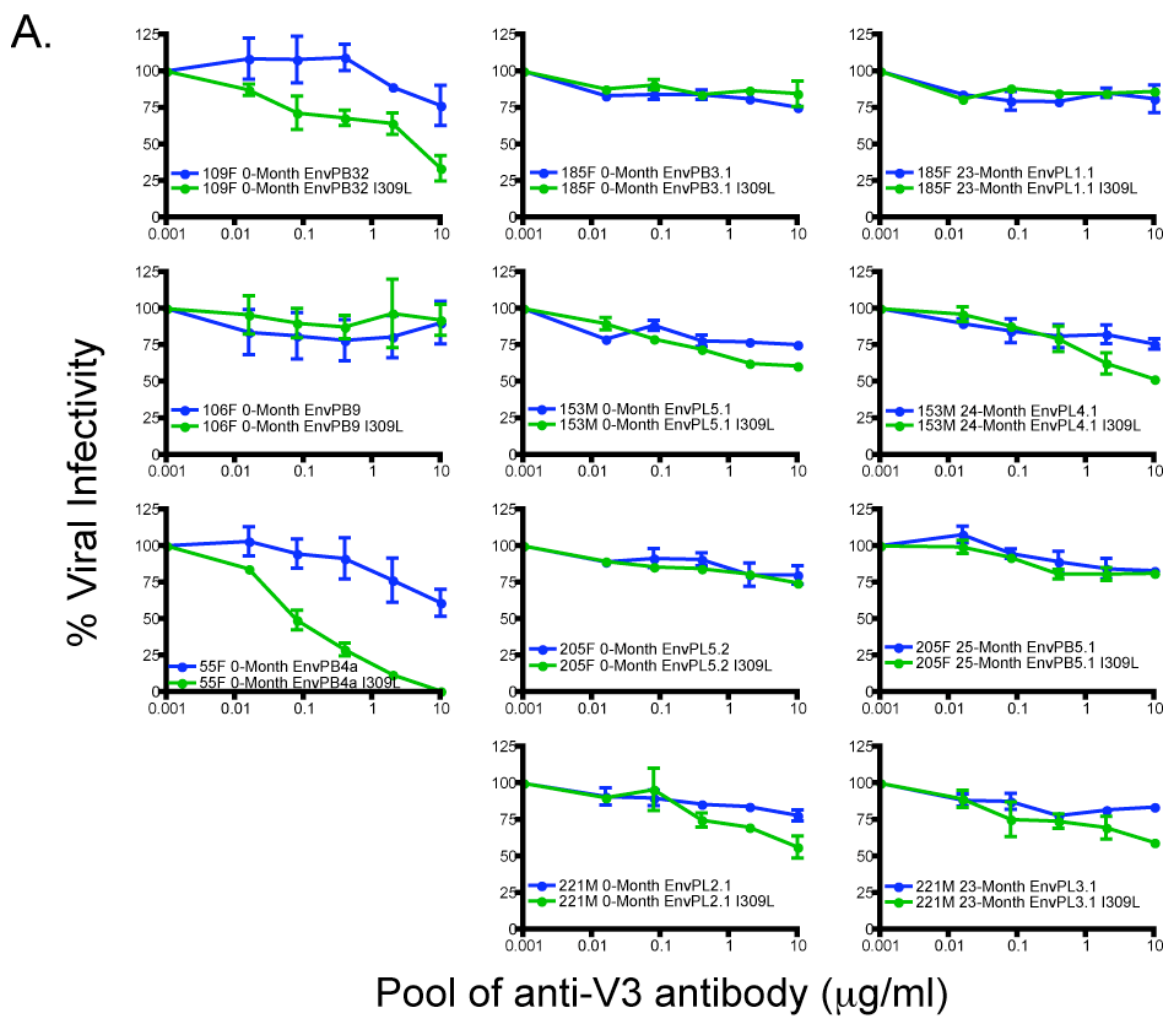


**Figure 6. I309L increases neutralization by anti-V3 antibodies.**

Neutralization sensitivity to a pool of three monoclonal antibodies against V3 derived from subtype C infected subjects in India was assessed for each mutant I309L and wildtype Env (A). The data is shown as the percent viral infectivity (luciferase units in the presence of antibody divided by in the presence of control anti-parvovirus antibody) on the y-axis. The concentration of the monoclonal antibodies is shown on the x-axis on a log-10 scale. Mutant I309L Envs are shown by green lines and wildtype Envs are shown by blue lines. Each line on the graph represents an individual Env pseudovirus. Error bars represent the standard error of the mean of at least 2 independent experiments. A vertical point plot of the mean percent viral infectivity at 10 $\mu$ g/ml of the monoclonal pool was generated using Graphpad Prism (B). I309 Envs in blue were compared to L309 Envs in green. A paired Wilcoxon test was performed to generate the p-value shown.



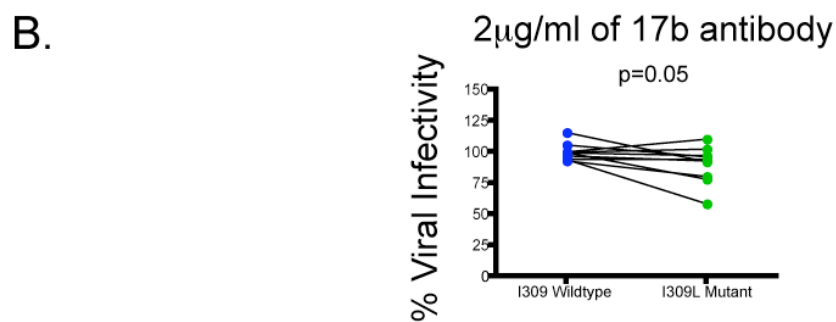
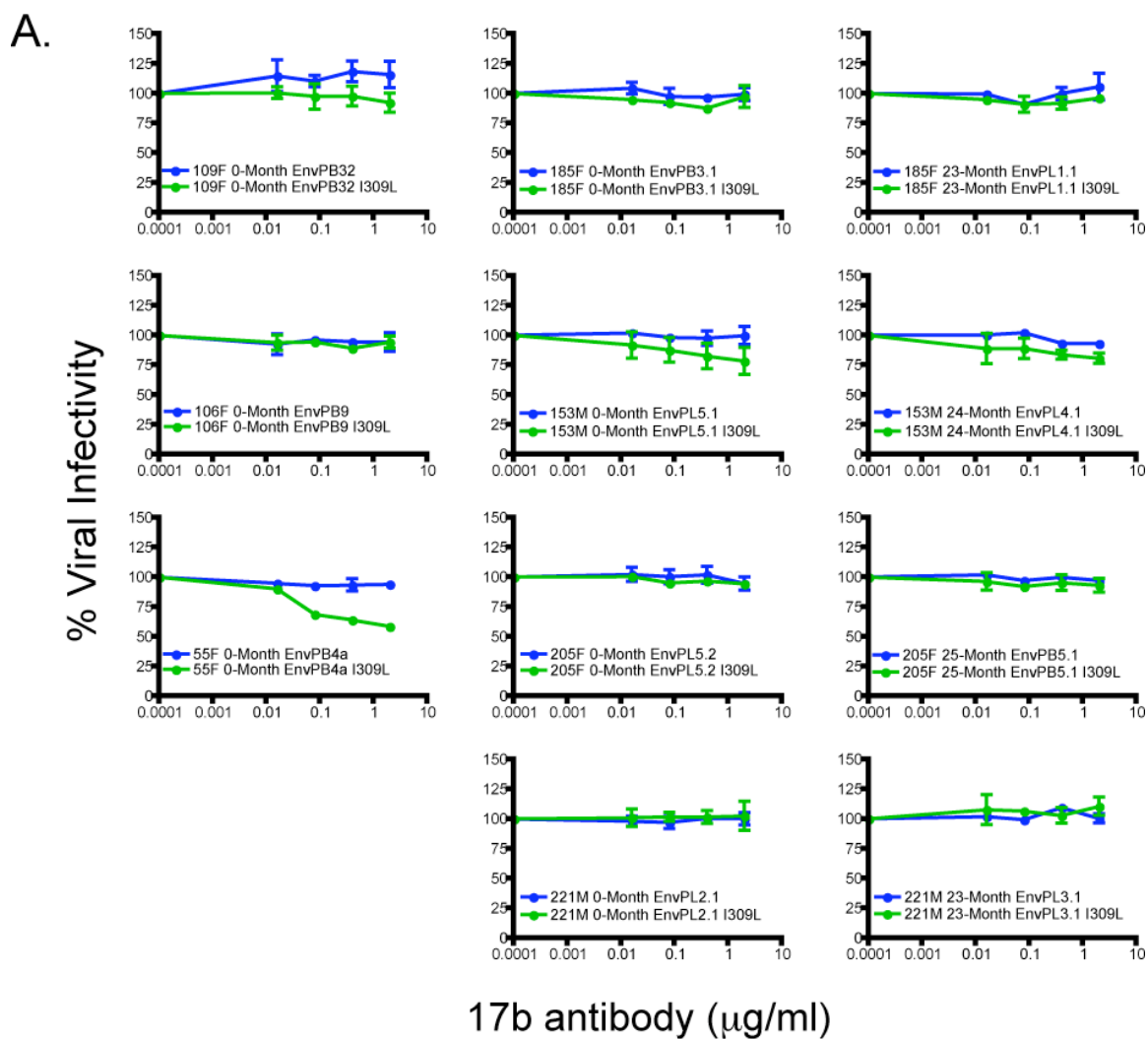


**Figure 7. I309L slightly increases neutralization of pre-triggered Envs by an anti-coreceptor binding site antibody 17b.**

Mutant I309L and wildtype Envs pseudoviruses were incubated with their cognate IC<sub>50</sub> nM of sCD4 (100nM of sCD4 if 50% inhibition was never reached), and then neutralization sensitivity was assessed by monoclonal antibody 17b (A). The data is shown as the percent viral infectivity (luciferase units in the presence of antibody divided by in the presence of control anti-parvovirus antibody) on the y-axis. The concentration of 17b is shown on the x-axis on a log-10 scale. Mutant I309L Envs are shown by green lines and wildtype Envs are shown by blue lines. Each line on the graph represents an individual Env pseudovirus. Error bars represent the standard error of the mean of at least 2 independent experiments. A vertical point plot of the mean percent viral infectivity at 2 $\mu$ g/ml of 17b was generated using Graphpad Prism (B). Wildtype Envs in blue were compared to I309L Envs in green while the mean infectivity for each group is represented by the black horizontal line. A paired Wilcoxon test was performed to generate the p-value shown.

## V. Discussion

In sequences representative of established infection, the subtype C V3 domain is more conserved than other subtypes. Consistent with this observation, we recently demonstrated that V3 remained remarkably conserved during the first two years of infection despite increasing sequence variation in V1V2, the gp120 outer domain, and gp41 (146). In the present study, we investigated the underlying biological basis for the conservation of V3 by focusing specifically on a residue that can exhibit high entropy in subtypes other than C. While this and other subtype-specific mutational patterns in V3 have been well established (54, 55, 86, 124, 145, 158), this study is among the first to delve into the biology that drives these observations.

**Replication is not dependent on conservation of I309.** As Ile is the highly conserved consensus residue for position 309 in subtype C, we evaluated whether a conservative substitution of Leu would lead to any defect reflected in the capacity for *in vitro* replication. Replication and spread in two primary target cells, CD4 T cells and MDM, was not overtly reduced by the I309L substitution. Although, it should be noted that we could not rule out subtle differences in replication kinetics between the wildtype and I309L mutants that might have been evident in a more sensitive growth competition assay. Overall, the subtype C Envs replicated to higher levels in CD4 T cells compared to MDM, suggesting that none of the wildtype Envs were inherently macrophage-tropic. This finding is consistent with our previous results in which subtype C Envs from recently and chronically infected subjects mediated single round infection of MDM much less

efficiently than CD4 T cells (77). Low efficiency replication in MDM compared to CD4 T cells has been attributed to an inability of patient-derived Envs to utilize the low CD4 levels expressed by MDM (7, 32, 45, 164). The moderate enhancement of replication in MDM when I309L was present suggests that this mutation could have altered the viral interaction with CD4. Indeed, a majority of the I309L mutant Envs more efficiently infected a cell line expressing a low level of CD4, focusing the effects of the mutation on utilization of CD4. Taken together, these results suggest that subtype-specific conservation of I309 is not driven by a detrimental effect on replication in CD4 T cells or MDM. Rather, this finding is consistent with the idea that Env residues that are critical for viral entry, like the GPG motif in V3, are conserved across all subtypes (49). Thus, subtype-specific conservation of I309 is more likely driven by properties that differ between subtypes, such as the antigenic nature of V3 and other Env regions.

**Conservation of I309 prevents exposure of neutralization targets.**

sCD4 sensitivity was used in this study as a surrogate for exposure of the CD4bs, and all but two Envs (both from subject 185F) became more sensitive to sCD4 when I309L was introduced. This finding supports the idea that V3, specifically I309, modulates exposure of the CD4bs, and is consistent with data from other studies (2, 76, 101, 183). Increased exposure of the CD4bs does not necessarily indicate that these Envs would be more sensitive to CD4bs-directed antibodies, however, a monoclonal targeting this region and capable of neutralizing these subtype C Envs was not available to test this hypothesis. However, increased sCD4 sensitivity was consistently observed, and this was accompanied by

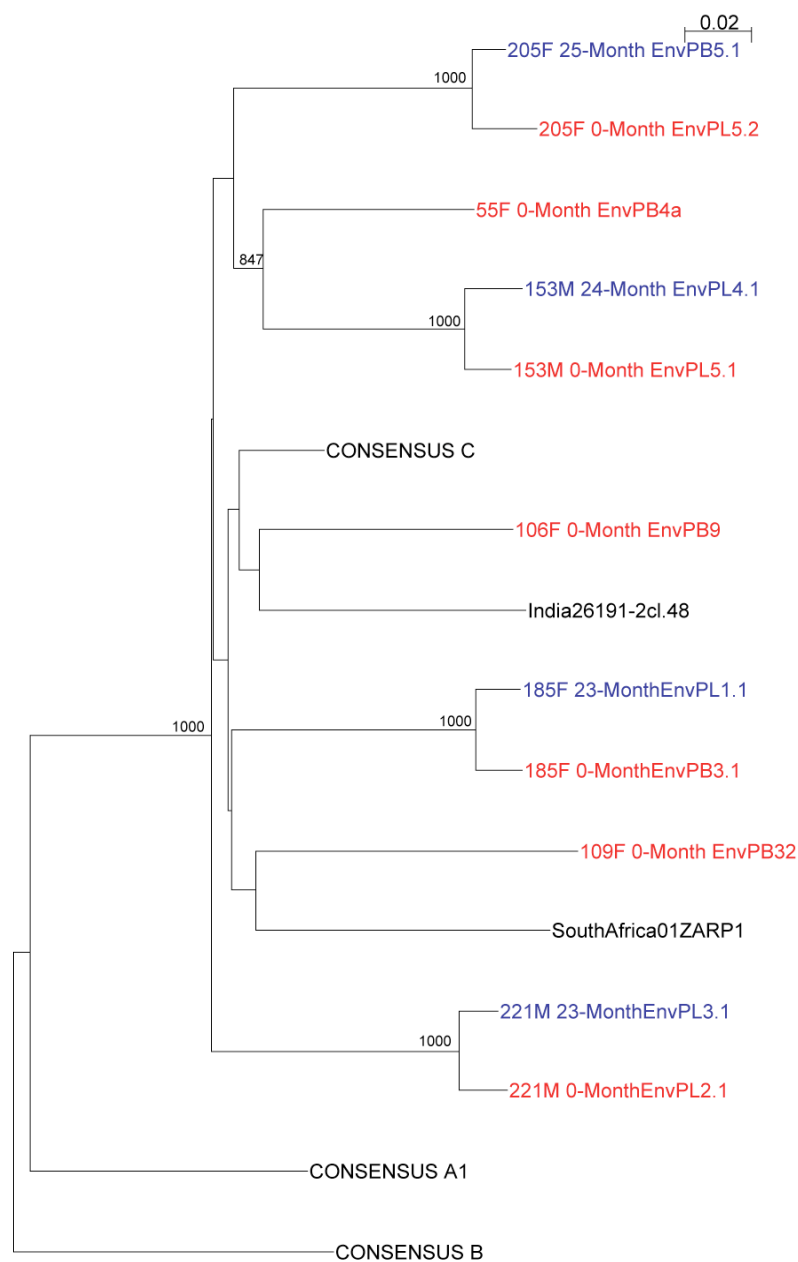
increased neutralization via V3 and CD4-induced epitopes to varying degrees. It has been shown that HIV-1 infected patients develop high titers of anti-CD4 induced and anti-V3 antibodies, and more variable titers of anti-CD4bs antibodies (10, 37, 38, 65, 96, 115, 154). It is plausible that I309L Envs could be more susceptible to these types of antibodies *in vivo*, and would therefore be selected against by immune pressure. It is important to note that we were unable to detect an increase in sensitivity to autologous patient plasma with I309L (data not shown). However, only the dominant circulating Nab specificities are measured in assays that utilize patient plasma, while other lower titer specificities may also exert selective pressure (12, 116, 146, 154). Alternatively, I309 could protect immunogenic structures so effectively that antibodies against these hidden epitopes are never induced. Since the number and potency of monoclonal antibodies available to probe differences between wildtype and I309L Envs was limited, the effect of I309L on neutralization sensitivity could be underestimated. Thus, even a subtle increase in susceptibility to neutralization by sCD4, anti-V3, and anti-CD4i monoclonal antibodies *in vitro* could reflect a substantial growth disadvantage *in vivo*. In fact, the differences in neutralization sensitivity between parent and mutant Envs were subtle, trending toward significance, but really driven by the Env from subject 55F. The impact of the L309 mutation was dramatic in this Env, a fact that may result from the unusual M307 residue (see Fig. 1) and highlights how many changes in Env sequence are context dependent and rarely result in a globally reproducible phenotype. We also acknowledge, that over-all neutralization sensitivity and immune evasion is clearly influenced by

multiple Env domains, as shown by our group and others (14, 115, 116, 131, 144, 146, 176).

**V3-mediated masking of the CD4 binding site.** We previously highlighted a cluster of hydrophobic residues flanking the V3 tip (anchored by residues I307, I309, and F317) that are highly conserved in subtype C sequences in the database and are largely restricted to hydrophobic amino acids across subtypes (55, 101, 145, 158). Coarse-grained calculations suggested that this hydrophobic cluster has the potential to interact with multiple gp120 core residues, several of which are proximal to the CD4 binding site and may impact CD4 binding (101). Based on these previous observations, and our current experimental results, we propose that the I309L substitution perturbs the hydrophobic cluster and, by altering the position of the V3 loop, impacts the CD4bs. Thus, for subtype C viruses, maintaining this residue could represent an intrinsic strategy of immune evasion, particularly concerning Nab recognition of the CD4bs. Consistent with this idea, I309 was not critical for viral replication or usage of CCR5, but its major effect was manifested in exposure of the CD4bs prior to receptor ligation.

Thus, V3 in subtype C Env could be placed in an optimal position to contribute to immune evasion prior to CD4 binding and additionally aid viral entry after CD4 binding. This theory provides a biologically plausible explanation for the I309L CD4 enhanced phenotype described here, as well as a compelling reason for the unique conservation pattern of specific residues within the subtype C V3 domain that may not be critical for viral entry functions. The idea of conformational

masking of neutralization targets is not new; and others have demonstrated concealment of epitopes on the native trimer (10, 37, 115, 181, 182). It is important to note that this tactic of V<sub>3</sub>-masking could also occur in other subtypes, but the specific mechanism may subtly differ. Thus, this specific feature of subtype C Envs may limit their inherent neutralization susceptibility to certain types of antibodies and could also influence their immunogenicity, which is of interest for vaccine design.

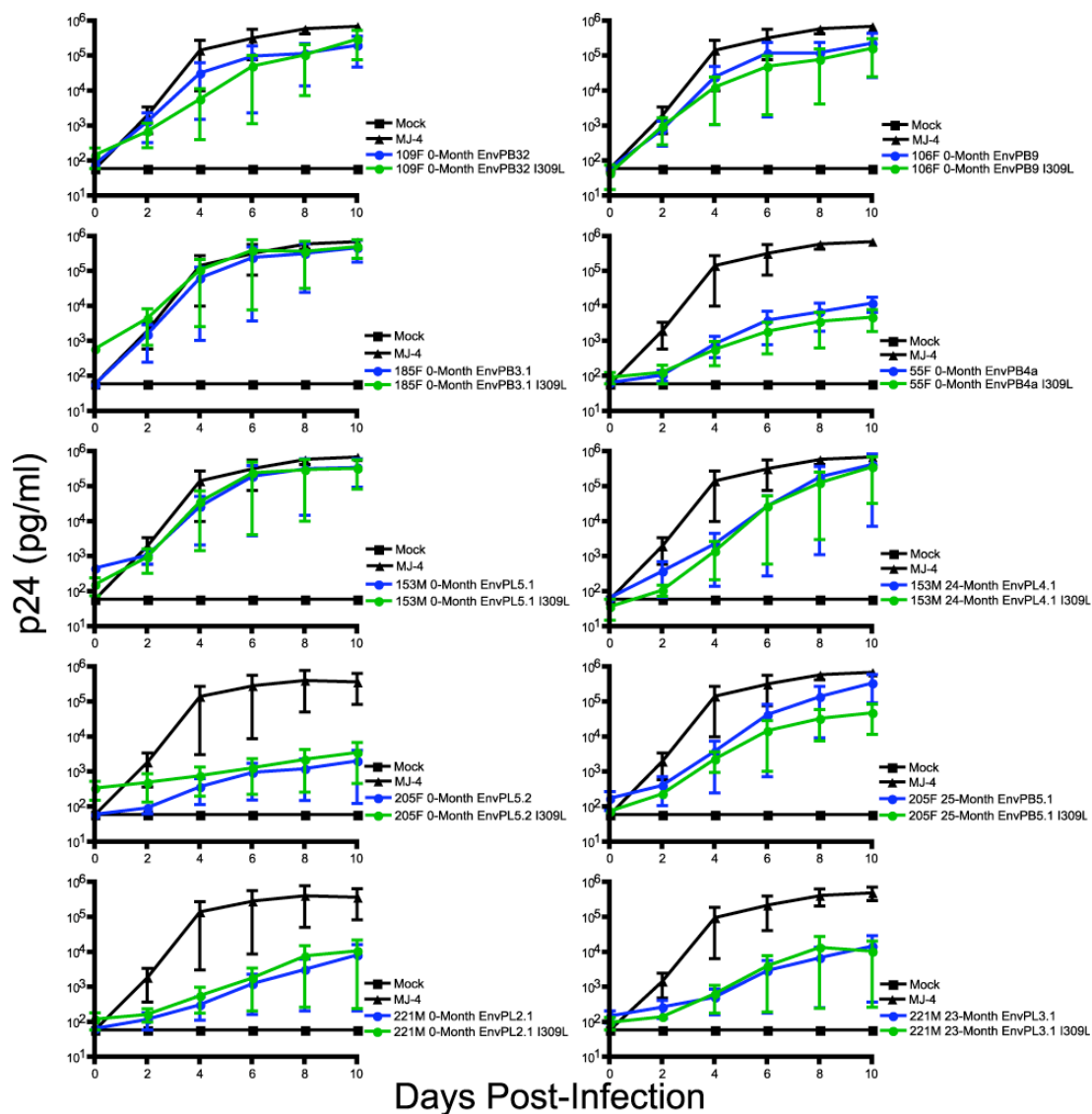


### Supplemental Figure 1. Phylogenetic tree of representative subtype C

**Envs.** The complete nucleotide sequence of the *env* genes from seven subjects with recent infection (red) and four Nab escape-variant Envs from a two-year time point post-infection (blue) are shown in a neighbor-joining tree generated using Clustal W. Reference subtype *env* sequences (black) for subtypes A, B and C were used to highlight the diversity of the 11 subtype C Envs. Significant



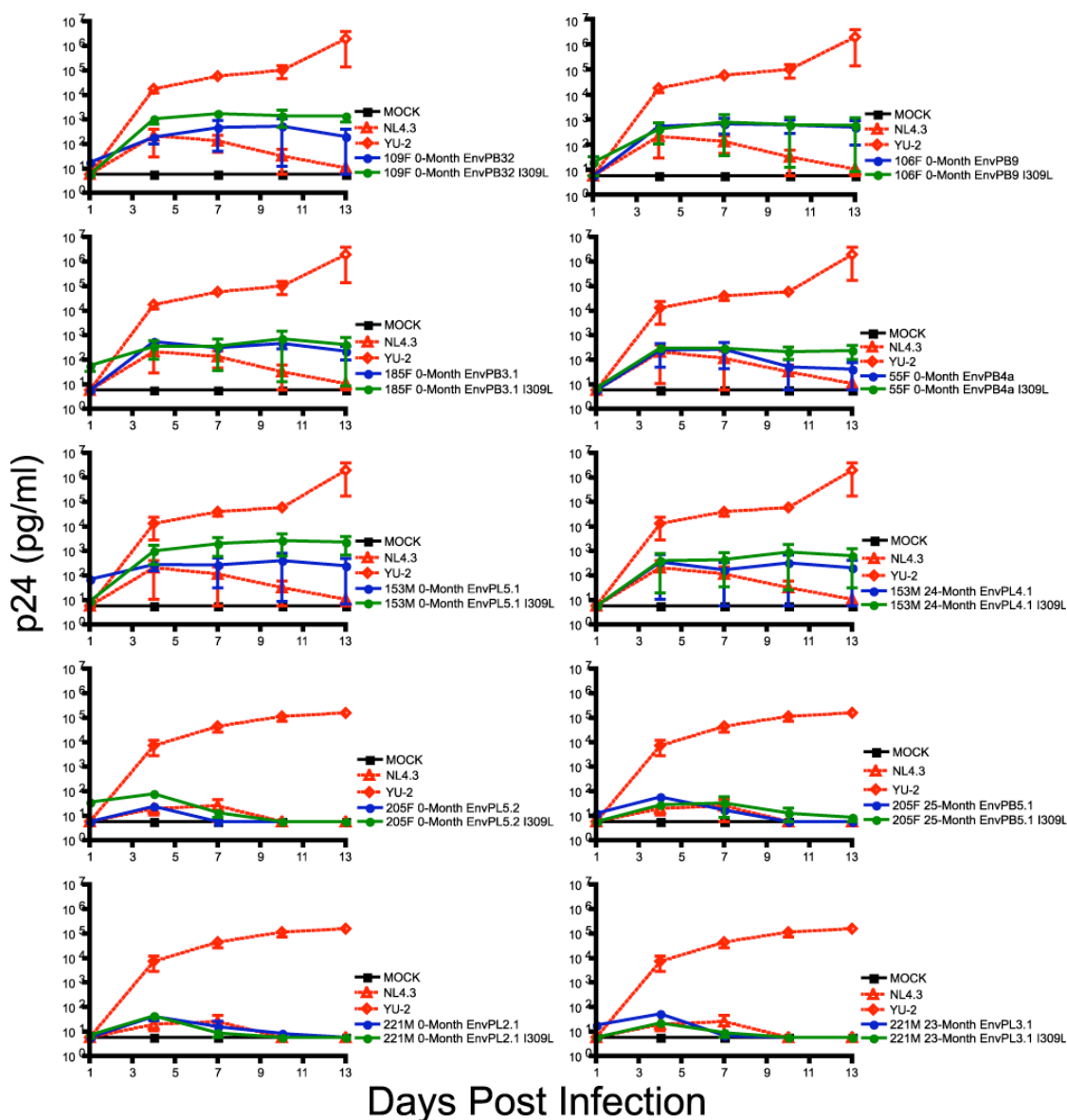
bootstraps from 1000 replicates are indicated.



### Supplemental Figure 2. Replication of virus containing a wildtype and I309L mutated Envs in PBMC.

10 wildtype and 10 I309L mutated Envs were placed into a replication competent NL4.3 backbone and used to infect CD8-depleted human PBMC. Viral p24 antigen production in the supernatant was measured by ELISA and is plotted (pg/ml) on the vertical axis on a log<sub>10</sub> scale while days post infection are on the horizontal axis. Mock-infected (squares) and positive control virus NL4.3 (triangles) are shown in black. Wildtype Envs are blue and I309L mutant Envs

are green. The error bars represent two independent experiments using two different donors.



### Supplemental Figure 3. Replication of I309 and I309L Env viruses in MDM.

10 wildtype and 10 I309L mutated Envs were placed into a replication competent NL4.3 backbone and used to infect MDM. Viral p24 antigen production in the supernatant was measured by ELISA and is plotted (pg/ml) on the vertical axis

on a log<sub>10</sub> scale while days post infection are on the horizontal axis. Mock-infected is shown in black squares, negative control virus NL4.3 (triangles) and positive control virus YU-2 (diamonds) are shown in red, wildtype I309 Envs are blue and I309L mutant Envs are green. The error bars represent two independent experiments from two different donors.

## **VI. Acknowledgements**

We would like to thank Drs. David Kabat and Emily Platt for providing the HeLa-CD4 cell lines; and the interns, staff, participants, and Project Management Group at ZEHRP. We gratefully acknowledge Dr. Susan Zolla-Pazner for providing us with the subtype C anti-V3 monoclonal antibodies, work that was supported by the New York University CFAR Immunology Core grant AI27742. The work in this paper was supported by NIH grants AI58706 and AI78410. SG was supported by LANL/DOE X1V5 grant.

## VII. Contributors

Rebecca M. Lynch,<sup>1</sup> Rong Rong,<sup>2,5</sup> Bing Li,<sup>5</sup> Tongye Shen,<sup>9</sup> William Honnen,<sup>7</sup>  
Joseph Mulenga,<sup>8</sup> Susan Allen,<sup>3,4</sup> Abraham Pinter,<sup>7</sup> S. Gnanakaran,<sup>10</sup>  
and Cynthia A. Derdeyn<sup>2,5,6</sup> \*

Immunology and Molecular Pathogenesis Program,<sup>1</sup> Department of Pathology  
and Laboratory Medicine,<sup>2</sup> Department of Global Health,<sup>3</sup> Rollins School of  
Public Health,<sup>4</sup> Yerkes National Primate Research Center,<sup>5</sup> Emory Vaccine  
Center,<sup>6</sup> Emory University, Atlanta, GA 30329.

Public Health Research Institute,<sup>7</sup> UMDNJ-New Jersey Medical School, Newark,  
NJ 07103.

Zambia Blood Transfusion Service,<sup>8</sup> Lusaka, Zambia.

Department of Biochemistry, Cellular & Molecular Biology,<sup>9</sup> University of  
Tennessee, Knoxville, TN 37996.

Theoretical Division,<sup>10</sup> Los Alamos National Laboratory, Los Alamos, NM 87545

### **Chapter Three:**

#### **The B cell response is redundant and highly focused on V1V2 during early subtype C infection in a Zambian seroconverter**

##### **I. Abstract**

High titer autologous neutralizing antibody responses have been demonstrated during early subtype C HIV-1 infection. However, characterization of this response at the monoclonal antibody level against autologous virus has not been performed. Here we describe five monoclonal antibodies derived from a subtype C infected seroconverter and their neutralizing activity against pseudoviruses that carry envelope glycoproteins from 48 days (0 month), 2 months, and 8 months after the estimated time of infection. Sequence analysis indicated that the Mabs arose from three distinct B cell clones and their pattern of neutralization compared to patient plasma suggested that they circulated between 2 and 8 months after infection. Neutralization by Mabs representative of each B-cell clone was mapped to two residues, positions 134 in V1 and 189 in V2. Mutational analysis revealed cooperative effects between glycans and residues at these two positions, arguing that they contribute to a single epitope. Analysis of the cognate gp120 sequence through homology modeling places this potential epitope near the interface between the V1 and V2 loops. Additionally, the escape mutation R189S in V2, which conferred resistance against all three Mabs, had no detrimental effect on virus replication in vitro. Taken together, our data demonstrate that independent B cells repeatedly targeted a single structure in V1V2 during early infection. Despite this assault, a single amino acid change was

sufficient to confer complete escape with minimal impact on replication fitness.



## II. Introduction

The UNAIDS organization estimates that in 2008 alone there were between 2.4 and 3 million new infections of HIV world-wide with over half of these occurring in sub-Saharan Africa (171). A vaccine to prevent these new infections is necessary; however, one major obstacle to this goal is the incredible genetic diversity of HIV-1 (54). This variation is categorized into viral subtypes and circulating recombinant forms, of which subtype C is essential to study because of its global preponderance and its dominance in sub-Saharan Africa (161). Within the viral genome, genetic variation is concentrated within the *env* gene, which encodes the surface unit gp120 and transmembrane unit gp41 (75, 84). These two glycoproteins are non-covalently linked and trimerize to form surface spikes on the virion. These trimers not only display the receptor (CD4) and co-receptor (CCR5 and/or CXCR4) binding sites for the virus, but are also the main targets of neutralizing antibodies (Nabs) during an immune response (8, 10, 65, 154). HIV vaccine research has recently focused on defining epitopes in gp120 that are associated with neutralization breadth for use in an antibody-based vaccine. However, Nab responses in early infection, raised against the founder virus or a limited set of variants, do not usually possess this desirable property and are readily escaped. Thus, a better understanding of the early Nab response during natural infection could lead to clues about how to improve Env immunogens and minimize the potential for escape.

It has been shown that early autologous antibody responses occur within the first few months in HIV-1 infection (1, 4, 19, 63, 92, 140, 176). In subtype C, this

response has been shown to be of high potency but strain-specific (20, 63, 92). Recent research has begun to illuminate how this Nab response develops. Moore et al., (116) demonstrated that the acute humoral response in four subtype C infected individuals was quite narrowly targeted against the virus. The Nabs during the first year of infection in these South African subjects only had 1-2 different specificities, mainly targeting either the V1V2 region or the C3 region of gp120. Furthermore, our group reported that in two subtype C infected individuals from Zambia, not only was the acute Nab response focused on one or a few regions of Env, but that the virus escaped by using multiple pathways. Rong et al. (146) demonstrated that in one subject, escape mainly occurred through mutations in the V3-V5 region of gp120. The requirements for escape; however, changed in this subject over time, sometimes relying on cooperative effects between different regions such as V1V2 and the gp41 ectodomain, confounding the identification of early Nab epitopes. In a second subject, escape was driven by changes in V1V2 continuously over a two-year period involving sequence changes as well as potential glycan shifts. Two B cell hybridomas that produced neutralizing monoclonal antibodies (Mabs) were isolated from this individual, allowing a more detailed analysis of viral escape. A potential glycan addition in V2 was suggested as the dominant escape pathway from these two Mabs. Thus, the potent Nab response in acute subtype C infection has been shown to involve only limited targets in gp120 (often V1V2) and to exert pressure on the virus that is easily escaped, sometimes only requiring a single amino acid change. The nature of the antibodies that make up this polyclonal plasma response in early infection has not yet been elucidated. Here we expand on our knowledge of

the B cell response and neutralization at the monoclonal antibody level during early subtype C infection. Using 5 Mabs isolated from peripheral memory B cells circulating in a subtype-C infected subject between 49 and 69 months post-seroconversion, we show that the Mabs produced by these B cells reflect the plasma pool at 8-months post-seroconversion. The Mabs represent antibodies produced from three individual B-cell clones that have undergone somatic hypermutation, and they rely on residues 134 and 189 in V1 and V2 respectively to neutralize the virus. The Mabs each have slightly different requirements for neutralization; however, the virus appears to develop an efficient escape pathway, becoming resistant to all 5 Mabs with a single amino acid change in V2. Our present study demonstrates how these clonally distinct antibodies from early infection target a single epitope formed at the interface of V1 and V2 and how the virus escapes without an overt replication fitness cost.

### III. Materials and Methods

**Env clones.** Details of the ZEHRP cohort, sample collection, and processing have been described previously (41, 108, 146, 166). The Envs studied here were derived from a newly infected subject from this cohort (205F) whose polyclonal antibody responses at the plasma level have been studied in detail (146). The Emory University Institutional Review Board, and the University of Zambia School of Medicine Research Ethics Committee approved informed consent and human subjects protocols. This subject did not receive antiretroviral therapy during the evaluation period. Single genome PCR amplification and cloning of the Envs has been described (67, 146). The env genes were cloned into the CMV-driven expression plasmids pcDNA 3.1/V5-His TOPO (Invitrogen), which were then used to generate viral pseudotypes. All Envs were derived from plasma or PBMC DNA according to protocols previously described (92) and are subtype C. Nucleotide sequences (either V1-V4 or full-length) have been deposited into Genbank under accession numbers GQ485415-427. All amino acid sequences are based on 205F 0-month FPL Env 6.3 numbering.

**PCR-based site mutagenesis and virus preparation.** To generate V1V2 mutations, PCR-directed site mutagenesis was performed using two overlapping primers that contained the mutated sequence for each Env using a strategy described in (144, 146). Briefly, the *env* gene (plus Rev and partial Nef coding sequences) for the 0-month FPL Env 6.3 was amplified using the following set of forward and reverse primer sequences (mutated nucleotide is underlined and HXB2 locations are provided):

N134S F: (6613-6644)(5'-GCTGTAGCAATTATAGCAATTGTAATGATACC-3')

N134S R: (6613-6644)(5'-GGTATCATTACAATTGCTTATAATTGCTACAGC-3')

N134Q F: (6613-6644)(5'-GCTGTAGCAATTATCAGAATTGTAATGATACC-3')

N134Q R: (6618-6659)(5'-

GGCAGTACTATAGGTATCATTACAATTCTGAATAATTGC-3')

N134T F: (6613-6644)(5'-GCTGTAGCAATTATACCAATTGTAATGATACC-3')

N134T R: (6618-6659)(5'-

GGCAGTACTATAGGTATCATTACAATTGGTTATAATTGC-3')

N132Q F: (6613-6644)(5'-GCTGTAGCCAGTATAACAATTGTAATGATACC-3')

N132Q R: (6618-6659)(5'-

GGCAGTACTATAGGTATCATTACAATTGTTATACTGGC-3')

N134T F: (6613-6644)(5'-GCTGTAGCAATTATACCAATTGTAATGATACC-3')

N134T R: (6618-6659)(5'-

GGCAGTACTATAGGTATCATTACAATTGGTTATAATTGC-3')

R189S F: (6779-6803)(5'-GCCTAATGATAGTAACTCTAGTGAGTATATATTA-3')

R189S R: (6779-6803)(5'-TAATATATACTCACTAGAGTTACTATCATTAGGC-3')

R189H F: (6779-6799)(5'-GCCTAATGATAGTAACTCTCACGAGTATAT-3')

R189H R: (6787-6811)(5'-CAATTTATTAATATATACTCGTGAGAGTTAC-3')

The amplification conditions were: 1 cycle of 95°C for 30 sec.; 18 cycles of 95°C for 30 sec.; 45°C for 1 min. (optimal annealing temperature was determined for each primer set), and 68°C for 9 min.; storage at 4°C. The 50 µl PCR reactions contained 100ng of each primer, 10 ng of the plasmid template, 0.2 mM dNTP, and 1X reaction buffer. PfuUltra II Fusion Hotstart DNA polymerase (Stratagene) was used to generate the PCR amplicons, which were digested with DpnI to

remove contaminating template DNA, and then transformed into maximum efficiency XL2-Blue ultracompetent cells ( $>5 \times 10^9$  cfu/ $\mu$ g DNA; Stratagene) so that the DNA volume did not exceed 5% of the cell volume. The entire transformation was plated onto LB-Ampicillin agar plates, generally resulting in 10 to 50 colonies.

Colonies were inoculated into LB-Ampicillin broth for overnight cultures and the plasmid was prepared using the QIAprep Spin Miniprep Kit. Each Env plasmid (1 $\mu$ g) was co-transfected into 293T cells along with 2 $\mu$ g of an Env-deficient subtype B proviral plasmid, pSG3 $\Delta$ Env, using Fugene-6 according to the manufacturer's instructions (Hoffman-La Roche). Transfection supernatants were collected at 48 hours post-transfection, clarified by low speed centrifugation for 20 minutes, aliquoted into 0.5 ml or less portions, and stored at  $-80^{\circ}\text{C}$ . The titer of each pseudotyped virus stock was determined by infecting JC53-BL (Tzm-bl) cells with 5-fold serial dilutions of virus as described previously (41, 92). All *env* sequences were confirmed by nucleotide sequencing.

**Generation of human monoclonal antibodies.** B cells from several viably frozen PBMC samples of subject 205F collected at 49 and 69 months after infection were inoculated with EBV and plated at low cell densities in multiple 96-well tissue culture plates containing irradiated, mature human macrophage feeder cells prepared from HIV-seronegative subjects as previously described (184). Two and three weeks later culture fluids were screened for antibodies that were reactive by ELISA and could neutralize the founder autologous virus envelope 0-month FPB Env 1.1. B cells in antibody positive wells were serially

subcultured at increasing dilutions as described in (143). Clones of antibody producing B cell lines from subject 205F did not grow well enough to allow scaling up Mab production. Therefore, cells producing Mab 6.4C were converted to a hybridoma by fusion with HAT sensitive HMMA cells as previously described (184). The four remaining Mabs were produced by molecular cloning (66). RNA was isolated from antibody positive cells and used in RT-PCR reactions to amplify VH and VL or VK genes for cloning into expression vectors (kindly provided by Yongjun Guan and George Lewis, U of Maryland). Subsequently functional pairs of heavy and light chain vectors were co-transfected into 293T cells for Mab expression. Mabs were purified from culture supernatants by protein A affinity chromatography.

**Screening ELISA for Mabs.** For antibody screening we used a “reverse capture” immunoassay, as previously described (143). Briefly, B cell culture fluids were incubated in plates coated with goat anti-human IgG antibodies. Detergent (Triton X-100) treated supernatant from cells transfected with plasmid expressing 205F 0-month FPB Env 1.1 gp160 was added to the wells. Bound HIV-1 Env was detected using a mixture of biotin-labeled human Mabs recognizing several non-overlapping conserved sites in gp120 and gp41 (143). The wells were incubated with peroxidase-streptavidin and signal was developed with TMBH<sub>2</sub>O<sub>2</sub> as substrate. The color reaction was stopped with 1M phosphoric acid and color read as OD/absorbance at 450 nm. An excess concentration (>100 µg/ml) of human IgG was added to the dilution buffers to prevent the capture of the biotin-labeled human Mabs by the goat anti-human IgG, which would otherwise cause

high background. OD readings greater than 1.500 were considered positive (usually >2.400) and background OD was usually less than 0.200.

**Neutralization Screening Assay for Mabs.** B cell culture fluids were screened for neutralizing activity in an adaptation of the single-cycle TZM-bl neutralization assay described previously (143). Briefly, supernatants from EBV transformed B-cells or transfected 293T cells were incubated with 205F 0-month FPB Env 1.1 pseudovirus in black 96-well culture plates. TZM-bl cells were added to a final concentration of  $5 \times 10^3$  cells/well with  $37.5 \mu\text{g/ml}$  DEAE-dextran and the plates were incubated for 48 hours. Neutralization was assessed by analyzing the amount of luciferase produced from the pseudovirus-infected cells. Luciferase was quantified using a commercially available kit (Promega BriteGlo). Typically neutralizing activity was evident when reduction in RLU was greater than 70% compared to the average RLU in the plate.

**Pseudovirus inhibition assays.** Neutralization assays using a panel of 5 autologous monoclonal antibodies were performed using viral pseudotypes to infect JC53-BL (Tzm-bl) indicator cells using a luciferase readout as described previously (41, 92, 144-146). Briefly, 2000 IU of pseudovirus was incubated for 1 hour in DMEM + 10% FBS (Hyclone) +  $40 \mu\text{g/ml}$  DEAE-Dextran with serial dilutions of monoclonal antibody, and subsequently  $100 \mu\text{l}$  was added to the indicator cells for a 48 hour infection before being lysed and evaluated for luciferase activity.



**Homology modeling of residues 134 and 189 in the V1V2 domain.**

The 205F EnvPL6.3 gp120 sequence was modeled using MODELLER (46). The template for the homology model was a subtype C gp120 obtained by longtime all-atom molecular dynamics simulation using the CHARMM27 (102) potential in NAMD (129). This simulated gp120 was modeled using all known CD4 bound gp120 structures (PDB IDs 1G9M (89), 1RZK (74), 2B4C (73), 2NY7 (187), 3JWD (122), 3JWO (122), and 3LMJ (42) as templates. In all of these structures, the core of gp120 was highly similar; however, it should be noted that 3LMJ was the only high-resolution structure of a subtype C gp120 sequence while the rest were subtype B. Multiple templates were used because it has been shown that this creates high quality homology models. In addition, each template has slightly different regions of gp120 resolved. Before modeling these templates, they were arranged in the trimeric state, which has been resolved using cryoelectron microscopy (PDB ID 3DNO (97)), in order to ensure that the hyper-variable loops did not sterically clash with the neighboring monomers. During modeling, disulfide constraints were added for the conserved cysteines present in all gp120 sequences. All sequence alignments used for modeling templates were based on the HIV-1 database ([www.hiv.lanl.gov](http://www.hiv.lanl.gov)). A 128 ns all-atom molecular dynamics simulation of the template described above was used to calculate the potential distance between N134 and R189.

**Replication in CD4+ cells using an NL4.3 proviral cassette.** A panel of Envs was subcloned into a replication competent NL4.3 backbone (98, 121) that we have used previously to evaluate replication of subtype C Envs (100). This

system is amenable to accepting diverse *env* genes, and facilitates substitution of virtually the entire coding region (only 36 and 6 amino acids at the N and C terminus respectively are derived from NL4.3). Peripheral blood mononuclear cells (PBMC) were isolated from the whole blood of a normal, seronegative donor by ficoll-hypaque centrifugation. CD8-depleted PBMC cultures were prepared by negative selection using Dynabeads (Invitrogen). The CD4-enriched PBMC were cultured in complete RPMI for 3 days in the presence of 3mg/ml phytohemagglutinin (PHA) for activation prior to infection. Infected cultures were maintained in complete RPMI supplemented with 30 U/ml recombinant human IL-2 (Roche) for up to 10 days. Every two days, 200µl of supernatant was collected for p24 analysis (Perkin-Elmer), and this volume was replaced with fresh complete media with IL-2. The subtype C Env MJ-4 was cloned into the NL4.3 backbone and used as a positive control for these experiments. The infectious subtype C proviral clone MJ4 (contributed by Drs. Thumbi Ndung'u, Boris Renjifo, and Max Essex) (119) was obtained from the NIH AIDS Research and Reference and Reagent Program, Division of AIDS, NIAID, NIH.

## **IV. Results**

### **Characterization of monoclonal antibodies isolated from a subtype C infected patient and selected for neutralization activity against the founder Env.**

Here we investigated autologous neutralization at the single antibody level by generating monoclonal antibodies isolated from subject 205F, a subtype C infected seroconverter in the Zambia-Emory HIV Research Project (ZEHRP). This subject was identified at a time of antigen positive; antibody negative status, allowing a date of infection to be accurately estimated (Fig. 1). After seroconversion, Envs were cloned every two to three months from both the plasma and PBMC of 205F and used to create a longitudinal panel of pseudoviruses against which autologous plasma was tested (146). At 49 and 69 months post-seroconversion, viable PBMC were collected from 205F and used for selection of memory B cells and production of monoclonal antibodies (Fig 1). Specificity was tested by screening the antibodies for neutralization activity against a 0-month Env that was representative of the founder virus (146).

Five Mabs that neutralized the founder virus were recovered by cloning of Ig heavy and light chains. The sequences of the 5 Mabs revealed that all antibodies were IgG with a gamma heavy chain and lambda light chain. Furthermore, analysis of the VH regions suggested that these Mabs arose from 3 distinct B cell clones and had undergone somatic hypermutation. A neighbor-joining tree of the nucleic acid sequences revealed three significant lineages suggesting that Mabs 6.4C and 8.9D were clonally distinct from the three other Mabs (6.1C, 10.9D, and

13.6A) (Fig 2A). All 5 Mabs were derived from heavy-chain alleles IGHV3-15\*01 and IGHJ4\*02 with 6.4C and 8.9D using IGHD4-04\*01 and 6.1C, 10.9D and 13.6A using IGHD5-12\*01. An amino acid alignment highlighted the fact that although 6.1C, 10.9D, and 13.6A have nearly identical sequences, there were 1-2 amino acid differences between them indicating somatic variation (Fig. 2B). Further analysis using the Joinsolver program confirmed that these latter three antibodies have the same DJ joining sequence and the same number of nucleotides (nontemplated junctional additions) at this junction, thus verifying that these are three somatic variants that arose from the same B cell clone (Suppl. Table 1). All five antibodies had a heavy chain CDR3 region composed of 16 amino acids although the sequences differed according to clone (Fig. 2B). The Mabs showed evidence of affinity maturation as well. The frequency of mutations as compared to germline was 8.84% for 8.9D, 12.93% for 6.4C and ranging between 3.74 and 4.42% for the three Mab variants 6.1C, 10.9D, and 13.6A. These non-silent mutations were preferentially found in the CDR regions (Suppl. Table 1). Thus, there appeared to be three genetically distinct B cell clones that were isolated from 205F.

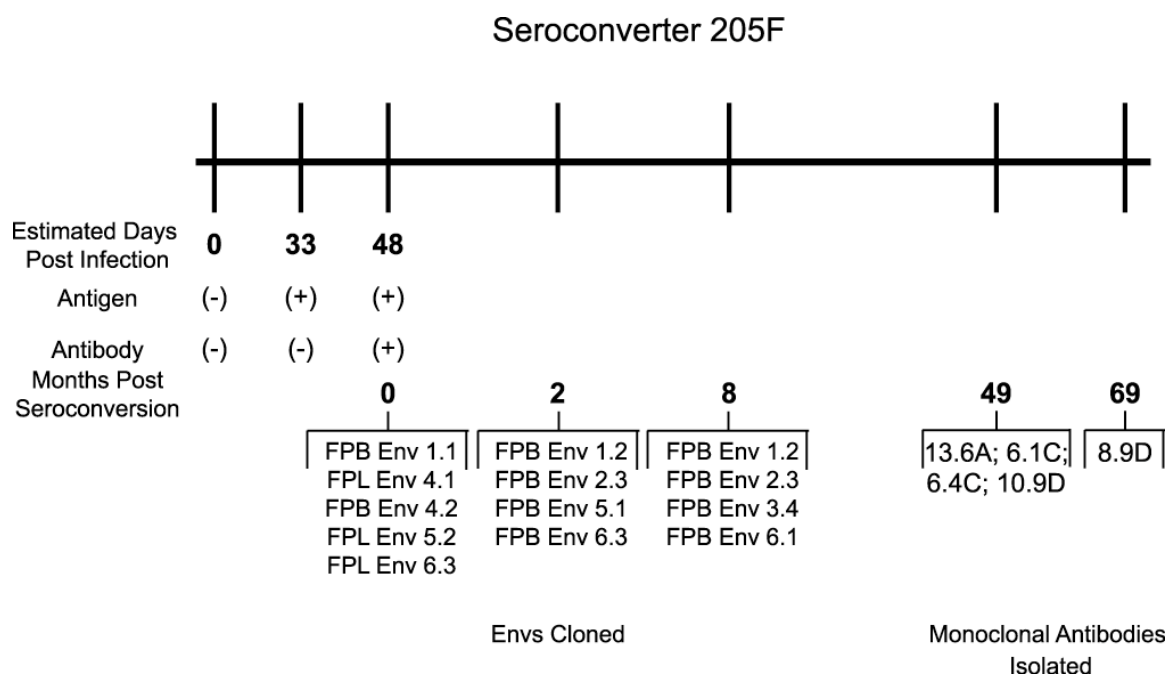


**Figure 1. Timeline of seroconverter 205F from a Zambian cohort.**

A timeline was created to detail the stages of infection of a female sero-positive subject from Zambia. Indicated are the days from estimated infection when 205F was antigen and/or antibody positive, and the months when Envs were cloned out of plasma or PBMC and when the Ig genes were cloned out of memory B cells to produce monoclonal antibodies.

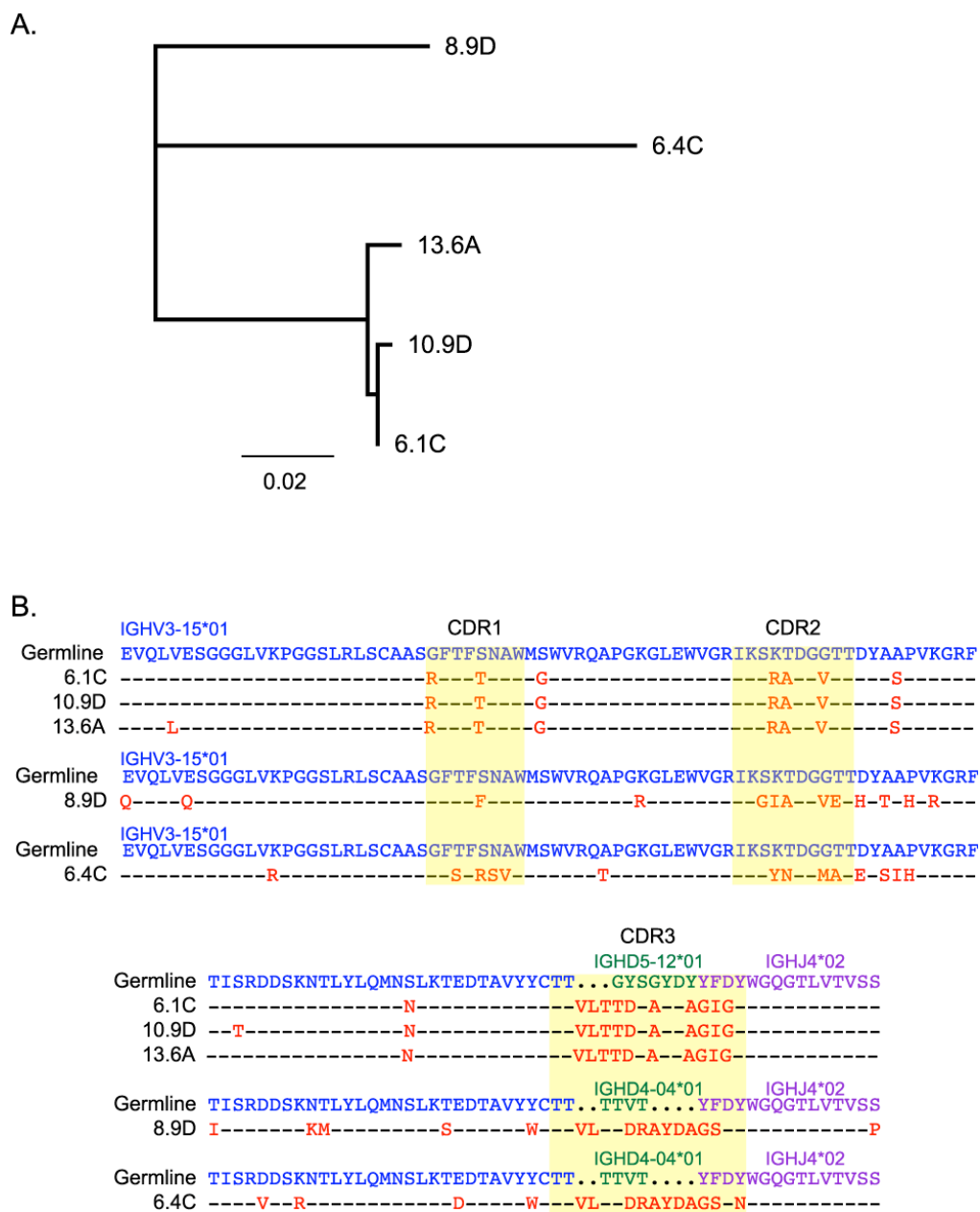


**Figure 2. Sequence analysis of Mabs isolated from seroconverter 205F.**

A Neighbor-Joining tree of the nucleotide sequences of the 5 Mabs was created using the Jukes-Cantor model in Geneious (A). Scale is indicated. An amino acid alignment of the VH genes of these 5 Mabs plus the germline sequences was generated using ClustalX in Geneious (B). Germline V alleles were obtained from

Joinsolver and are indicated in blue, D in green and J in purple. CDR regions are highlighted in yellow, while mutations from the germline are in red.

**The monoclonal antibodies likely arose before eight months post-seroconversion.** Previous studies suggested that two of these monoclonal antibodies arose during early infection of 205F (146). Here all five monoclonal antibodies were tested for neutralization activity against a panel of Envs cloned from samples collected between 0-8 months post-seroconversion (Table 1). The Mabs neutralized four of the five 0-month Envs fairly potently with 50% inhibitory concentrations (IC<sub>50</sub>s) ranging between 0.09-0.69µg/ml. Surprisingly, the 0-month Env 6.3 was not neutralized by all of the Mabs. Three of the five antibodies could not reach 50% neutralization at the highest concentration tested (25µg/ml); however, antibodies 6.4C and 8.9D did neutralize this Env with IC<sub>50</sub>s of 0.34 and 0.1 µg/ml respectively. At 2-months post-seroconversion, all four Envs tested were sensitive to neutralization by the Mabs, although, again 6.4C and 8.9D were the most potent antibodies with IC<sub>50</sub>s all under 0.2 µg/ml. By 8 months post-seroconversion, two Envs were resistant to all five monoclonals, and this pattern of sensitivity and resistance to neutralization by the Mabs mirrored exactly the neutralization pattern of the contemporaneous 8-month plasma. The fact that 8-month Envs 2.3 and 6.1 were resistant to both plasma and Mabs while Envs 1.2 and 3.4 were sensitive to both suggests that these Mabs likely represent the antibodies circulating in the plasma near this time point after seroconversion.

Table 1.

| 205F Envs   |                | Monoclonal Antibodies (IC50<br>μg/ml) <sup>a</sup> |       |       |      |      | Contemporaneous<br>Plasma |
|-------------|----------------|--|-------|-------|------|------|---------------------------|
|             |                | 6.1C   | 13.6A | 10.9D | 8.9D | 6.4C |                           |
| 0-<br>month | FPB Env<br>1.1 | 0.61   | 0.69  | 0.67  | 0.09 | 0.12 |                           |
|             | FPL Env<br>4.1 | 0.31   | 0.35  | 0.35  | 0.10 | 0.10 |                           |
|             | FPB Env<br>4.2 | 0.40   | 0.60  | 0.52  | 0.09 | 0.10 |                           |
|             | FPL Env<br>5.2 | 0.19   | 0.37  | 0.23  | 0.11 | 0.13 |                           |
|             | FPL Env<br>6.3 | >25  | >25   | >25   | 0.10 | 0.34 |                           |
| 2-<br>month | FPB Env<br>1.2 | 0.35   | 0.53  | 0.50  | 0.09 | 0.11 | Sensitive                 |
|             | FPB Env<br>2.3 | 0.45   | 2.23  | 1.94  | 0.10 | 0.16 | Resistant                 |
|             | FPB Env<br>5.1 | 0.24   | 0.59  | 0.40  | 0.10 | 0.12 | Sensitive                 |
|             | FPB Env<br>6.3 | 0.30   | 0.63  | 0.45  | 0.09 | 0.10 | Sensitive                 |
| 8-<br>month | FPB Env<br>1.2 | 0.35   | 0.32  | 0.31  | 0.10 | 0.10 | Sensitive                 |
|             | FPB Env<br>2.3 | >25  | >25   | >25   | >25  | >25  | Resistant                 |
|             | FPB Env<br>3.4 | 0.21   | 0.22  | 0.24  | 0.10 | 0.10 | Sensitive                 |
|             | FPB Env<br>6.1 | >25  | >25   | >25   | >25  | >25  | Resistant                 |

<sup>a</sup> The inhibitory concentration that neutralizes the virus by 50%.



**Glycosylation in V1 can confer sensitivity to monoclonal antibodies.**

Previously it had been shown that V1V2 was the major determinant of resistance to neutralizing antibodies in subject 205F during the first two years of infection (146). Specifically, two residues at position 134 in V1 and 189 in V2 that were each part of a potential N-linked glycosylation site were shown to influence neutralization sensitively to 6.4C and 13.6A, but it was not clear whether the amino acid substitution or altered glycan motif at each site was responsible (position 189 was numbered 197 in (146)). Here, the requirement for these specific residues and for N-linked glycosylation at both positions was more fully explored using a mutagenesis strategy to detect neutralization determinants of three Mabs representative of the three distinct B-cell lineages (6.4C; 13.6A; and 8.9D). 0-month Env 6.3, which lacks potential glycosylation motifs at both of these positions, was used as the background Env for these experiments.

Env 6.3 contains the sequence NYN at positions 132-134 in V1 (Fig 3B) and is highly sensitive to neutralization by Mab 8.9D, sensitive to 6.4C, and resistant to 13.6A (Fig 3A). When the N134S mutation was introduced, thereby inserting the glycosylation motif NYS into V1, the Env remained sensitive to 8.9D, and sensitivity to 6.4C increased, lowering the IC<sub>50</sub> from 0.34 to 0.1 µg/ml. Most interestingly, Env 6.3 became fully sensitive to Mab 13.6A, indicating that either the Serine or the glycan at this position might comprise a target for this antibody. The role of the potential glycan was further investigated by creating additional mutations that either did (NYT) or did not (NYQ, QYS) create glycosylation

motifs in Env 6.3 (Fig. 3B). Sensitivity to 8.9D did not appear to be affected by any of the mutations, and so all Envs remained potentially neutralized. 6.4C neutralized all Envs as well regardless of glycan motif; however, the V1 NYS Env remained especially sensitive to neutralization when compared to the other four Envs, despite the fact that the NYT variant also introduced a glycosylation site at this position. Mab 13.6A required a glycan motif (either NYS or NYT) for neutralization while all other non-glycosylated mutations were resistant to this Mab. Once again, the V1-NYS Env was almost one log<sub>10</sub> more sensitive than V1-NYT with IC<sub>50</sub>s of 0.77 and 7.19 µg/ml respectively. The results for Mabs 6.4C and 13.6A suggest that although glycosylation status can play a role in neutralization sensitivity, the amino acid at residue 134 (either Ser or Thr) can also dramatically modulate this effect.



mean of at least 2 independent experiments. An amino acid alignment of all Envs used is shown with a red box highlighting residue 134 (B).

**Amino acid sequence rather than glycosylation status in V2 defines neutralization sensitivity to Mabs.**

As shown previously, Mab 8.9D potently neutralized 0-month Env 6.3 regardless of whether the N134S (V1-NYS) was present. However, an R189S mutation, present in an 8-month escape variant, inserted the NSS glycan motif at the terminal end of V2 (Fig. 4B) and was sufficient to render the Env completely resistant to this Mab (Fig. 4A; Env V1-NYN V2-NSS). Surprisingly, glycosylation at this site was not necessary to induce resistance to Mab 8.9D. Substitution of a histidine for R189 resulted in a 200-fold increase in resistance to the Mab (Fig. 4A). Interestingly, the effect of mutating R189 was further modulated by the presence of the NYS glycan motif in V1. While the V1-NYN V2-NSS Env was resistant to 25 µg/ml of 8.9D, it was neutralized 50% at this same concentration when the V1-NYS motif was present (Env V1-NYS V2-NSS). A similar result was seen when V1-NYN V2-NSH and V1-NYS V2-NSH were compared, with the V1 glycosylation motif increasing net sensitivity 10-fold. Collectively these data suggest a cooperative effect between these two positions in neutralization by Mab 8.9D, with R189 acting as the dominant neutralization determinant. Thus although R189 was necessary for potent neutralization by 8.9D, changes at both 189 and 134 modulate sensitivity to this Mab.

A somewhat different synergy between residues 134 and 189 was seen with Mab 6.4C. As previously shown, the 0-month Env 6.3 was sensitive to neutralization by this Mab and changes at position 134 did increase neutralization sensitivity by

10-fold (Fig. 3A & 4A). Interestingly, substitutions at position 134 had no effect on neutralization in the context of the R189 mutations for 6.4C. When either the V2-NSS mutation or the V2-NSH mutation was introduced, the Envs became completely resistant irrespective of whether the V1 glycan motif was present or not. Thus, like 8.9D, 6.4C requires an R189 residue for neutralization, but in this case the requirement is absolute and loss of this residue resulted in complete resistance.

In contrast, Mab 13.6A exhibited an absolute requirement for the V1 glycosylation site and the R189 residue for neutralization. Thus, despite containing the V1 NYS glycan motif, Envs V1-NYS V2-NSS and V1-NYS-NSH were resistant to 13.6A (Fig 4A). Similarly, any Env that lacked the V1 glycosylation site was resistant as well (Fig 3A & 4A). Therefore, the two residues at 134 and 189 play a key cooperative role in antibody neutralization by Mab 13.6A.

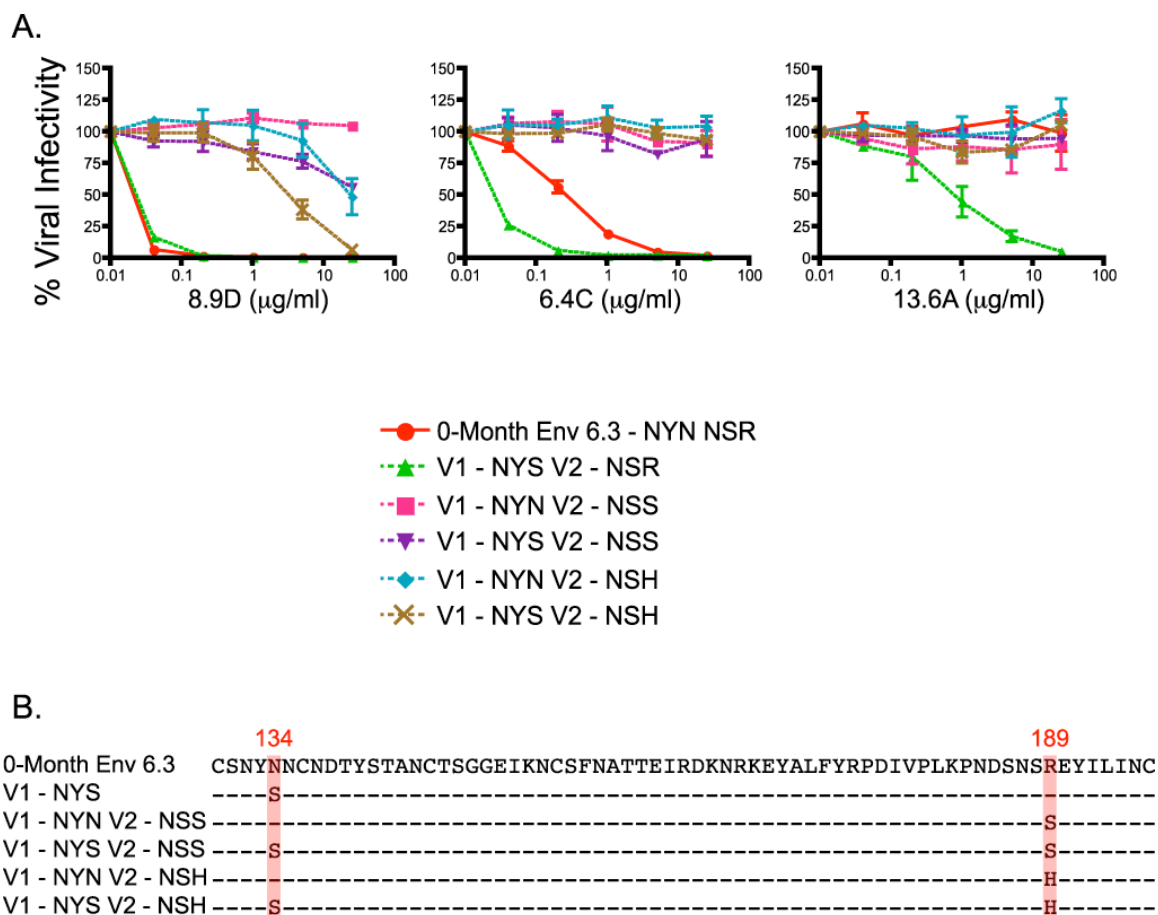


**Figure 4. Mab neutralization of Env 6.3 and V2 mutants.**

0-month FPL Env 6.3 was used as a backbone for mutations at residue 189 in conjunction with residue 134, and these Envs were assessed for sensitivity to Mabs 8.9D, 6.4C and 13.6A using pseudoviruses (A). Each line on the graph represents an individual Env pseudovirus as listed in the key. Percent viral infectivity compared to no Mab is shown on the vertical axis and was calculated from luciferase units by dividing virus-infected wells in the presence of antibody by the virus-infected well in the absence of antibody. The concentration of each Mab (in  $\mu\text{g/ml}$ ) is plotted on the horizontal axis on a  $\log_{10}$  scale. Error bars represent the standard error of the mean of at least 2 independent experiments.

An amino acid alignment of all Envs used is shown with a red box highlighting residues 134 and 189 (B).

**Residues 134 and 189 may contribute to a single epitope near the V1V2 stem.**

On the linear amino acid sequence, positions 134 and 189 occur in the N- and C-terminal regions, respectively, of the V1V2 domain. To gain insight into their position with respect to the 3-dimensional gp120, and in particular the V1V2 loop, residues 134 and 189 were viewed on a composite, CD4 bound gp120 structure onto which the 205F Env

6.3 sequence was homology modeled. Fig. 5 displays one possible conformation in which these residues coalesce at the interface of the V1 and V2 loops in a region that could be stabilized by multiple disulfide bonds, including an unusual pair of cysteines in the V1 loop that are found in most 205F Envs. This potential epitope is also located directly above the V1V2 stem, which is a highly conserved structure. The mean distance between the C-alpha atoms of N134 and R189 based on the molecular dynamics simulation is 27 (+/- 2) Angstroms, which is consistent with the formation of an antibody epitope. For example, amino acids that comprise the epitope for Mab b12 can be as far apart as 37 Angstroms (187). Thus it is feasible that the 205F Mabs recognize slightly different versions of a novel conformational epitope at the interface of V1 and V2 comprised of these two residues and, in the case of 13.6A, carbohydrate moieties. Furthermore, the variations in neutralization determinants of the three Mabs suggest that this region of V1V2 may exist in multiple conformations, or orientations, several of which elicited a B cell response.

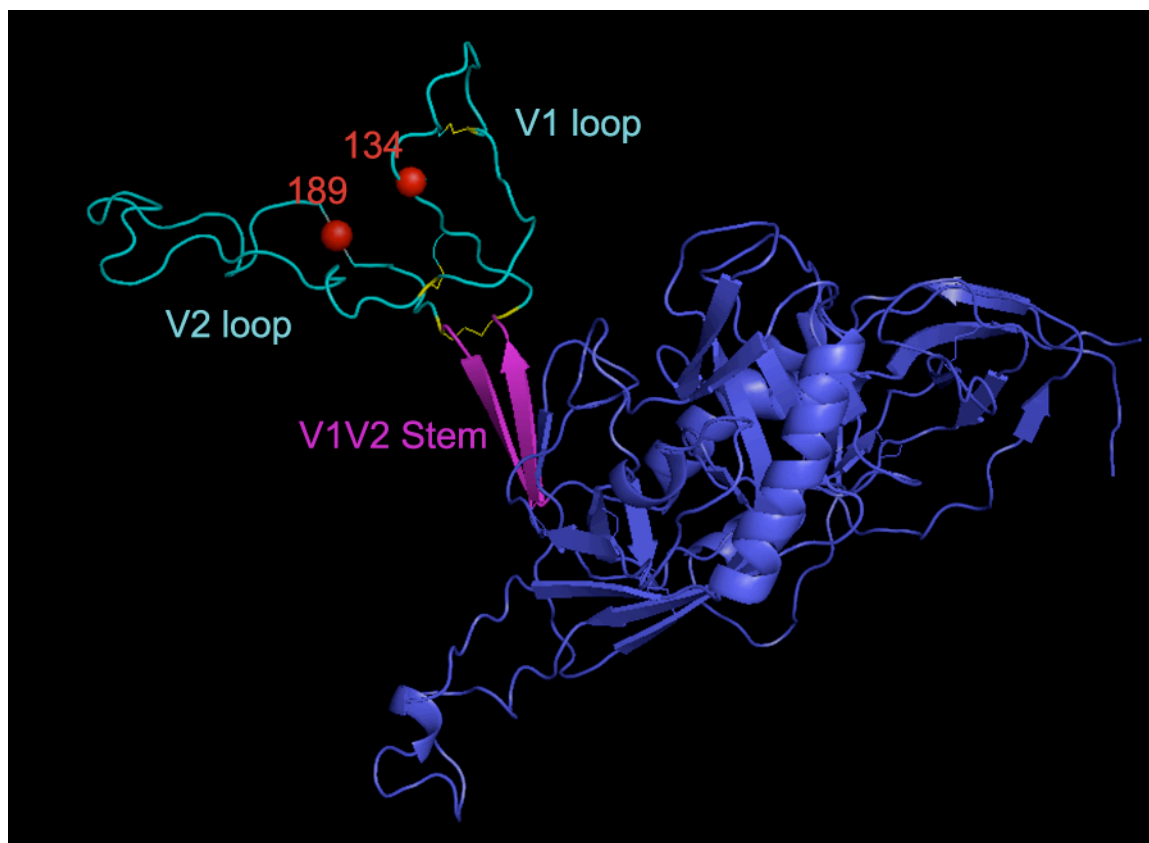


**Figure 5. Model of residues 134 and 189 in the V1V2 domain of o-month FPL Env 6.3.**

Homology modeling was used (see Materials and Methods) to generate a 3-D structure of o-month FPL Env 6.3 gp120 (in blue) and visualized in MacPyMOL. The V1V2 domain is shown in cyan with disulfide bonds in this region highlighted in yellow. The V1V2 stem is labeled and shown in magenta. Residues 134 and 189 are represented by red spheres.



**Amino acid changes at residues 134 and 189 do not overtly affect replication fitness in vitro.**

To date, the question of whether specific autologous neutralization escape mutations exact a replication cost on the virus has not been explored. To investigate this possibility, the 0-month Env 1.1 and the 0-month Env 6.3 with the V1-NYS and V2-NSS motifs introduced singly and in combination were cloned into a replication competent NL4.3 proviral backbone and used to infect PBMC enriched for CD4 T cells by CD8 depletion. Supernatant was collected every two days and viral p24 was quantified for a measure of viral replication for a 10-day period (Fig. 6). The subtype C provirus MJ4 was used as a positive control for replication in CD4 T cells (119), and none of the Envs tested replicated as well as MJ-4. The 0-month Env1.1, which contained the V1 to V4 region of the founder virus (146), replicated moderately well, while the 0-month Env 6.3 which resisted neutralization by 13.6A due to its lack of a glycosylation motif in V1 replicated to similar if slightly better levels by day 10 (Fig 6A). Thus in this assay, the ability to escape Mab neutralization by losing a glycan sequon did not adversely affect replication. To completely escape neutralization by all three Mabs (13.6A, 6.4C and 8.9D); however, the 0-month Env 6.3 required a change at position R189, which in one 8-month escape virus was a serine (Fig. 4A). Interestingly, introducing this autologous escape mutation (NSS) into the Env 6.3 had a detrimental effect on replication (Fig 6B), a fact which may explain why the V1-NYN V2-NSS lineage is not seen circulating at later timepoints in seroconverter 205F (146). Instead, the escape pathway utilized by later Envs was to create the R198S change while preserving the V1 glycosylation motif. Indeed,

when the V2-NSS mutation was introduced into Env 6.3 in combination with V1-NYS, the virus replicated better than the V2-NSS Env, suggesting that the V1 NYS may in some way compensate for the V2-NSS replication cost (Fig 6C). Thus, these results argue that the R189S mutation that confers resistance against autologous Mabs had only a minor effect on replication in this in vitro assay system in the context of the V1 glycosylation site, although it is important to note that this mutation was tested in the absence of other compensatory changes that may have been present in vivo.

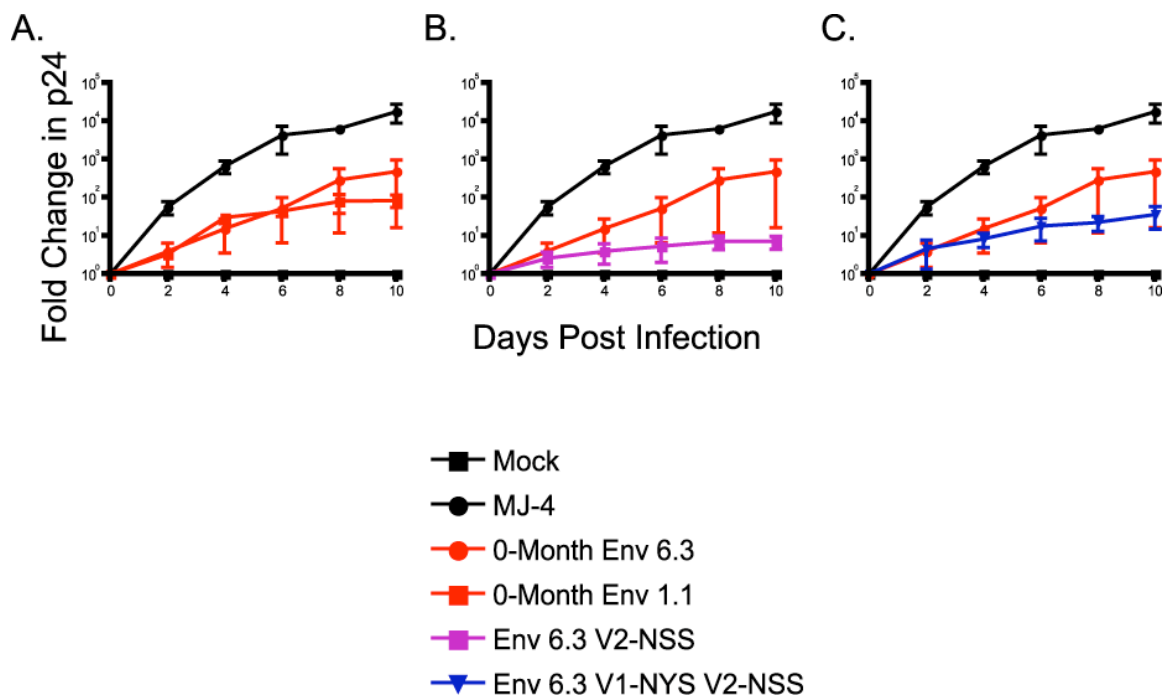


**Figure 6. Replication kinetics of parent and mutant Envs in PMBC.**

o-month Envs 6.3 and 1.1 (A) as well as mutant Envs V2-NSS (B) and V1-NYS V2-NSS (C) were placed into a replication competent NL4.3 backbone and used to infect CD8-depleted human PBMC. Viral p24 antigen (pg/ml) production in the supernatant was measured by ELISA on day 10 and is plotted as fold change over day 0 on the vertical axis on a log<sub>10</sub> scale. The positive control virus MJ-4 is shown in black circles and the mock-infected negative control is shown by black squares. The error bars for each Env were calculated from three independent experiments using PBMC from three different seronegative donors.

## V. Discussion

### **By 8-months post-seroconversion, multiple B-cell clones produced somatic variations of antibodies that neutralize the virus.**

In HIV-1 infection, V1V2 has been shown to be a target of Nabs (81, 173), and multiple monoclonals isolated from sero-positive subjects bind this region (59, 60, 72). This domain can confer escape from Nabs as well either through shielding affects or sequence change (131, 144, 147). Furthermore, V1V2 has been shown to confer strain specificity to the Nab response during SHIV infection of rhesus macaques (91). Thus, it is not surprising that in addition to V5 and C3 in gp120, the V1V2 region is targeted by early antibodies during subtype C infection.

The current report is one of the first to reveal that in one subtype C infected subject, the early Nab response is focused upon V1V2 but is actually comprised of multiple antibody specificities, all targeting the same structure within V1V2.

Sequence analysis revealed that these five antibodies were mostly likely derived from 3 distinct B-cell clones, although all five showed variation from germline preferentially in the CDR regions, indicating somatic hypermutation. Mabs 6.4C and 8.9D were more highly mutated than the other three Mabs, and also displayed greater breadth and potency against the autologous Envs. These observations suggest that 6.4C and 8.9D had undergone more extensive affinity maturation that increased their efficacy against autologous viral variants.

Collectively, the five 205F Mabs neutralized all Envs from 0 and 2 months post-seroconversion; however, by 8-months, the plasma escape variants were also refractory to neutralization by the Mabs. These data suggest that although these

Mabs were isolated from B cells circulating four to five years after infection, they are representative of the major plasma pool at 8-months post-seroconversion. Furthermore, what appeared to be a mono-specific response against V1V2 in plasma is actually multiple B cell clones producing distinct neutralizing antibodies against this target.

**Mutational analysis reveals that residues 134 and 189 contribute to a novel epitope near the V1V2 stem.**

It has been well documented that V1V2 can contain neutralization and escape determinants from Nabs (116, 131, 144, 146, 147, 172), and in seroconverter 205F, escape through sequence changes in V1V2 was demonstrated previously (146). Here we define a potential conformational epitope at the V1V2 interface in this subject that is glycan dependent in one case. The three Mabs from 205F evaluated in this study (13.6A, 6.4C and 8.9D) are dependent upon positions 134 and 189 in V1V2 for neutralization to varying degrees, with the Mabs showing a decreasing dependence on glycosylation at residue N132 (13.6A>6.4C>8.9D). Mab 13.6A was the only one that absolutely required a glycan sequon (residues 132-134) in V1 for neutralization; however, the NYS and NYT glycosylation motifs were not equivalent in neutralization sensitivity, differing by 10-fold. One possible explanation for this observation is that serine and threonine are recognized differentially by the antibody, but conversely, mutants containing asparagine or glutamine were not neutralized, a fact that argues against tolerance for variation at this position. It is also possible that NYS and NYT are differentially glycosylated and/or that protein folding in this region is affected by

the S134T change, causing a slight structural variation that affects antibody binding. Indeed, removal of a single glycan has been shown to affect trimer conformation (9). In any case, this finding is consistent with the idea that N-linked glycan motifs are not equivalent (80).

Overall, the results imply that the three Mabs recognize a common epitope formed by positions 134 and 189 at the interface of the V1V2 loop. Alternatively, one position may not be included in the epitope, but rather could allosterically influence the other. However, each Mab appears to have a slightly different requirement for neutralization, suggesting that this region may adopt multiple conformations or orientations within a single Env variant that are recognized by different B cell receptors. It is possible that each Mab binds the epitope in a subtly different orientation and thus is influenced differentially by surrounding residues. This phenomenon would be similar to the variations seen in Mabs that recognize the CD4 binding site (25). Alternatively, the virus that elicited each of these Mabs could have differed slightly in this region. A similar phenomenon was reported for a series of Mabs that were generated against SHIV162P in macaques. These Mabs recognize a series of overlapping epitopes within a common V2 structure, and vary in their recognition of amino acid sequence and glycosylation pattern (143). The region encompassing the V1V2 stem has been shown to affect both CD4 binding as well as formation of the bridging sheet, leading to the possibility that the 205F Mabs neutralize by a common mechanism in which they block gp120 interactions with CD4 or CCR5.

## **Glycosylation plays varying roles in neutralization during early infection.**

Studies of glycosylation patterns in gp120 are commonly performed on sequence alone, with the addition of putative N-linked glycan motifs often associated with neutralization resistance. Indeed there is ample evidence for the role of the ‘glycan shield’ as a robust mechanism of viral escape from Nab (23, 83, 93, 99, 105, 176, 179). Nevertheless, we here provide further data indicating that the reverse is also true. Mab 2G12 has long been identified as a broadly neutralizing antibody that is directed against glycans in gp120 (149, 153, 169), and other monoclonals that require a glycan for binding have been described (43, 173, 175). Our data offer another demonstration that anti-glycan specificities occur naturally during infection and provide an example of how removing a glycosylation motif in V1 can result in autologous neutralization resistance.

The sequence changes associated with creating glycan motifs can themselves be important for neutralization. For 6.4C and 13.6A, it is the amino acid change as opposed to the creation of a glycan motif in V2 that disrupts antibody neutralization. This observation is consistent with recent studies demonstrating that sequence changes in the context of a glycan motif are sufficient to disrupt neutralization sensitivity or resistance (16, 143). It should be noted; however, that in none of these studies was it confirmed that the NXS/T motifs are glycosylated. Nevertheless, other studies have provided evidence that the majority of glycan motifs in HIV-1 gp120 are glycosylated, arguing that the motifs in V1 and V2 under study are indeed likely to be modified by carbohydrate addition (57).

Overall, changes in glycan motifs can affect neutralization in multiple ways, not all requiring glycosylation, making this an efficient scheme for the virus to utilize for Nab escape.

### **Replication kinetics of neutralization resistant Envs is similar to neutralization sensitive Envs.**

In addition to reducing neutralization sensitivity, escape mutations in Env could potentially affect replication fitness and result in lower viral load. One study found a negative correlation between autologous titer and viral load in chronic infection, but another demonstrated no correlation between these two parameters in long-term non-progressors (39, 104). In subtype C infection, a slight dip in viral load was observed concurrent with the appearance of certain autologous Nab specificities (116). In vitro data has demonstrated no correlation between resistance to broadly neutralizing antibodies and replication (136), but has found that alanine mutations of targeted epitopes may result in loss of infectivity (130). To date, specific mutations that arise naturally during infection and confer resistance to autologous Nabs have not been examined for their effect on replication kinetics in vitro. Here we investigated the in vitro replication kinetics in CD4 T cells of Envs with and without the V2-NSS motif, which confers global autologous Mab escape. In the context of the 0-month Env 6.3, the V2-NSS motif had a detrimental affect on replication, suggesting that fitness cost may play a role in autologous escape pathways. However, HIV-1 uses multiple escape pathways and compensatory mutations to overcome this disadvantage. It is possible that further differences could have been detected in a more sensitive



fitness competition assays; however, these data suggest that it is quite possible for Env to escape the humoral immune response without overt loss of replication capability.

Overall, this study describes a potential novel conformational epitope that is present in a subtype C infected subject during early infection and could be located at the interface of the V1 and V2 loops. This potential epitope was recognized by at least three different B cell receptors on the native Env trimer, and elicited both glycan dependent and independent Mabs. Thus, there are complex and immunogenic structures formed by V1V2 on the native Env, and these may exist in slightly different conformations or be recognized in slightly different ways by distinct B cells. While we presently studied only one subject, these Mabs are likely to be representative of those that arise during the early neutralizing response in many HIV-1 infected subjects, as this response is often focused on only one or a few targets and is readily escaped. The findings provide new insight into why the early autologous Nab response is ineffective and fails to contain the virus. The results also illustrate the power of a single, strategically placed amino acid change in viral escape. The redundant and highly focused nature of the Mabs in this subject suggests that to elicit Nab breadth with an Env immunogen, it will be critical to present only the desired epitope, such as the CD4 binding site, and eliminate others that might be divert the B cell response.

Supplemental Table 1

| Mab Name          | V-allele    | D-allele    | J-allele | CDR3 amino acid       | DJ n nucleotides <sup>a</sup> | DJ junction                 | Number of Mutations from Germline | Frequency of Mutations | R/S ratio FR <sup>b</sup> | R/S ratio CDR <sup>c</sup> |
|-------------------|-------------|-------------|----------|-----------------------|-------------------------------|-----------------------------|-----------------------------------|------------------------|---------------------------|----------------------------|
| 8.9D Heavy chain  | IGHV3-15*01 | IGHD4-04*01 | IGHJ4*02 | TTVLTTRRAY<br>DAGSDY  | 23                            | ATAGAGCCTAAG<br>ATGCAGGGAGC | 26                                | 8.84%                  | 13/5                      | 8/0                        |
| 6.4C Heavy chain  | IGHV3-15*01 | IGHD4-04*01 | IGHJ4*02 | TTVLTTRRAY<br>DAGSDN  | 22                            | ATCGTGCCTAAG<br>ATGCAGGGAG  | 38                                | 12.93%                 | 13/12                     | 10/3                       |
| 10.9D Heavy chain | IGHV3-15*01 | IGHD5-12*01 | IGHJ4*02 | TTVLTTRDSAY<br>DAGIGY | 11                            | GCAAGGATCGG                 | 13                                | 4.42%                  | 4/4                       | 5/0                        |
| 6.1C Heavy chain  | IGHV3-15*01 | IGHD5-12*01 | IGHJ4*02 | TTVLTTRDSAY<br>DAGIGY | 11                            | GCAAGGATCGG                 | 12                                | 4.08%                  | 3/4                       | 5/0                        |
| 13.6A Heavy chain | IGHV3-15*01 | IGHD5-12*01 | IGHJ4*02 | TTVLTTRDSAY<br>DAGIGY | 11                            | GCAAGGATCGG                 | 11                                | 3.74%                  | 4/2                       | 5/0                        |

<sup>a</sup> Non-templated nucleotides added at the DJ junction.

<sup>b</sup> The replacement to silent mutation ratio found in the framework regions.

<sup>c</sup> The replacement to silent mutation ratio found in the complementarity-determining regions.

## **VI. Acknowledgements**

We would like to thank the interns, staff, participants, and Project Management Group at ZEHRP. We also gratefully acknowledge productive input from Dr. Joshy Jacob. The work in this paper was supported by NIH grant AI-58706. SG was supported by LANL/DOE grant X9R8. AS was supported by CNLS.

## VII. Contributors

Rebecca M. Lynch<sup>1,3</sup>, Rong Rong<sup>2,3</sup>, Saikat Boliar<sup>2,3</sup>, Anurag Sethi<sup>8</sup>, Bing Li<sup>3</sup>,  
Joseph Mulenga<sup>6</sup>, Susan Allen<sup>4,5</sup>, James E. Robinson<sup>7</sup>, S. Gnanakaran<sup>8</sup> and  
Cynthia A. Derdeyn<sup>2,3\*</sup>

Immunology and Molecular Pathogenesis Program<sup>1</sup>, Department of Pathology  
and Laboratory Medicine<sup>2</sup>, Emory Vaccine Center<sup>3</sup>, Department of Global  
Health<sup>4</sup>, Rollins School of Public Health<sup>5</sup>, Emory University, Atlanta, GA.  
Zambia Blood Transfusion Service<sup>6</sup>, Lusaka, Zambia.

Department of Pediatrics<sup>7</sup>, Tulane University School of Medicine, New Orleans,  
LA.

Theoretical Division, Los Alamos National Laboratory<sup>8</sup>, Los Alamos, NM 87545.

## **Chapter Four:**

### **Thesis Discussion**

The extreme genetic diversity of HIV-1 poses a significant challenge for global vaccination approaches, and strategies to overcome this are extremely limited at present. In an effort to understand the biological consequences of inter-subtype diversity, recent research has linked genetic differences in Env to both phenotypic and antigenic properties. A particular focus has been on subtypes B and C, where differences have been associated with distinct autologous humoral responses that vary in gp120 targets as well as in cross-reactive breadth, especially in the V3 domain. It is important to note that differences between subtypes that circulate in distinct geographic regions, such as B and C, could also reflect dissimilarity in the host population from which the viruses were derived, epidemic patterns, the route of infection, etc. Nevertheless, as studies continue to uncover subtype-specific differences in Env function, structure, and antigenicity, these will be important to incorporate into global vaccine design. Furthermore, in light of the prevalence of subtype C infection worldwide, it becomes especially important to study the host immune response to this subtype in particular.

In this vein, I first explore in chapter two, possible explanations for a particular conservation pattern in subtype C V3 domains. In an analysis of sequences in the Los Alamos HIV Database, the subtype C V3 domain is more conserved than other subtypes (data not shown and (124)). My lab has recently observed as well that V3 remains remarkably conserved during the first two years of infection despite increasing sequence variation in V1V2, the gp120 outer domain, and gp41

(146). In particular, I observe a highly conserved residue (I309) in subtype C Envs that exhibits high entropy in other subtypes. While this and other subtype-specific mutational patterns in V3 have been well established (54, 55, 86, 124, 145, 158), this study is among the first to delve into the biology that might explain these observations.

Variability in entropy between subtypes B and C in V3 occurs between residues 304-321. Position 309 is the only one of these 16 residues where subtype C stays essentially the same (Ile) and subtype B toggles between 4 amino acids (Ile, Met, Leu and Val). Therefore I would propose that residue 309 is representative of differences in conservation between subtype B and C V3. A caveat to these studies is that they are limited to this one position; however, it is likely that sequence patterns conserved in all subtypes represent residues highly necessary for correct viral function. For example, the GPG turn motif at the V3 tip is well conserved in all subtypes (<http://www.hiv.lanl.gov>) and previous mutational studies have shown that changes to the GPG motif led to drastically lower fusion and infectivity (49). In contrast, subtype C Envs carrying L309 use limiting CD4 more efficiently in entry experiments and replicate to wildtype levels *in vitro* in the absence of antibody suggesting no detectable detrimental effect on either infectivity or replication. Furthermore, this proficient use of CD4 appeared to expand the ability of these Envs to infect macrophages, albeit inefficiently. In no case, however, did the wildtype subtype C virus replicate in macrophages to any detectable degree rendering the macrophage tropism of I309L Envs all the more

interesting. This expanded tropism should, in theory, be advantageous to the virus, not detrimental.

A possible reason that this I309L mutation allowing macrophage tropism does not occur in vivo is my findings that these Envs were over-all more sensitive to sCD4, anti-V3 antibody, and 17b after triggering with sCD4. Although there was no difference between L309 and I309 Envs when examining neutralization by autologous or heterologous plasma pools, the monoclonal antibody data suggests a subtle difference in neutralization susceptibility between mutant and wildtype Envs. It is possible that the autologous plasma more accurately corresponds to the antibody-containing microenvironment that pressures these viruses, and that the neutralization by monoclonals is only superficially representative. However, there is evidence that when examining subtle differences in neutralization sensitivity and escape, monoclonals may reveal differences that are drowned out in the presence of large polyclonal antibody pools in plasma ((12, 146) and Chp.3). Although most of the targeted epitopes in patient plasma remain unknown, it has been shown that HIV-infected patients have large titers of anti-co-receptor and anti-V3 antibodies, and to varying degrees anti-CD4bs antibodies, (11, 37, 38, 65, 95, 115, 173). Therefore, it is plausible that L309 Envs are more susceptible to these antibodies specifically within the plasma, especially if increased exposure of the CD4bs also leads to 'pre-triggering' of these Envs. Taken together these data suggest that any increased advantage in terms of cell tropism conferred by L309 may be outweighed by the increased neutralization sensitivity due to exposure of epitopes such as the CD4bs. These data begin to

suggest a biological explanation for the strict conservation of the subtype C V3 domain by linking it to the prevention of neutralization epitope exposure, although structural concealment of V3 epitopes has been observed previously (10, 37, 115). This chapter provides novel insight at a population or subtype level into the delicate balance the virus must have between infectivity (CD4bs exposure and increased cell tropism) and evasion of the host immune response.

What is the possible mechanism by which subtype C HIV uses conservation of V3 to hide neutralization targets? The V3 domain does not exhibit the types of mutations that other neutralization escape mechanisms require, such as an evolving glycan shield (176) or an expanding V1V2 domain (131, 144, 147). An all-atom molecular dynamics simulation previously performed supports the existence of a cluster of hydrophobic residues flanking the V3 tip (anchored by residues I307, I309, and F317) (101), and further evidence for this cluster or 'hydrophobic face' has recently been published using structural analysis of V3 peptide-antibody complexes (78). These 3 positions are highly conserved in subtype C sequences in the database and are largely restricted to hydrophobic amino acids (55, 145, 158). Thus, stabilizing forces may drive this hydrophobic cluster to avoid solvent exposure by burying itself within the V3 loop or into the gp120 core, in the vicinity of the CD4bs and V1V2 on the same or a neighboring protomer. In fact, coarse-grained calculations have demonstrated that V3 (and perhaps the hydrophobic cluster) has the potential to interact with multiple core residues, several of which are proximal to the CD4 binding site and may impact CD4 binding ((101) and Fig. 1). For subtype C viruses, maintaining this cluster in



an optimal position by limiting sequence variation in the V3 tip could be critical for immune avoidance. This paradigm, therefore, provides a biologically plausible explanation for the I309L phenotype I observed, as well as a compelling reason for conservation of subtype C V3.

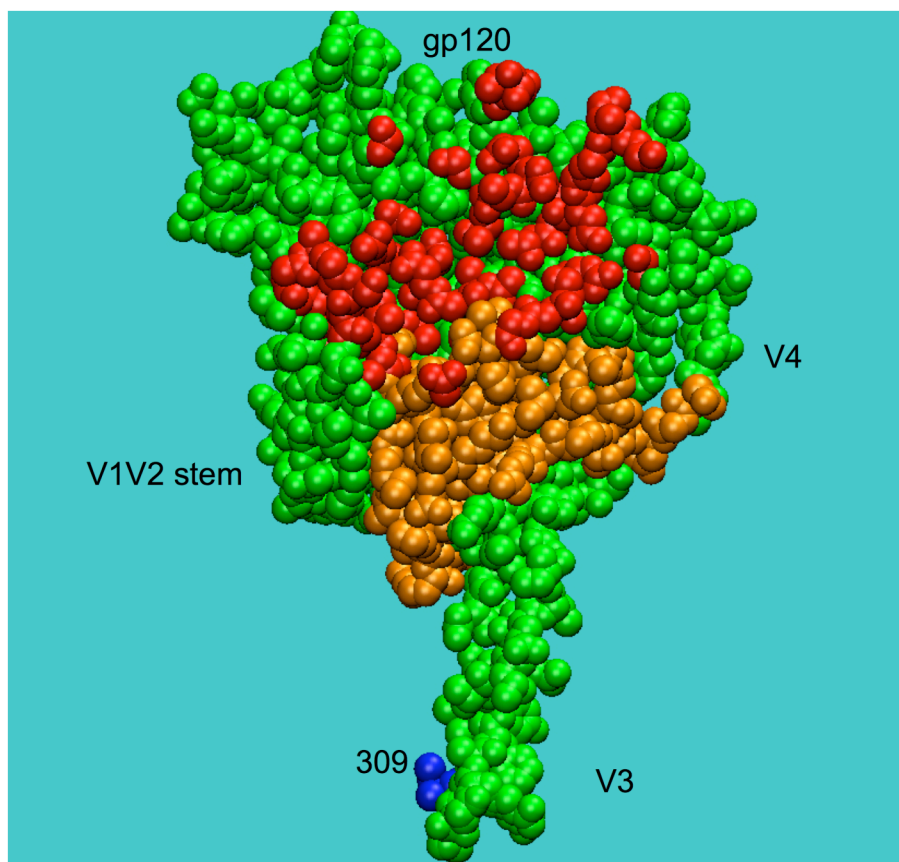


**Figure 1. Regions in core gp120 that could potentially interact with Ile 309.**

To identify regions of gp120 that could potentially interact with V3, a coarse-grained model was used, and residues that showed any contact probability with Ile 309 are mapped onto the gp120 structure (2B4C; (73)) in orange. Residues that have been previously shown to participate in CD4 binding are red. The position of Ile 309 at the V3 crown is highlighted in blue.

While conservation of sequence as a mechanism of immune avoidance may be observed at a population level, it is more likely that sequence variation will be used to escape host immune pressure within an individual. In chapter three, I explore this latter escape method in more detail by using autologous monoclonal antibodies to elucidate a potential epitope targeted in early infection as well as residues that confer resistance to this neutralization. These data begin to reveal how the virus escapes humoral immune pressure through sequence variation without crippling effects on replication.

Five antibodies were cloned out of peripheral memory B-cells isolated at 49 and 69 months post-seroconversion from a Zambian subject. These antibodies were screened for neutralizing activity against 0-month FPB Env 1.1, which has the V1-V4 sequence of the founder virus (146). Sequence analysis revealed that these five antibodies were mostly likely derived from 3 distinct B-cells, although all five showed variation from germline, indicating somatic hypermutation. These Mabs were next analyzed for their ability to neutralize autologous Envs from longitudinal time-points. This functional analysis revealed that these Mabs neutralized all but one Env from 0 and 2 months post-seroconversion, but that by 8-months, the Envs that were plasma escape variants were also refractory to neutralization by the Mabs. These data suggest that although these Mabs were isolated at a later time point, they represent the major plasma pool at 8-months post-seroconversion.

These Mabs likely arose between 2-8 months post seroconversion, and it was previously established by Rong et al. (146) that Nab in this seroconverter mainly targeted the V1V2 domain within the first two years of infection, making it the likely target for all five Mabs. This fact is not surprising considering that V1V2 has frequently been shown to be a target of Nabs (81, 115, 116, 173), and multiple monoclonals isolated from sero-positive subjects bind this region (59, 60, 72). This domain can confer escape from Nabs as well either through shielding effects or sequence change (131, 144, 147). My studies with autologous Mabs add to this body of literature by illuminating that this singular response against V1V2 in plasma is actually multiple B cell clones producing distinct neutralizing antibodies against this target.

Using a mutagenesis strategy I demonstrate that three Mabs isolated from this subject have varying requirements of positions 134 and 189 in the V1V2 domain for neutralization. Mab 13.6A requires a glycan motif at 132-134 in V1 as well as an arginine at 189; however, the glycan-encoding motifs NYS and NYT are not equivalent in neutralization sensitivity. Mabs 6.4C and 8.9D require R189 for neutralization, but this sensitivity is affected to varying degrees by the V1 glycan motif. Overall, these data suggest that the Mabs bind, albeit in different ways, a common epitope formed by these two residues at the stem of the V1V2 loop.

Using computer modeling to view a possible conformation of this epitope (Chp. 3 Fig. 5), I can propose a mechanism for neutralization by these Mabs. Since the V1V2 stem has been shown to affect both CD4 binding as well as formation of the bridging sheet, antibody binding to this putative epitope could potentially block

viral binding to either CD4 or CCR5. It should be noted, however, that this epitope is putative and further binding studies will need to be performed to rule out the possibility that 134 and 189 affect neutralization through allosteric effects on a distant epitope.

The 'glycan shield' is a commonly cited term for a mechanism of viral Nab escape (see Chapter 1) whereby the virion is covered by glycans that hide or shift Nab targeted epitopes (9, 176). The Mab data presented in chapter three; however, emphasizes a complicated role for glycosylation in humoral immune escape. The Mabs highlight the fact that anti-glycan specificities do occur during natural infection meaning that potential N-linked glycosylation sites (PNGS) are not synonymous with Nab escape but rather can indicate sensitivity as well.

Interestingly, the neutralization profile of Mab 13.6A implies that even though NXT and NXS are both N-linked glycan motifs, they are not structurally equivalent in their presentation of the 13.6A epitope. A second reason that PNGS should not be automatically correlated with Nab escape is that my data along with other recent reports (16, 143) reveal that the sequence change associated with the insertion of a glycan sequon may be sufficient to affect neutralization. In other words, it is the amino acid that is the determinant of sensitivity not the linked glycan. For the three Mabs I studied (13.6A, 6.4C & 8.9D), the R189S mutation conferred escape because of the loss of the arginine as opposed to the insertion of a glycan motif (NSR to NSS).

Thus, the single R189S mutation escapes all three Mabs 13.6A, 6.4C and 8.9D, suggesting that this is an efficient escape pathway for the virus to follow. In addition to reducing neutralization sensitivity, escape mutations in Env could potentially affect replication fitness and result in lower viral load. To date, specific mutations that arise naturally during infection and confer resistance to autologous Nabs have not been examined for their effect on replication kinetics in vitro. In chapter 3, I investigate the ability of Envs with and without the Mab escape V2-NSS motif to replicate in CD4 T cells. It appears that in the background of 0-month Env 6.3, this R189S V2 mutation can detrimentally affect replication; however, in the presence of the V1 N134S mutation, replication returns to parental level kinetics. Thus these data demonstrate for the first time that it is possible for the virus to escape multiple Nabs while maintaining replication fitness.

## **Conclusion**

In conclusion, studying the natural humoral immune response may provide insight into how an effective vaccine might be designed. In this thesis, I attempt to determine mechanisms of viral escape from neutralizing antibody pressure. Often, areas of conservation in gp120 are thought to be ideal candidates for immunogens that would provide broad vaccine coverage. I first show that in subtype C Envs, the V3 domain may be particularly conserved to sterically conceal Nab targets such as the CD4bs. Thus, areas of conservation may elicit antibodies with broad neutralization potential but if the epitope is hidden on the

trimer, neutralization will not be possible. This observation is particularly important because of the current focus on the CD4bs as a conserved vaccine target. This avenue of research must take into account structural differences between subtypes, and recent publications have, in fact, widened the number and diversity of viruses a Mab must neutralize in order to be labeled as “broadly neutralizing”. Furthermore, the lack of sequence change in V3 may be the reason that CXCR4 viruses are less frequently seen in subtype C infection as compared to subtype B (22, 26, 28, 29, 109, 120, 160), and therefore, may have consequences for antiviral treatment with entry inhibitors against CCR5.

Another reason that broad vaccine coverage remains unattainable is the tolerance Env shows for high levels of sequence diversity. Here in chapter three, I demonstrate that during early subtype C infection in one seroconverter, the antibody response is comprised of multiple B-cell clones targeting the same region of gp210 (V1V2). Thus, one reason that antibodies may fail to control the virus, is that this limited response is easily escaped with minimal sequence change, giving the virus time to discover an escape pathway with the least effect on replication kinetics. These data suggest that future vaccine design might be well served to include multiple epitopes and expand the antibody response beyond the limited one that naturally arises in order to ‘box’ the virus in with the fewest possible escape pathways.

## Bibliography

1. **Aasa-Chapman, M. M., A. Hayman, P. Newton, D. Cornforth, I. Williams, P. Borrow, P. Balfe, and A. McKnight.** 2004. Development of the antibody response in acute HIV-1 infection. *Aids* **18**:371-81.
2. **Agrawal-Gamse, C., F. H. Lee, B. Haggarty, A. P. Jordan, Y. Yi, B. Lee, R. G. Collman, J. A. Hoxie, R. W. Doms, and M. M. Laakso.** 2009. Adaptive mutations in a human immunodeficiency virus type 1 envelope protein with a truncated V3 loop restore function by improving interactions with CD4. *J Virol* **83**:11005-15.
3. **Alexander, M., R. Lynch, J. Mulenga, S. Allen, C. A. Derdeyn, and E. Hunter.** 2010. Donor and recipient envs from heterosexual human immunodeficiency virus subtype C transmission pairs require high receptor levels for entry. *J Virol* **84**:4100-4.
4. **Arendrup, M., C. Nielsen, J. E. Hansen, C. Pedersen, L. Mathiesen, and J. O. Nielsen.** 1992. Autologous HIV-1 neutralizing antibodies: emergence of neutralization-resistant escape virus and subsequent development of escape virus neutralizing antibodies. *J Acquir Immune Defic Syndr* **5**:303-7.
5. **Armstrong, K. L., T. H. Lee, and M. Essex.** 2009. Replicative capacity differences of thymidine analog resistance mutations in subtype B and C human immunodeficiency virus type 1. *J Virol* **83**:4051-9.
6. **Ashkenazi, A., D. H. Smith, S. A. Marsters, L. Riddle, T. J. Gregory, D. D. Ho, and D. J. Capon.** 1991. Resistance of primary isolates of human immunodeficiency virus type 1 to soluble CD4 is independent of CD4-rgp120 binding affinity. *Proc Natl Acad Sci U S A* **88**:7056-60.
7. **Bannert, N., D. Schenten, S. Craig, and J. Sodroski.** 2000. The level of CD4 expression limits infection of primary rhesus monkey macrophages by a T-tropic simian immunodeficiency virus and macrophagetropic human immunodeficiency viruses. *J Virol* **74**:10984-93.
8. **Barin, F., M. F. McLane, J. S. Allan, T. H. Lee, J. E. Groopman, and M. Essex.** 1985. Virus envelope protein of HTLV-III represents major target antigen for antibodies in AIDS patients. *Science* **228**:1094-6.
9. **Binley, J. M., Y. E. Ban, E. T. Crooks, D. Eggink, K. Osawa, W. R. Schief, and R. W. Sanders.** 2010. Role of complex carbohydrates in human immunodeficiency virus type 1 infection and resistance to antibody neutralization. *J Virol* **84**:5637-55.
10. **Binley, J. M., E. A. Lybarger, E. T. Crooks, M. S. Seaman, E. Gray, K. L. Davis, J. M. Decker, D. Wycuff, L. Harris, N. Hawkins, B. Wood, C. Nathe, D. Richman, G. D. Tomaras, F. Bibollet-Ruche, J. E. Robinson, L. Morris, G. M. Shaw, D. C. Montefiori, and J. R. Mascola.** 2008. Profiling the specificity of neutralizing antibodies in a large panel of plasmas from patients



- chronically infected with human immunodeficiency virus type 1 subtypes B and C. *J Virol* **82**:11651-68.
11. **Binley, J. M., T. Wrin, B. Korber, M. B. Zwick, M. Wang, C. Chappey, G. Stiegler, R. Kunert, S. Zolla-Pazner, H. Katinger, C. J. Petropoulos, and D. R. Burton.** 2004. Comprehensive cross-clade neutralization analysis of a panel of anti-human immunodeficiency virus type 1 monoclonal antibodies. *J Virol* **78**:13232-52.
  12. **Blish, C. A., Z. Jalalian-Lechak, S. Rainwater, M. A. Nguyen, O. C. Dogan, and J. Overbaugh.** 2009. Cross-subtype neutralization sensitivity despite monoclonal antibody resistance among early subtype A, C, and D envelope variants of human immunodeficiency virus type 1. *J Virol* **83**:7783-8.
  13. **Blish, C. A., R. Nedellec, K. Mandaliya, D. E. Mosier, and J. Overbaugh.** 2007. HIV-1 subtype A envelope variants from early in infection have variable sensitivity to neutralization and to inhibitors of viral entry. *Aids* **21**:693-702.
  14. **Blish, C. A., M. A. Nguyen, and J. Overbaugh.** 2008. Enhancing exposure of HIV-1 neutralization epitopes through mutations in gp41. *PLoS Med* **5**:e9.
  15. **Borrow, P., H. Lewicki, X. Wei, M. S. Horwitz, N. Peffer, H. Meyers, J. A. Nelson, J. E. Gairin, B. H. Hahn, M. B. Oldstone, and G. M. Shaw.** 1997. Antiviral pressure exerted by HIV-1-specific cytotoxic T lymphocytes (CTLs) during primary infection demonstrated by rapid selection of CTL escape virus. *Nat Med* **3**:205-11.
  16. **Bosch, K. A., S. Rainwater, W. Jaoko, and J. Overbaugh.** 2010. Temporal analysis of HIV envelope sequence evolution and antibody escape in a subtype A-infected individual with a broad neutralizing antibody response. *Virology* **398**:115-24.
  17. **Boutwell, C. L., C. F. Rowley, and M. Essex.** 2009. Reduced viral replication capacity of human immunodeficiency virus type 1 subtype C caused by cytotoxic-T-lymphocyte escape mutations in HLA-B57 epitopes of capsid protein. *J Virol* **83**:2460-8.
  18. **Brown, B. K., L. Wiczorek, E. Sanders-Buell, A. Rosa Borges, M. L. Robb, D. L. Birx, N. L. Michael, F. E. McCutchan, and V. R. Polonis.** 2008. Cross-clade neutralization patterns among HIV-1 strains from the six major clades of the pandemic evaluated and compared in two different models. *Virology* **375**:529-38.
  19. **Bunnik, E. M., L. Pisas, A. C. van Nuenen, and H. Schuitemaker.** 2008. Autologous neutralizing humoral immunity and evolution of the viral envelope in the course of subtype B human immunodeficiency virus type 1 infection. *J Virol* **82**:7932-41.
  20. **Bures, R., L. Morris, C. Williamson, G. Ramjee, M. Deers, S. A. Fiscus, S. Abdool-Karim, and D. C. Montefiori.** 2002. Regional clustering of shared neutralization determinants on primary isolates of clade C human immunodeficiency virus type 1 from South Africa. *J Virol* **76**:2233-44.

21. **Cardozo, T., T. Kimura, S. Philpott, B. Weiser, H. Burger, and S. Zolla-Pazner.** 2007. Structural basis for coreceptor selectivity by the HIV type 1 V3 loop. *AIDS Res Hum Retroviruses* **23**:415-26.
22. **Cecilia, D., S. S. Kulkarni, S. P. Tripathy, R. R. Gangakhedkar, R. S. Paranjape, and D. A. Gadkari.** 2000. Absence of coreceptor switch with disease progression in human immunodeficiency virus infections in India. *Virology* **271**:253-8.
23. **Chackerian, B., L. M. Rudensey, and J. Overbaugh.** 1997. Specific N-linked and O-linked glycosylation modifications in the envelope V1 domain of simian immunodeficiency virus variants that evolve in the host alter recognition by neutralizing antibodies. *J Virol* **71**:7719-27.
24. **Chen, B., E. M. Vogan, H. Gong, J. J. Skehel, D. C. Wiley, and S. C. Harrison.** 2005. Structure of an unliganded simian immunodeficiency virus gp120 core. *Nature* **433**:834-41.
25. **Chen, L., Y. D. Kwon, T. Zhou, X. Wu, S. O'Dell, L. Cavacini, A. J. Hessel, M. Pancera, M. Tang, L. Xu, Z. Y. Yang, M. Y. Zhang, J. Arthos, D. R. Burton, D. S. Dimitrov, G. J. Nabel, M. R. Posner, J. Sodroski, R. Wyatt, J. R. Mascola, and P. D. Kwong.** 2009. Structural basis of immune evasion at the site of CD4 attachment on HIV-1 gp120. *Science* **326**:1123-7.
26. **Choge, I., T. Cilliers, P. Walker, N. Taylor, M. Phoswa, T. Meyers, J. Viljoen, A. Violari, G. Gray, P. L. Moore, M. Papathanosopoulos, and L. Morris.** 2006. Genotypic and phenotypic characterization of viral isolates from HIV-1 subtype C-infected children with slow and rapid disease progression. *AIDS Res Hum Retroviruses* **22**:458-65.
27. **Choisy, M., C. H. Woelk, J. F. Guegan, and D. L. Robertson.** 2004. Comparative study of adaptive molecular evolution in different human immunodeficiency virus groups and subtypes. *J Virol* **78**:1962-70.
28. **Cilliers, T., J. Nhlapo, M. Coetzer, D. Orlovic, T. Ketas, W. C. Olson, J. P. Moore, A. Trkola, and L. Morris.** 2003. The CCR5 and CXCR4 coreceptors are both used by human immunodeficiency virus type 1 primary isolates from subtype C. *J Virol* **77**:4449-56.
29. **Coetzer, M., T. Cilliers, M. Papathanosopoulos, G. Ramjee, S. A. Karim, C. Williamson, and L. Morris.** 2007. Longitudinal analysis of HIV type 1 subtype C envelope sequences from South Africa. *AIDS Res Hum Retroviruses* **23**:316-21.
30. **Coetzer, M., T. Cilliers, L. H. Ping, R. Swanstrom, and L. Morris.** 2006. Genetic characteristics of the V3 region associated with CXCR4 usage in HIV-1 subtype C isolates. *Virology* **356**:95-105.
31. **Coffin, J. M.** 1992. Genetic diversity and evolution of retroviruses. *Curr Top Microbiol Immunol* **176**:143-64.
32. **Collman, R., B. Godfrey, J. Cutilli, A. Rhodes, N. F. Hassan, R. Sweet, S. D. Douglas, H. Friedman, N. Nathanson, and F. Gonzalez-Scarano.** 1990. Macrophage-tropic strains of human immunodeficiency virus type 1 utilize the CD4 receptor. *J Virol* **64**:4468-76.

33. **Connor, R. I., K. E. Sheridan, D. Ceradini, S. Choe, and N. R. Landau.** 1997. Change in coreceptor use correlates with disease progression in HIV-1--infected individuals. *J Exp Med* **185**:621-8.
34. **Cormier, E. G., Dragic, T.** 2002. The crown and stem of the V3 loop play distinct roles in human immunodeficiency virus type 1 envelope glycoprotein interactions with the CCR5 coreceptor. *J Virol* **76**:8953-7.
35. **Crawford, H., J. G. Prado, A. Leslie, S. Hue, I. Honeyborne, S. Reddy, M. van der Stok, Z. Mncube, C. Brander, C. Rousseau, J. I. Mullins, R. Kaslow, P. Goepfert, S. Allen, E. Hunter, J. Mulenga, P. Kiepiela, B. D. Walker, and P. J. Goulder.** 2007. Compensatory mutation partially restores fitness and delays reversion of escape mutation within the immunodominant HLA-B\*5703-restricted Gag epitope in chronic human immunodeficiency virus type 1 infection. *J Virol* **81**:8346-51.
36. **Daar, E. S., X. L. Li, T. Moudgil, and D. D. Ho.** 1990. High concentrations of recombinant soluble CD4 are required to neutralize primary human immunodeficiency virus type 1 isolates. *Proc Natl Acad Sci U S A* **87**:6574-8.
37. **Davis, K. L., F. Bibollet-Ruche, H. Li, J. M. Decker, O. Kutsch, L. Morris, A. Salomon, A. Pinter, J. A. Hoxie, B. H. Hahn, P. D. Kwong, and G. M. Shaw.** 2009. Human immunodeficiency virus type 2 (HIV-2)/HIV-1 envelope chimeras detect high titers of broadly reactive HIV-1 V3-specific antibodies in human plasma. *J Virol* **83**:1240-59.
38. **Decker, J. M., F. Bibollet-Ruche, X. Wei, S. Wang, D. N. Levy, W. Wang, E. Delaporte, M. Peeters, C. A. Derdeyn, S. Allen, E. Hunter, M. S. Saag, J. A. Hoxie, B. H. Hahn, P. D. Kwong, J. E. Robinson, and G. M. Shaw.** 2005. Antigenic conservation and immunogenicity of the HIV coreceptor binding site. *J Exp Med* **201**:1407-19.
39. **Deeks, S. G., B. Schweighardt, T. Wrin, J. Galovich, R. Hoh, E. Sinclair, P. Hunt, J. M. McCune, J. N. Martin, C. J. Petropoulos, and F. M. Hecht.** 2006. Neutralizing antibody responses against autologous and heterologous viruses in acute versus chronic human immunodeficiency virus (HIV) infection: evidence for a constraint on the ability of HIV to completely evade neutralizing antibody responses. *J Virol* **80**:6155-64.
40. **Deng, H., R. Liu, W. Ellmeier, S. Choe, D. Unutmaz, M. Burkhart, P. Di Marzio, S. Marmon, R. E. Sutton, C. M. Hill, C. B. Davis, S. C. Peiper, T. J. Schall, D. R. Littman, and N. R. Landau.** 1996. Identification of a major co-receptor for primary isolates of HIV-1. *Nature* **381**:661-6.
41. **Derdeyn, C. A., J. M. Decker, F. Bibollet-Ruche, J. L. Mokili, M. Muldoon, S. A. Denham, M. L. Heil, F. Kasolo, R. Musonda, B. H. Hahn, G. M. Shaw, B. T. Korber, S. Allen, and E. Hunter.** 2004. Envelope-constrained neutralization-sensitive HIV-1 after heterosexual transmission. *Science* **303**:2019-22.

42. **Diskin, R., P. M. Marcovecchio, and P. J. Bjorkman.** 2010. Structure of a clade C HIV-1 gp120 bound to CD4 and CD4-induced antibody reveals anti-CD4 polyreactivity. *Nat Struct Mol Biol* **17**:608-13.
43. **Doores, K. J., and D. R. Burton.** 2010. Variable loop glycan dependency of the broad and potent HIV-1 neutralizing antibodies PG9 and PG16. *J Virol*.
44. **Dragic, T., V. Litwin, G. P. Allaway, S. R. Martin, Y. Huang, K. A. Nagashima, C. Cayanan, P. J. Maddon, R. A. Koup, J. P. Moore, and W. A. Paxton.** 1996. HIV-1 entry into CD4+ cells is mediated by the chemokine receptor CC-CKR-5. *Nature* **381**:667-73.
45. **Duenas-Decamp, M. J., P. J. Peters, D. Burton, and P. R. Clapham.** 2009. Determinants flanking the CD4 binding loop modulate macrophage tropism of human immunodeficiency virus type 1 R5 envelopes. *J Virol* **83**:2575-83.
46. **Eswar, N., B. Webb, M. A. Marti-Renom, M. S. Madhusudhan, D. Eramian, M. Y. Shen, U. Pieper, and A. Sali.** 2006. Comparative protein structure modeling using Modeller. *Curr Protoc Bioinformatics* **Chapter 5**:Unit 5 6.
47. **Felsovalyi, K., A. Nadas, S. Zolla-Pazner, and T. Cardozo.** 2006. Distinct sequence patterns characterize the V3 region of HIV type 1 gp120 from subtypes A and C. *AIDS Res Hum Retroviruses* **22**:703-8.
48. **Feng, Y., C. C. Broder, P. E. Kennedy, and E. A. Berger.** 1996. HIV-1 entry cofactor: functional cDNA cloning of a seven-transmembrane, G protein-coupled receptor. *Science* **272**:872-7.
49. **Freed, E. O., D. J. Myers, and R. Risser.** 1991. Identification of the principal neutralizing determinant of human immunodeficiency virus type 1 as a fusion domain. *J Virol* **65**:190-4.
50. **Frost, S. D., T. Wrin, D. M. Smith, S. L. Kosakovsky Pond, Y. Liu, E. Paxinos, C. Chappey, J. Galovich, J. Beauchaine, C. J. Petropoulos, S. J. Little, and D. D. Richman.** 2005. Neutralizing antibody responses drive the evolution of human immunodeficiency virus type 1 envelope during recent HIV infection. *Proc Natl Acad Sci U S A* **102**:18514-9.
51. **Gao, F., E. Bailes, D. L. Robertson, Y. Chen, C. M. Rodenburg, S. F. Michael, L. B. Cummins, L. O. Arthur, M. Peeters, G. M. Shaw, P. M. Sharp, and B. H. Hahn.** 1999. Origin of HIV-1 in the chimpanzee *Pan troglodytes troglodytes*. *Nature* **397**:436-41.
52. **Gao, F., L. Yue, A. T. White, P. G. Pappas, J. Barchue, A. P. Hanson, B. M. Greene, P. M. Sharp, G. M. Shaw, and B. H. Hahn.** 1992. Human infection by genetically diverse SIVSM-related HIV-2 in west Africa. *Nature* **358**:495-9.
53. **Garlick, R. L., R. J. Kirschner, F. M. Eckenrode, W. G. Tarpley, and C. S. Tomich.** 1990. *Escherichia coli* expression, purification, and biological activity of a truncated soluble CD4. *AIDS Res Hum Retroviruses* **6**:465-79.
54. **Gaschen, B., J. Taylor, K. Yusim, B. Foley, F. Gao, D. Lang, V. Novitsky, B. Haynes, B. H. Hahn, T. Bhattacharya, and B.**

- Korber.** 2002. Diversity considerations in HIV-1 vaccine selection. *Science* **296**:2354-60.
55. **Gilbert, P. B., V. Novitsky, and M. Essex.** 2005. Covariability of selected amino acid positions for HIV type 1 subtypes C and B. *AIDS Res Hum Retroviruses* **21**:1016-30.
56. **Gnanakaran, S., D. Lang, M. Daniels, T. Bhattacharya, C. A. Derdeyn, and B. Korber.** 2007. Clade-specific differences between human immunodeficiency virus type 1 clades B and C: diversity and correlations in C3-V4 regions of gp120. *J Virol* **81**:4886-91.
57. **Go, E. P., Q. Chang, H. X. Liao, L. L. Sutherland, S. M. Alam, B. F. Haynes, and H. Desaire.** 2009. Glycosylation site-specific analysis of clade C HIV-1 envelope proteins. *J Proteome Res* **8**:4231-42.
58. **Goepfert, P. A., W. Lumm, P. Farmer, P. Matthews, A. Prendergast, J. M. Carlson, C. A. Derdeyn, J. Tang, R. A. Kaslow, A. Bansal, K. Yusim, D. Heckerman, J. Mulenga, S. Allen, P. J. Goulder, and E. Hunter.** 2008. Transmission of HIV-1 Gag immune escape mutations is associated with reduced viral load in linked recipients. *J Exp Med* **205**:1009-17.
59. **Gorny, M. K., J. P. Moore, A. J. Conley, S. Karwowska, J. Sodroski, C. Williams, S. Burda, L. J. Boots, and S. Zolla-Pazner.** 1994. Human anti-V2 monoclonal antibody that neutralizes primary but not laboratory isolates of human immunodeficiency virus type 1. *J Virol* **68**:8312-20.
60. **Gorny, M. K., L. Stamatatos, B. Volsky, K. Revesz, C. Williams, X. H. Wang, S. Cohen, R. Staudinger, and S. Zolla-Pazner.** 2005. Identification of a new quaternary neutralizing epitope on human immunodeficiency virus type 1 virus particles. *J Virol* **79**:5232-7.
61. **Gorny, M. K. a. Z.-P., S. (ed.).** 2004. *Human Monoclonal Antibodies that Neutralize HIV-1.* Los Alamos National Laboratory, Theoretical Biology and Biophysics, Los Alamos.
62. **Gray, E. S., M. C. Madiga, P. L. Moore, K. Mlisana, S. S. Abdool Karim, J. M. Binley, G. M. Shaw, J. R. Mascola, and L. Morris.** 2009. Broad neutralization of human immunodeficiency virus type 1 mediated by plasma antibodies against the gp41 membrane proximal external region. *J Virol* **83**:11265-74.
63. **Gray, E. S., P. L. Moore, I. A. Choge, J. M. Decker, F. Bibollet-Ruche, H. Li, N. Leseka, F. Treurnicht, K. Mlisana, G. M. Shaw, S. S. Karim, C. Williamson, and L. Morris.** 2007. Neutralizing antibody responses in acute human immunodeficiency virus type 1 subtype C infection. *J Virol* **81**:6187-96.
64. **Gray, E. S., P. L. Moore, R. A. Pantophlet, and L. Morris.** 2007. N-linked glycan modifications in gp120 of human immunodeficiency virus type 1 subtype C render partial sensitivity to 2G12 antibody neutralization. *J Virol* **81**:10769-76.
65. **Gray, E. S., N. Taylor, D. Wycuff, P. L. Moore, G. D. Tomaras, C. K. Wibmer, A. Puren, A. DeCamp, P. B. Gilbert, B. Wood, D. C. Montefiori, J. M. Binley, G. M. Shaw, B. F. Haynes, J. R.**

- Mascola, and L. Morris.** 2009. Antibody specificities associated with neutralization breadth in plasma from human immunodeficiency virus type 1 subtype C-infected blood donors. *J Virol* **83**:8925-37.
66. **Guan, Y., M. M. Sajadi, R. Kamin-Lewis, T. R. Fouts, A. Dimitrov, Z. Zhang, R. R. Redfield, A. L. DeVico, R. C. Gallo, and G. K. Lewis.** 2009. Discordant memory B cell and circulating anti-Env antibody responses in HIV-1 infection. *Proc Natl Acad Sci U S A* **106**:3952-7.
67. **Haaland, R. E., P. A. Hawkins, J. Salazar-Gonzalez, A. Johnson, A. Tichacek, E. Karita, O. Manigart, J. Mulenga, B. F. Keele, G. M. Shaw, B. H. Hahn, S. A. Allen, C. A. Derdeyn, and E. Hunter.** 2009. Inflammatory genital infections mitigate a severe genetic bottleneck in heterosexual transmission of subtype A and C HIV-1. *PLoS Pathog* **5**:e1000274.
68. **Hahn, B. H., G. M. Shaw, K. M. De Cock, and P. M. Sharp.** 2000. AIDS as a zoonosis: scientific and public health implications. *Science* **287**:607-14.
69. **Hemelaar, J., E. Gouws, P. D. Ghys, and S. Osmanov.** 2006. Global and regional distribution of HIV-1 genetic subtypes and recombinants in 2004. *Aids* **20**:W13-23.
70. **Hirsch, V. M., R. A. Olmsted, M. Murphy-Corb, R. H. Purcell, and P. R. Johnson.** 1989. An African primate lentivirus (SIVsm) closely related to HIV-2. *Nature* **339**:389-92.
71. **Ho, D. D., A. U. Neumann, A. S. Perelson, W. Chen, J. M. Leonard, and M. Markowitz.** 1995. Rapid turnover of plasma virions and CD4 lymphocytes in HIV-1 infection. *Nature* **373**:123-6.
72. **Honnen, W. J., C. Krachmarov, S. C. Kayman, M. K. Gorny, S. Zolla-Pazner, and A. Pinter.** 2007. Type-specific epitopes targeted by monoclonal antibodies with exceptionally potent neutralizing activities for selected strains of human immunodeficiency virus type 1 map to a common region of the V2 domain of gp120 and differ only at single positions from the clade B consensus sequence. *J Virol* **81**:1424-32.
73. **Huang, C. C., M. Tang, M. Y. Zhang, S. Majeed, E. Montabana, R. L. Stanfield, D. S. Dimitrov, B. Korber, J. Sodroski, I. A. Wilson, R. Wyatt, and P. D. Kwong.** 2005. Structure of a V3-containing HIV-1 gp120 core. *Science* **310**:1025-8.
74. **Huang, C. C., M. Venturi, S. Majeed, M. J. Moore, S. Phogat, M. Y. Zhang, D. S. Dimitrov, W. A. Hendrickson, J. Robinson, J. Sodroski, R. Wyatt, H. Choe, M. Farzan, and P. D. Kwong.** 2004. Structural basis of tyrosine sulfation and VH-gene usage in antibodies that recognize the HIV type 1 coreceptor-binding site on gp120. *Proc Natl Acad Sci U S A* **101**:2706-11.
75. **Hunter, E.** 1997. Viral Entry and Receptors, p. 71-121. *In* J. M. C. a. H. E. Varmus (ed.), *Retroviruses*. Cold Spring Harbor Laboratory, Plainview.
76. **Hwang, S. S., T. J. Boyle, H. K. Lyerly, and B. R. Cullen.** 1992. Identification of envelope V3 loop as the major determinant of CD4 neutralization sensitivity of HIV-1. *Science* **257**:535-7.

77. **Isaacman-Beck, J., E. A. Hermann, Y. Yi, S. J. Ratcliffe, J. Mulenga, S. Allen, E. Hunter, C. A. Derdeyn, and R. G. Collman.** 2009. Heterosexual transmission of human immunodeficiency virus type 1 subtype C: Macrophage tropism, alternative coreceptor use, and the molecular anatomy of CCR5 utilization. *J Virol* **83**:8208-20.
78. **Jiang, X., V. Burke, M. Totrov, C. Williams, T. Cardozo, M. K. Gorny, S. Zolla-Pazner, and X. P. Kong.** 2010. Conserved structural elements in the V3 crown of HIV-1 gp120. *Nat Struct Mol Biol* **17**:955-61.
79. **Kabat, D., S. L. Kozak, K. Wehrly, and B. Chesebro.** 1994. Differences in CD4 dependence for infectivity of laboratory-adapted and primary patient isolates of human immunodeficiency virus type 1. *J Virol* **68**:2570-7.
80. **Kasturi, L., H. Chen, and S. H. Shakin-Eshleman.** 1997. Regulation of N-linked core glycosylation: use of a site-directed mutagenesis approach to identify Asn-Xaa-Ser/Thr sequons that are poor oligosaccharide acceptors. *Biochem J* **323 ( Pt 2)**:415-9.
81. **Kayman, S. C., Z. Wu, K. Revesz, H. Chen, R. Kopelman, and A. Pinter.** 1994. Presentation of native epitopes in the V1/V2 and V3 regions of human immunodeficiency virus type 1 gp120 by fusion glycoproteins containing isolated gp120 domains. *J Virol* **68**:400-10.
82. **Keele, B. F., E. E. Giorgi, J. F. Salazar-Gonzalez, J. M. Decker, K. T. Pham, M. G. Salazar, C. Sun, T. Grayson, S. Wang, H. Li, X. Wei, C. Jiang, J. L. Kirchherr, F. Gao, J. A. Anderson, L. H. Ping, R. Swanstrom, G. D. Tomaras, W. A. Blattner, P. A. Goepfert, J. M. Kilby, M. S. Saag, E. L. Delwart, M. P. Busch, M. S. Cohen, D. C. Montefiori, B. F. Haynes, B. Gaschen, G. S. Athreya, H. Y. Lee, N. Wood, C. Seoighe, A. S. Perelson, T. Bhattacharya, B. T. Korber, B. H. Hahn, and G. M. Shaw.** 2008. Identification and characterization of transmitted and early founder virus envelopes in primary HIV-1 infection. *Proc Natl Acad Sci U S A* **105**:7552-7.
83. **Koch, M., M. Pancera, P. D. Kwong, P. Kolchinsky, C. Grundner, L. Wang, W. A. Hendrickson, J. Sodroski, and R. Wyatt.** 2003. Structure-based, targeted deglycosylation of HIV-1 gp120 and effects on neutralization sensitivity and antibody recognition. *Virology* **313**:387-400.
84. **Korber, B., B. Gaschen, K. Yusim, R. Thakallapally, C. Kesmir, and V. Detours.** 2001. Evolutionary and immunological implications of contemporary HIV-1 variation. *Br Med Bull* **58**:19-42.
85. **Korber, B., M. Muldoon, J. Theiler, F. Gao, R. Gupta, A. Lapedes, B. H. Hahn, S. Wolinsky, and T. Bhattacharya.** 2000. Timing the ancestor of the HIV-1 pandemic strains. *Science* **288**:1789-96.
86. **Korber, B. T., K. MacInnes, R. F. Smith, and G. Myers.** 1994. Mutational trends in V3 loop protein sequences observed in different genetic lineages of human immunodeficiency virus type 1. *J Virol* **68**:6730-44.
87. **Krachmarov, C., A. Pinter, W. J. Honnen, M. K. Gorny, P. N. Nyambi, S. Zolla-Pazner, and S. C. Kayman.** 2005. Antibodies that are cross-reactive for human immunodeficiency virus type 1 clade a and

- clade B v3 domains are common in patient sera from Cameroon, but their neutralization activity is usually restricted by epitope masking. *J Virol* **79**:780-90.
88. **Kwong, P. D., M. L. Doyle, D. J. Casper, C. Cicala, S. A. Leavitt, S. Majeed, T. D. Steenbeke, M. Venturi, I. Chaiken, M. Fung, H. Katinger, P. W. Parren, J. Robinson, D. Van Ryk, L. Wang, D. R. Burton, E. Freire, R. Wyatt, J. Sodroski, W. A. Hendrickson, and J. Arthos.** 2002. HIV-1 evades antibody-mediated neutralization through conformational masking of receptor-binding sites. *Nature* **420**:678-82.
  89. **Kwong, P. D., R. Wyatt, S. Majeed, J. Robinson, R. W. Sweet, J. Sodroski, and W. A. Hendrickson.** 2000. Structures of HIV-1 gp120 envelope glycoproteins from laboratory-adapted and primary isolates. *Structure* **8**:1329-39.
  90. **Kwong, P. D., R. Wyatt, J. Robinson, R. W. Sweet, J. Sodroski, and W. A. Hendrickson.** 1998. Structure of an HIV gp120 envelope glycoprotein in complex with the CD4 receptor and a neutralizing human antibody. *Nature* **393**:648-59.
  91. **Laird, M. E., T. Igarashi, M. A. Martin, and R. C. Desrosiers.** 2008. Importance of the V1/V2 loop region of simian-human immunodeficiency virus envelope glycoprotein gp120 in determining the strain specificity of the neutralizing antibody response. *J Virol* **82**:11054-65.
  92. **Li, B., J. M. Decker, R. W. Johnson, F. Bibollet-Ruche, X. Wei, J. Mulenga, S. Allen, E. Hunter, B. H. Hahn, G. M. Shaw, J. L. Blackwell, and C. A. Derdeyn.** 2006. Evidence for potent autologous neutralizing antibody titers and compact envelopes in early infection with subtype C human immunodeficiency virus type 1. *J Virol* **80**:5211-8.
  93. **Li, Y., B. Cleveland, I. Klots, B. Travis, B. A. Richardson, D. Anderson, D. Montefiori, P. Polacino, and S. L. Hu.** 2008. Removal of a single N-linked glycan in human immunodeficiency virus type 1 gp120 results in an enhanced ability to induce neutralizing antibody responses. *J Virol* **82**:638-51.
  94. **Li, Y., H. Hui, C. J. Burgess, R. W. Price, P. M. Sharp, B. H. Hahn, and G. M. Shaw.** 1992. Complete nucleotide sequence, genome organization, and biological properties of human immunodeficiency virus type 1 in vivo: evidence for limited defectiveness and complementation. *J Virol* **66**:6587-600.
  95. **Li, Y., S. A. Migueles, B. Welcher, K. Svehla, A. Phogat, M. K. Louder, X. Wu, G. M. Shaw, M. Connors, R. T. Wyatt, and J. R. Mascola.** 2007. Broad HIV-1 neutralization mediated by CD4-binding site antibodies. *Nat Med* **13**:1032-4.
  96. **Li, Y., K. Svehla, M. K. Louder, D. Wycuff, S. Phogat, M. Tang, S. A. Migueles, X. Wu, A. Phogat, G. M. Shaw, M. Connors, J. Hoxie, J. R. Mascola, and R. Wyatt.** 2009. Analysis of neutralization specificities in polyclonal sera derived from human immunodeficiency virus type 1-infected individuals. *J Virol* **83**:1045-59.



97. **Liu, J., A. Bartesaghi, M. J. Borgnia, G. Sapiro, and S. Subramaniam.** 2008. Molecular architecture of native HIV-1 gp120 trimers. *Nature* **455**:109-13.
98. **Lohrengel, S., F. Hermann, I. Hagmann, H. Oberwinkler, L. Scrivano, C. Hoffmann, D. von Laer, and M. T. Dittmar.** 2005. Determinants of human immunodeficiency virus type 1 resistance to membrane-anchored gp41-derived peptides. *J Virol* **79**:10237-46.
99. **Ly, A., and L. Stamatatos.** 2000. V2 loop glycosylation of the human immunodeficiency virus type 1 SF162 envelope facilitates interaction of this protein with CD4 and CCR5 receptors and protects the virus from neutralization by anti-V3 loop and anti-CD4 binding site antibodies. *J Virol* **74**:6769-76.
100. **Lynch, R. M., R. Rong, B. Li, T. Shen, W. Honnen, J. Mulenga, S. Allen, A. Pinter, S. Gnanakaran, and C. A. Derdeyn.** 2010. Subtype-specific conservation of isoleucine 309 in the envelope V3 domain is linked to immune evasion in subtype C HIV-1 infection. *Virology* **404**:59-70.
101. **Lynch, R. M., T. Shen, S. Gnanakaran, and C. A. Derdeyn.** 2009. Appreciating HIV type 1 diversity: subtype differences in Env. *AIDS Res Hum Retroviruses* **25**:237-48.
102. **MacKerell, J. A.** 1998. All-atom empirical potential for molecular modeling and dynamics studies of proteins. *J Phys Chem B* **102**:3586-3616.
103. **Maddon, P. J., A. G. Dalgleish, J. S. McDougal, P. R. Clapham, R. A. Weiss, and R. Axel.** 1986. The T4 gene encodes the AIDS virus receptor and is expressed in the immune system and the brain. *Cell* **47**:333-48.
104. **Mahalanabis, M., P. Jayaraman, T. Miura, F. Pereyra, E. M. Chester, B. Richardson, B. Walker, and N. L. Haigwood.** 2009. Continuous viral escape and selection by autologous neutralizing antibodies in drug-naïve human immunodeficiency virus controllers. *J Virol* **83**:662-72.
105. **McCaffrey, R. A., C. Saunders, M. Hensel, and L. Stamatatos.** 2004. N-linked glycosylation of the V3 loop and the immunologically silent face of gp120 protects human immunodeficiency virus type 1 SF162 from neutralization by anti-gp120 and anti-gp41 antibodies. *J Virol* **78**:3279-95.
106. **McCutchan, F. E.** 2006. Global epidemiology of HIV. *J Med Virol* **78 Suppl 1**:S7-S12.
107. **McDougal, J. S., P. J. Maddon, A. G. Dalgleish, P. R. Clapham, D. R. Littman, M. Godfrey, D. E. Maddon, L. Chess, R. A. Weiss, and R. Axel.** 1986. The T4 glycoprotein is a cell-surface receptor for the AIDS virus. *Cold Spring Harb Symp Quant Biol* **51 Pt 2**:703-11.
108. **McKenna, S. L., G. K. Muyinda, D. Roth, M. Mwali, N. Ng'andu, A. Myrick, C. Luo, F. H. Priddy, V. M. Hall, A. A. von Lieven, J. R. Sabatino, K. Mark, and S. A. Allen.** 1997. Rapid HIV testing and

- counseling for voluntary testing centers in Africa. *Aids* **11 Suppl 1**:S103-10.
109. **Michler, K., B. J. Connell, W. D. Venter, W. S. Stevens, A. Capovilla, and M. A. Papathanasopoulos.** 2008. Genotypic characterization and comparison of full-length envelope glycoproteins from South African HIV type 1 subtype C primary isolates that utilize CCR5 and/or CXCR4. *AIDS Res Hum Retroviruses* **24**:743-51.
  110. **Moore, J. P.** 1993. The reactivities of HIV-1+ human sera with solid-phase V3 loop peptides can be poor predictors of their reactivities with V3 loops on native gp120 molecules. *AIDS Res Hum Retroviruses* **9**:209-19.
  111. **Moore, J. P., L. C. Burkly, R. I. Connor, Y. Cao, R. Tizard, D. D. Ho, and R. A. Fisher.** 1993. Adaptation of two primary human immunodeficiency virus type 1 isolates to growth in transformed T cell lines correlates with alterations in the responses of their envelope glycoproteins to soluble CD4. *AIDS Res Hum Retroviruses* **9**:529-39.
  112. **Moore, J. P., Y. Cao, D. D. Ho, and R. A. Koup.** 1994. Development of the anti-gp120 antibody response during seroconversion to human immunodeficiency virus type 1. *J Virol* **68**:5142-55.
  113. **Moore, J. P., J. A. McKeating, Y. X. Huang, A. Ashkenazi, and D. D. Ho.** 1992. Virions of primary human immunodeficiency virus type 1 isolates resistant to soluble CD4 (sCD4) neutralization differ in sCD4 binding and glycoprotein gp120 retention from sCD4-sensitive isolates. *J Virol* **66**:235-43.
  114. **Moore, P. L., E. T. Crooks, L. Porter, P. Zhu, C. S. Cayan, H. Grise, P. Corcoran, M. B. Zwick, M. Franti, L. Morris, K. H. Roux, D. R. Burton, and J. M. Binley.** 2006. Nature of nonfunctional envelope proteins on the surface of human immunodeficiency virus type 1. *J Virol* **80**:2515-28.
  115. **Moore, P. L., E. S. Gray, I. A. Choge, N. Ranchobe, K. Mlisana, S. S. Abdool Karim, C. Williamson, and L. Morris.** 2008. The c3-v4 region is a major target of autologous neutralizing antibodies in human immunodeficiency virus type 1 subtype C infection. *J Virol* **82**:1860-9.
  116. **Moore, P. L., N. Ranchobe, B. E. Lambson, E. S. Gray, E. Cave, M. R. Abrahams, G. Bandawe, K. Mlisana, S. S. Abdool Karim, C. Williamson, and L. Morris.** 2009. Limited neutralizing antibody specificities drive neutralization escape in early HIV-1 subtype C infection. *PLoS Pathog* **5**:e1000598.
  117. **Morris, L., T. Cilliers, H. Bredell, M. Phoswa, and D. J. Martin.** 2001. CCR5 is the major coreceptor used by HIV-1 subtype C isolates from patients with active tuberculosis. *AIDS Res Hum Retroviruses* **17**:697-701.
  118. **Navis, M., D. E. Matas, A. Rachinger, F. A. Koning, P. van Swieten, N. A. Kootstra, and H. Schuitemaker.** 2008. Molecular evolution of human immunodeficiency virus type 1 upon transmission between human leukocyte antigen disparate donor-recipient pairs. *PLoS One* **3**:e2422.

119. **Ndung'u, T., B. Renjifo, and M. Essex.** 2001. Construction and analysis of an infectious human Immunodeficiency virus type 1 subtype C molecular clone. *J Virol* **75**:4964-72.
120. **Ndung'u, T., E. Sepako, M. F. McLane, F. Chand, K. Bedi, S. Gaseitsiwe, F. Doualla-Bell, T. Peter, I. Thior, S. M. Moyo, P. B. Gilbert, V. A. Novitsky, and M. Essex.** 2006. HIV-1 subtype C in vitro growth and coreceptor utilization. *Virology* **347**:247-60.
121. **Neumann, T., I. Hagmann, S. Lohrengel, M. L. Heil, C. A. Derdeyn, H. G. Krausslich, and M. T. Dittmar.** 2005. T20-insensitive HIV-1 from naive patients exhibits high viral fitness in a novel dual-color competition assay on primary cells. *Virology* **333**:251-62.
122. **Pancera, M., S. Majeed, Y. E. Ban, L. Chen, C. C. Huang, L. Kong, Y. D. Kwon, J. Stuckey, T. Zhou, J. E. Robinson, W. R. Schief, J. Sodroski, R. Wyatt, and P. D. Kwong.** 2010. Structure of HIV-1 gp120 with gp41-interactive region reveals layered envelope architecture and basis of conformational mobility. *Proc Natl Acad Sci U S A* **107**:1166-71.
123. **Paredes, R., M. Sagar, V. C. Marconi, R. Hoh, J. N. Martin, N. T. Parkin, C. J. Petropoulos, S. G. Deeks, and D. R. Kuritzkes.** 2009. In vivo fitness cost of the M184V mutation in multidrug-resistant human immunodeficiency virus type 1 in the absence of lamivudine. *J Virol* **83**:2038-43.
124. **Patel, M. B., N. G. Hoffman, and R. Swanstrom.** 2008. Subtype-specific conformational differences within the V3 region of subtype B and subtype C human immunodeficiency virus type 1 Env proteins. *J Virol* **82**:903-16.
125. **Pathak, V. K., and H. M. Temin.** 1990. Broad spectrum of in vivo forward mutations, hypermutations, and mutational hotspots in a retroviral shuttle vector after a single replication cycle: substitutions, frameshifts, and hypermutations. *Proc Natl Acad Sci U S A* **87**:6019-23.
126. **Peeters, M., C. Toure-Kane, and J. N. Nkengasong.** 2003. Genetic diversity of HIV in Africa: impact on diagnosis, treatment, vaccine development and trials. *Aids* **17**:2547-60.
127. **Peters, P. J., M. J. Duenas-Decamp, W. M. Sullivan, R. Brown, C. Ankghuambom, K. Luzuriaga, J. Robinson, D. R. Burton, J. Bell, P. Simmonds, J. Ball, and P. R. Clapham.** 2008. Variation in HIV-1 R5 macrophage-tropism correlates with sensitivity to reagents that block envelope: CD4 interactions but not with sensitivity to other entry inhibitors. *Retrovirology* **5**:5.
128. **Peters, P. J., W. M. Sullivan, M. J. Duenas-Decamp, J. Bhattacharya, C. Ankghuambom, R. Brown, K. Luzuriaga, J. Bell, P. Simmonds, J. Ball, and P. R. Clapham.** 2006. Non-macrophage-tropic human immunodeficiency virus type 1 R5 envelopes predominate in blood, lymph nodes, and semen: implications for transmission and pathogenesis. *J Virol* **80**:6324-32.

129. **Phillips, J. C., R. Braun, W. Wang, J. Gumbart, E. Tajkhorshid, E. Villa, C. Chipot, R. D. Skeel, L. Kale, and K. Schulten.** 2005. Scalable molecular dynamics with NAMD. *J Comput Chem* **26**:1781-802.
130. **Pietzsch, J., J. F. Scheid, H. Mouquet, F. Klein, M. S. Seaman, M. Jankovic, D. Corti, A. Lanzavecchia, and M. C. Nussenzweig.** 2010. Human anti-HIV-neutralizing antibodies frequently target a conserved epitope essential for viral fitness. *J Exp Med*.
131. **Pinter, A., W. J. Honnen, Y. He, M. K. Gorny, S. Zolla-Pazner, and S. C. Kayman.** 2004. The V1/V2 domain of gp120 is a global regulator of the sensitivity of primary human immunodeficiency virus type 1 isolates to neutralization by antibodies commonly induced upon infection. *J Virol* **78**:5205-15.
132. **Platt, E. J., K. Wehrly, S. E. Kuhmann, B. Chesebro, and D. Kabat.** 1998. Effects of CCR5 and CD4 cell surface concentrations on infections by macrophagetropic isolates of human immunodeficiency virus type 1. *J Virol* **72**:2855-64.
133. **Prado, J. G., S. Franco, T. Matamoros, L. Ruiz, B. Clotet, L. Menendez-Arias, M. A. Martinez, and J. Martinez-Picado.** 2004. Relative replication fitness of multi-nucleoside analogue-resistant HIV-1 strains bearing a dipeptide insertion in the fingers subdomain of the reverse transcriptase and mutations at codons 67 and 215. *Virology* **326**:103-12.
134. **Prado, J. G., I. Honeyborne, I. Brierley, M. C. Puertas, J. Martinez-Picado, and P. J. Goulder.** 2009. Functional consequences of human immunodeficiency virus escape from an HLA-B\*13-restricted CD8+ T-cell epitope in p1 Gag protein. *J Virol* **83**:1018-25.
135. **Pugach, P., S. E. Kuhmann, J. Taylor, A. J. Marozsan, A. Snyder, T. Ketas, S. M. Wolinsky, B. T. Korber, and J. P. Moore.** 2004. The prolonged culture of human immunodeficiency virus type 1 in primary lymphocytes increases its sensitivity to neutralization by soluble CD4. *Virology* **321**:8-22.
136. **Quakkelaar, E. D., E. M. Bunnik, F. P. van Alphen, B. D. Boeser-Nunnink, A. C. van Nuenen, and H. Schuitemaker.** 2007. Escape of human immunodeficiency virus type 1 from broadly neutralizing antibodies is not associated with a reduction of viral replicative capacity in vitro. *Virology* **363**:447-53.
137. **Rademeyer, C., P. L. Moore, N. Taylor, D. P. Martin, I. A. Choge, E. S. Gray, H. W. Sheppard, C. Gray, L. Morris, and C. Williamson.** 2007. Genetic characteristics of HIV-1 subtype C envelopes inducing cross-neutralizing antibodies. *Virology* **368**:172-81.
138. **Ramirez, B. C., E. Simon-Loriere, R. Galetto, and M. Negroni.** 2008. Implications of recombination for HIV diversity. *Virus Res* **134**:64-73.
139. **Richman, D. D., and S. A. Bozzette.** 1994. The impact of the syncytium-inducing phenotype of human immunodeficiency virus on disease progression. *J Infect Dis* **169**:968-74.

140. **Richman, D. D., T. Wrin, S. J. Little, and C. J. Petropoulos.** 2003. Rapid evolution of the neutralizing antibody response to HIV type 1 infection. *Proc Natl Acad Sci U S A* **100**:4144-9.
141. **Rizzuto, C., and J. Sodroski.** 2000. Fine definition of a conserved CCR5-binding region on the human immunodeficiency virus type 1 glycoprotein 120. *AIDS Res Hum Retroviruses* **16**:741-9.
142. **Rizzuto, C. D., R. Wyatt, N. Hernandez-Ramos, Y. Sun, P. D. Kwong, W. A. Hendrickson, and J. Sodroski.** 1998. A conserved HIV gp120 glycoprotein structure involved in chemokine receptor binding. *Science* **280**:1949-53.
143. **Robinson, J. E., K. Franco, D. H. Elliott, M. J. Maher, A. Reyna, D. C. Montefiori, S. Zolla-Pazner, M. K. Gorny, Z. Kraft, and L. Stamatatos.** 2010. Quaternary epitope specificities of anti-HIV-1 neutralizing antibodies generated in rhesus macaques infected by the simian/human immunodeficiency virus SHIVSF162P4. *J Virol* **84**:3443-53.
144. **Rong, R., F. Bibollet-Ruche, J. Mulenga, S. Allen, J. L. Blackwell, and C. A. Derdeyn.** 2007. Role of V1V2 and other human immunodeficiency virus type 1 envelope domains in resistance to autologous neutralization during clade C infection. *J Virol* **81**:1350-9.
145. **Rong, R., S. Gnanakaran, J. M. Decker, F. Bibollet-Ruche, J. Taylor, J. N. Sfakianos, J. L. Mokili, M. Muldoon, J. Mulenga, S. Allen, B. H. Hahn, G. M. Shaw, J. L. Blackwell, B. T. Korber, E. Hunter, and C. A. Derdeyn.** 2007. Unique mutational patterns in the envelope alpha 2 amphipathic helix and acquisition of length in gp120 hypervariable domains are associated with resistance to autologous neutralization of subtype C human immunodeficiency virus type 1. *J Virol* **81**:5658-68.
146. **Rong, R., B. Li, R. M. Lynch, R. E. Haaland, M. K. Murphy, J. Mulenga, S. A. Allen, A. Pinter, G. M. Shaw, E. Hunter, J. E. Robinson, S. Gnanakaran, and C. A. Derdeyn.** 2009. Escape from autologous neutralizing antibodies in acute/early subtype C HIV-1 infection requires multiple pathways. *PLoS Pathog* **5**:e1000594.
147. **Sagar, M., X. Wu, S. Lee, and J. Overbaugh.** 2006. Human immunodeficiency virus type 1 V1-V2 envelope loop sequences expand and add glycosylation sites over the course of infection, and these modifications affect antibody neutralization sensitivity. *J Virol* **80**:9586-98.
148. **Salazar-Gonzalez, J. F., M. G. Salazar, B. F. Keele, G. H. Learn, E. E. Giorgi, H. Li, J. M. Decker, S. Wang, J. Baalwa, M. H. Kraus, N. F. Parrish, K. S. Shaw, M. B. Guffey, K. J. Bar, K. L. Davis, C. Ochsenbauer-Jambor, J. C. Kappes, M. S. Saag, M. S. Cohen, J. Mulenga, C. A. Derdeyn, S. Allen, E. Hunter, M. Markowitz, P. Hraber, A. S. Perelson, T. Bhattacharya, B. F. Haynes, B. T. Korber, B. H. Hahn, and G. M. Shaw.** 2009. Genetic identity, biological phenotype, and evolutionary pathways of

- transmitted/founder viruses in acute and early HIV-1 infection. *J Exp Med* **206**:1273-89.
149. **Sanders, R. W., M. Venturi, L. Schiffner, R. Kalyanaraman, H. Katinger, K. O. Lloyd, P. D. Kwong, and J. P. Moore.** 2002. The mannose-dependent epitope for neutralizing antibody 2G12 on human immunodeficiency virus type 1 glycoprotein gp120. *J Virol* **76**:7293-305.
  150. **Santiago, M. L., F. Range, B. F. Keele, Y. Li, E. Bailes, F. Bibollet-Ruche, C. Fruteau, R. Noe, M. Peeters, J. F. Brookfield, G. M. Shaw, P. M. Sharp, and B. H. Hahn.** 2005. Simian immunodeficiency virus infection in free-ranging sooty mangabeys (*Cercocebus atys atys*) from the Tai Forest, Cote d'Ivoire: implications for the origin of epidemic human immunodeficiency virus type 2. *J Virol* **79**:12515-27.
  151. **Sather, D. N., J. Armann, L. K. Ching, A. Mavrantoni, G. Sellhorn, Z. Caldwell, X. Yu, B. Wood, S. Self, S. Kalams, and L. Stamatatos.** 2009. Factors associated with the development of cross-reactive neutralizing antibodies during human immunodeficiency virus type 1 infection. *J Virol* **83**:757-69.
  152. **Sattentau, Q. J., Moore, J. P.** 1995. Human immunodeficiency virus type 1 neutralization is determined by epitope exposure on the gp120 oligomer. *J Exp Med* **182**:185-96.
  153. **Scanlan, C. N., R. Pantophlet, M. R. Wormald, E. Ollmann Saphire, R. Stanfield, I. A. Wilson, H. Katinger, R. A. Dwek, P. M. Rudd, and D. R. Burton.** 2002. The broadly neutralizing anti-human immunodeficiency virus type 1 antibody 2G12 recognizes a cluster of alpha1-->2 mannose residues on the outer face of gp120. *J Virol* **76**:7306-21.
  154. **Scheid, J. F., H. Mouquet, N. Feldhahn, M. S. Seaman, K. Velinzon, J. Pietzsch, R. G. Ott, R. M. Anthony, H. Zebroski, A. Hurley, A. Phogat, B. Chakrabarti, Y. Li, M. Connors, F. Pereyra, B. D. Walker, H. Wardemann, D. Ho, R. T. Wyatt, J. R. Mascola, J. V. Ravetch, and M. C. Nussenzweig.** 2009. Broad diversity of neutralizing antibodies isolated from memory B cells in HIV-infected individuals. *Nature* **458**:636-40.
  155. **Schneidewind, A., M. A. Brockman, R. Yang, R. I. Adam, B. Li, S. Le Gall, C. R. Rinaldo, S. L. Craggs, R. L. Allgaier, K. A. Power, T. Kuntzen, C. S. Tung, M. X. LaBute, S. M. Mueller, T. Harrer, A. J. McMichael, P. J. Goulder, C. Aiken, C. Brander, A. D. Kelleher, and T. M. Allen.** 2007. Escape from the dominant HLA-B27-restricted cytotoxic T-lymphocyte response in Gag is associated with a dramatic reduction in human immunodeficiency virus type 1 replication. *J Virol* **81**:12382-93.
  156. **Schuitmaker, H., M. Koot, N. A. Kootstra, M. W. Dercksen, R. E. de Goede, R. P. van Steenwijk, J. M. Lange, J. K. Schattenkerk, F. Miedema, and M. Tersmette.** 1992. Biological phenotype of human immunodeficiency virus type 1 clones at different

- stages of infection: progression of disease is associated with a shift from monocytotropic to T-cell-tropic virus population. *J Virol* **66**:1354-60.
157. **Shen, X., R. J. Parks, D. C. Montefiori, J. L. Kirchherr, B. F. Keele, J. M. Decker, W. A. Blattner, F. Gao, K. J. Weinhold, C. B. Hicks, M. L. Greenberg, B. H. Hahn, G. M. Shaw, B. F. Haynes, and G. D. Tomaras.** 2009. In vivo gp41 antibodies targeting the 2F5 monoclonal antibody epitope mediate human immunodeficiency virus type 1 neutralization breadth. *J Virol* **83**:3617-25.
  158. **Stanfield, R. L., M. K. Gorny, S. Zolla-Pazner, and I. A. Wilson.** 2006. Crystal structures of human immunodeficiency virus type 1 (HIV-1) neutralizing antibody 2219 in complex with three different V3 peptides reveal a new binding mode for HIV-1 cross-reactivity. *J Virol* **80**:6093-105.
  159. **Streeck, H., B. Li, A. F. Poon, A. Schneidewind, A. D. Gladden, K. A. Power, D. Daskalakis, S. Bazner, R. Zuniga, C. Brander, E. S. Rosenberg, S. D. Frost, M. Altfeld, and T. M. Allen.** 2008. Immune-driven recombination and loss of control after HIV superinfection. *J Exp Med* **205**:1789-96.
  160. **Sullivan, P., W. D. Decker, J. Mulenga, J. Decker, U. Fideli, E. Hunter, and S. Allen.** 2008. Presented at the AIDS Vaccine, Capetown, South Africa.
  161. **Taylor, B. S., M. E. Sobieszczyk, F. E. McCutchan, and S. M. Hammer.** 2008. The challenge of HIV-1 subtype diversity. *N Engl J Med* **358**:1590-602.
  162. **Tersmette, M., J. M. Lange, R. E. de Goede, F. de Wolf, J. K. Eeftink-Schattenkerk, P. T. Schellekens, R. A. Coutinho, J. G. Huisman, J. Goudsmit, and F. Miedema.** 1989. Association between biological properties of human immunodeficiency virus variants and risk for AIDS and AIDS mortality. *Lancet* **1**:983-5.
  163. **Thali, M., J. P. Moore, C. Furman, M. Charles, D. D. Ho, J. Robinson, and J. Sodroski.** 1993. Characterization of conserved human immunodeficiency virus type 1 gp120 neutralization epitopes exposed upon gp120-CD4 binding. *J Virol* **67**:3978-88.
  164. **Thomas, E. R., R. L. Dunfee, J. Stanton, D. Bogdan, J. Taylor, K. Kunstman, J. E. Bell, S. M. Wolinsky, and D. Gabuzda.** 2007. Macrophage entry mediated by HIV Envs from brain and lymphoid tissues is determined by the capacity to use low CD4 levels and overall efficiency of fusion. *Virology* **360**:105-19.
  165. **Tomaras, G. D., N. L. Yates, P. Liu, L. Qin, G. G. Fouda, L. L. Chavez, A. C. Decamp, R. J. Parks, V. C. Ashley, J. T. Lucas, M. Cohen, J. Eron, C. B. Hicks, H. X. Liao, S. G. Self, G. Landucci, D. N. Forthal, K. J. Weinhold, B. F. Keele, B. H. Hahn, M. L. Greenberg, L. Morris, S. S. Karim, W. A. Blattner, D. C. Montefiori, G. M. Shaw, A. S. Perelson, and B. F. Haynes.** 2008. Initial B-cell responses to transmitted human immunodeficiency virus type 1: virion-binding immunoglobulin M (IgM) and IgG antibodies

- followed by plasma anti-gp41 antibodies with ineffective control of initial viremia. *J Virol* **82**:12449-63.
166. **Trask, S. A., C. A. Derdeyn, U. Fideli, Y. Chen, S. Meleth, F. Kasolo, R. Musonda, E. Hunter, F. Gao, S. Allen, and B. H. Hahn.** 2002. Molecular epidemiology of human immunodeficiency virus type 1 transmission in a heterosexual cohort of discordant couples in Zambia. *J Virol* **76**:397-405.
  167. **Travers, S. A., M. J. O'Connell, G. P. McCormack, and J. O. McInerney.** 2005. Evidence for heterogeneous selective pressures in the evolution of the env gene in different human immunodeficiency virus type 1 subtypes. *J Virol* **79**:1836-41.
  168. **Trkola, A., T. Dragic, J. Arthos, J. M. Binley, W. C. Olson, G. P. Allaway, C. Cheng-Mayer, J. Robinson, P. J. Maddon, and J. P. Moore.** 1996. CD4-dependent, antibody-sensitive interactions between HIV-1 and its co-receptor CCR-5. *Nature* **384**:184-7.
  169. **Trkola, A., M. Purtscher, T. Muster, C. Ballaun, A. Buchacher, N. Sullivan, K. Srinivasan, J. Sodroski, J. P. Moore, and H. Katinger.** 1996. Human monoclonal antibody 2G12 defines a distinctive neutralization epitope on the gp120 glycoprotein of human immunodeficiency virus type 1. *J Virol* **70**:1100-8.
  170. **Troyer, R. M., J. McNevin, Y. Liu, S. C. Zhang, R. W. Krizan, A. Abraha, D. M. Tebit, H. Zhao, S. Avila, M. A. Lobritz, M. J. McElrath, S. Le Gall, J. I. Mullins, and E. J. Arts.** 2009. Variable fitness impact of HIV-1 escape mutations to cytotoxic T lymphocyte (CTL) response. *PLoS Pathog* **5**:e1000365.
  171. **UNAIDS.** 2009. AIDS Epidemic Update. World Health Organization.
  172. **Walker, L. M., S. K. Phogat, P. Y. Chan-Hui, D. Wagner, P. Phung, J. L. Goss, T. Wrin, M. D. Simek, S. Fling, J. L. Mitcham, J. K. Lehrman, F. H. Priddy, O. A. Olsen, S. M. Frey, P. W. Hammond, S. Kaminsky, T. Zamb, M. Moyle, W. C. Koff, P. Poignard, and D. R. Burton.** 2009. Broad and potent neutralizing antibodies from an African donor reveal a new HIV-1 vaccine target. *Science* **326**:285-9.
  173. **Walker, L. M., M. D. Simek, F. Priddy, J. S. Gach, D. Wagner, M. B. Zwick, S. K. Phogat, P. Poignard, and D. R. Burton.** 2010. A limited number of antibody specificities mediate broad and potent serum neutralization in selected HIV-1 infected individuals. *PLoS Pathog* **6**.
  174. **Wang, J., C. Dykes, R. A. Domaol, C. E. Koval, R. A. Bambara, and L. M. Demeter.** 2006. The HIV-1 reverse transcriptase mutants G190S and G190A, which confer resistance to non-nucleoside reverse transcriptase inhibitors, demonstrate reductions in RNase H activity and DNA synthesis from tRNA(Lys, 3) that correlate with reductions in replication efficiency. *Virology* **348**:462-74.
  175. **Warrier, S. V., A. Pinter, W. J. Honnen, M. Girard, E. Muchmore, and S. A. Tilley.** 1994. A novel, glycan-dependent epitope in the V2 domain of human immunodeficiency virus type 1 gp120 is



- recognized by a highly potent, neutralizing chimpanzee monoclonal antibody. *J Virol* **68**:4636-42.
176. **Wei, X., J. M. Decker, S. Wang, H. Hui, J. C. Kappes, X. Wu, J. F. Salazar-Gonzalez, M. G. Salazar, J. M. Kilby, M. S. Saag, N. L. Komarova, M. A. Nowak, B. H. Hahn, P. D. Kwong, and G. M. Shaw.** 2003. Antibody neutralization and escape by HIV-1. *Nature* **422**:307-12.
  177. **Wei, X., S. K. Ghosh, M. E. Taylor, V. A. Johnson, E. A. Emini, P. Deutsch, J. D. Lifson, S. Bonhoeffer, M. A. Nowak, B. H. Hahn, and et al.** 1995. Viral dynamics in human immunodeficiency virus type 1 infection. *Nature* **373**:117-22.
  178. **Willey, R. L., M. A. Martin, and K. W. Peden.** 1994. Increase in soluble CD4 binding to and CD4-induced dissociation of gp120 from virions correlates with infectivity of human immunodeficiency virus type 1. *J Virol* **68**:1029-39.
  179. **Wolk, T., and M. Schreiber.** 2006. N-Glycans in the gp120 V1/V2 domain of the HIV-1 strain NL4-3 are indispensable for viral infectivity and resistance against antibody neutralization. *Med Microbiol Immunol* **195**:165-72.
  180. **Worobey, M., M. Gemmel, D. E. Teuwen, T. Haselkorn, K. Kunstman, M. Bunce, J. J. Muyembe, J. M. Kabongo, R. M. Kalengayi, E. Van Marck, M. T. Gilbert, and S. M. Wolinsky.** 2008. Direct evidence of extensive diversity of HIV-1 in Kinshasa by 1960. *Nature* **455**:661-4.
  181. **Wu, X., A. Sambor, M. C. Nason, Z. Y. Yang, L. Wu, S. Zolla-Pazner, G. J. Nabel, and J. R. Mascola.** 2008. Soluble CD4 broadens neutralization of V3-directed monoclonal antibodies and guinea pig vaccine sera against HIV-1 subtype B and C reference viruses. *Virology* **380**:285-95.
  182. **Wu, X., T. Zhou, S. O'Dell, R. T. Wyatt, P. D. Kwong, and J. R. Mascola.** 2009. Mechanism of human immunodeficiency virus type 1 resistance to monoclonal antibody B12 that effectively targets the site of CD4 attachment. *J Virol* **83**:10892-907.
  183. **Wyatt, R., M. Thali, S. Tilley, A. Pinter, M. Posner, D. Ho, J. Robinson, and J. Sodroski.** 1992. Relationship of the human immunodeficiency virus type 1 gp120 third variable loop to a component of the CD4 binding site in the fourth conserved region. *J Virol* **66**:6997-7004.
  184. **Xiang, S. H., N. Doka, R. K. Choudhary, J. Sodroski, and J. E. Robinson.** 2002. Characterization of CD4-induced epitopes on the HIV type 1 gp120 envelope glycoprotein recognized by neutralizing human monoclonal antibodies. *AIDS Res Hum Retroviruses* **18**:1207-17.
  185. **Zhang, M., B. Foley, A. K. Schultz, J. P. Macke, I. Bulla, M. Stanke, B. Morgenstern, B. Korber, and T. Leitner.** 2010. The role of recombination in the emergence of a complex and dynamic HIV epidemic. *Retrovirology* **7**:25.

186. **Zhang, P. F., P. Bouma, E. J. Park, J. B. Margolick, J. E. Robinson, S. Zolla-Pazner, M. N. Flora, and G. V. Quinnan, Jr.** 2002. A variable region 3 (V3) mutation determines a global neutralization phenotype and CD4-independent infectivity of a human immunodeficiency virus type 1 envelope associated with a broadly cross-reactive, primary virus-neutralizing antibody response. *J Virol* **76**:644-55.
187. **Zhou, T., L. Xu, B. Dey, A. J. Hessel, D. Van Ryk, S. H. Xiang, X. Yang, M. Y. Zhang, M. B. Zwick, J. Arthos, D. R. Burton, D. S. Dimitrov, J. Sodroski, R. Wyatt, G. J. Nabel, and P. D. Kwong.** 2007. Structural definition of a conserved neutralization epitope on HIV-1 gp120. *Nature* **445**:732-7.
188. **Zhu, T., B. T. Korber, A. J. Nahmias, E. Hooper, P. M. Sharp, and D. D. Ho.** 1998. An African HIV-1 sequence from 1959 and implications for the origin of the epidemic. *Nature* **391**:594-7.
189. **Zolla-Pazner, S., S. S. Cohen, C. Krachmarov, S. Wang, A. Pinter, and S. Lu.** 2008. Focusing the immune response on the V3 loop, a neutralizing epitope of the HIV-1 gp120 envelope. *Virology* **372**:233-46.